Alma Mater Studiorum – Università di Bologna

DOTTORATO DI RICERCA IN
ONCOLOGIA, EMATOLOGIA E PATOLOGIA

Ciclo XXXI

Settore Concorsuale: 06/D3

Settore Scientifico Disciplinare: MED/06

RESISTANCE MECHANISMS AND NOVEL THERAPEUTIC OPPORTUNITIES IN GASTROINTESTINAL STROMAL TUMORS (GISTs)

Presentata da:
Gloria Ravegnini

Coordinatore Dottorato
Chiar.Mo Prof.
Pier-Luigi Lollini

Supervisore
Chiar.Ma Prof.ssa
Maria Abbondanza Pantaleo

Esame finale anno 2019

Index

General background

1. Gastrointestinal Stromal Tumor

1.1. Brief history of GISTs

Gastrointestinal stromal tumors (GISTs) are rare sarcomas, which represent the most common mesenchymal tumor of the gastrointestinal (GI) tract [1]. Three milestones have characterized the history of GISTs. In 1941, for the first time, Golden and Stout characterized a group of mesenchymal tumor arising in the bowel wall [2], but in 1983 Mazur and Clark proposed the term "stromal tumor" for this specific disease [3]. The second milestone was in 1998, when a groundbreaking publication by Hirota and colleagues reported activating mutations in the *KIT* receptor tyrosine kinase (RTK) gene in GISTs as well as expression of KIT protein by immunohistochemistry (IHC) [4]. Finally, the last milestone took place with the introduction of tyrosine kinase receptor inhibitor (TKI), imatinib, which led to a terrific improvement of GIST patients' prognosis [5].

1.2. Epidemiology, clinical features and prognosis of GISTs

Even if rare, GISTs represent the most common mesenchymal neoplasia of the GI tract. The true incidence of GIST in the US and Europe is hard to determine, as GISTs have only been accurately recognized and diagnosed as an entity since the late '90s. The incidence of these tumors is geographically variable, from 4.3–6.8 cases per million to 19–22 cases per million [6]. It is estimated that incidence rates of GIST in US is 11-14 cases/ 1000000 with 4000-6000 new cases per year [7]; similar incidence rates have been found in Europe [8,9].

Regarding to sex differences, there is a slight prevalence in males. The median age is around 60–65 years, but cases in patients younger than 40 are rare, and only 1% interest patients aged < 21. However, pediatric GISTs represent a clinically and molecularly distinct subset [10,11].

GISTs occur throughout the GI tract and are most commonly found in the stomach (60%), small intestine (35%, specifically, jejunum and ileum (30%) and duodenum (5%)), colorectum (4%), and rarely in the esophagus and appendix (Figure 1) [10,12,13].

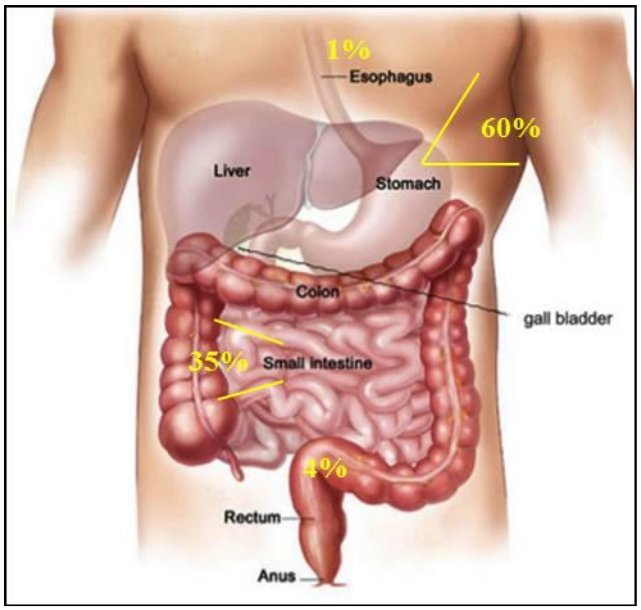

Figure 1. GISTs may be found anywhere in or near the GI tract

The tumors are generally between 1 and 40 cm in diameter at the time of diagnosis and may cause mass-related symptoms or anemia as a result of mucosal ulceration [14]. Patients with GIST, often, do not experience any specific symptoms or signs and when symptoms do occur, they may be vague. Clinical symptoms associated with GIST include abdominal pain, fatigue, dysphagia, satiety, nausea and vomiting, vomiting blood, blood in the stool and obstruction. Patients may present with chronic GI bleeding (causing anemia), or acute GI bleeding (caused by erosion through the gastric or bowel mucosa) or rupture into the abdominal cavity causing life-threatening intraperitoneal hemorrhage. It is not uncommon that a GIST is discovered by chance when a person has an imaging test for an unrelated concern or condition [15].

1.3. **Histopathology**

As mentioned above, GISTs – commonly arising within the muscle of GI tract – may range from 1 cm to more than 40 cm in size, and 5 cm is considered the average size.

GISTs probably originate from the interstitial cells of Cajal (ICC) or their precursors [16]. ICCs generate a periodic depolarization – referred to as pacemaker activity – in the GI tract controlling intestinal motility [16,17]. Moreover, similar to GISTs, ICCs express the RTK KIT, encoded by *c-KIT* gene. In general, small GISTs tend to form intramural masses, while larger GISTs make external masses and involve muscular layers [14]. Morphologically, it is possible to distinguish three main histological subtypes in GISTs: i) spindle cell type (~70% of the cases), ii) epithelioid type (~20%), and iii) mixed spindle cell and epithelioid type (~10%) (Figure 2). The spindle cells are monomorphic, with rounded to elongated nuclei and made up of cells in short fascicles. Epithelioid cell GISTs are characterized by round cells arranged in nests or sheets and with eosinophilic to clear cytoplasm; cells are polygonal with round, centrally located nuclei. Finally, approximately 10% of GISTs show mixed morphology, being composed of both spindle and epithelioid cells [18].

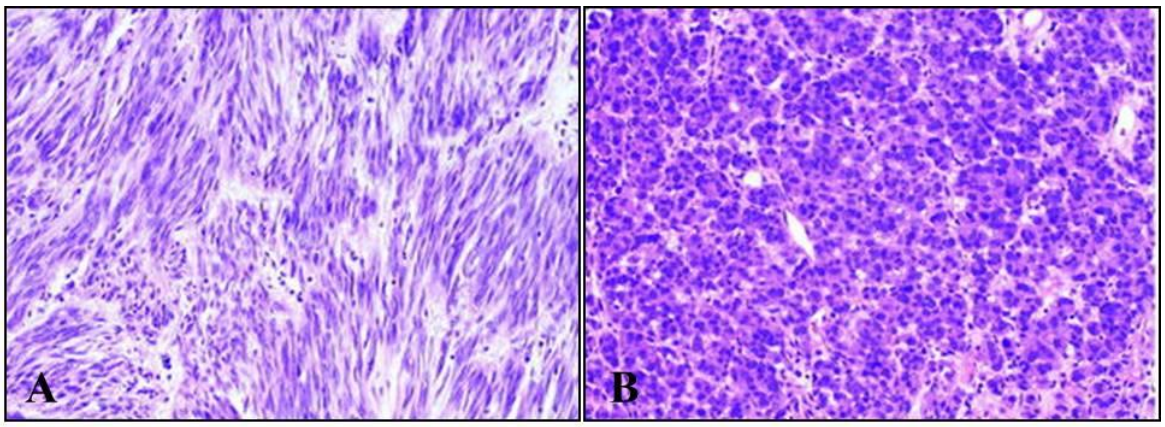

Figure 2. Example of GIST cells' morphology. **A)** GIST composed of spindle cells (hematoxylin-eosin, original magnification ×200). **B)** GIST composed of epithelioid cells (hematoxylin-eosin, original magnification ×200) [18]

1.4. Oncogenic mutations in *KIT* and *PDGFRA* genes

With the identification of the specific mutation in *KIT* gene in 1998 by Hirota et al [4], the history of this tumor was completely changed. Today, it is well established that about 80-85% of GISTs harbor a gain of function mutation in *KIT* or *PDGFRA* genes. *KIT* and *PDGFRA* genes are adjacently located on chromosome 4q12 and encode RTK class 3. KIT and PDGFRA receptors share structural features and are composed of an extracellular (EC) ligand-binding domain, a transmembrane domain, a juxtamembrane domain (JM), and two cytoplasmic kinase domains (TK1, which includes ATP binding pocket, and TK2, the kinase activation loop) (Figure 3) [19,20]. In physiological conditions, KIT and PDGFRA are activated by binding of their ligands to the EC domain, stem cell factor (SCF) and Platelet Derived Growth Factor Subunit A (PDGFA), respectively. Ligand binding leads to the receptor homodimerization and subsequent cross phosphorylation of specific cytoplasmic tyrosine residues, which act as binding sites for a plethora of signaling proteins involved in pivotal processes, such as cell proliferation, adhesion, motility, apoptosis, chemotaxis, and survival [21]. The via activated by phosphorylation includes RAS/RAF/MEK, and PI3K/AKT/mTOR, and MAPK cascade [21,22] (Figure 4).

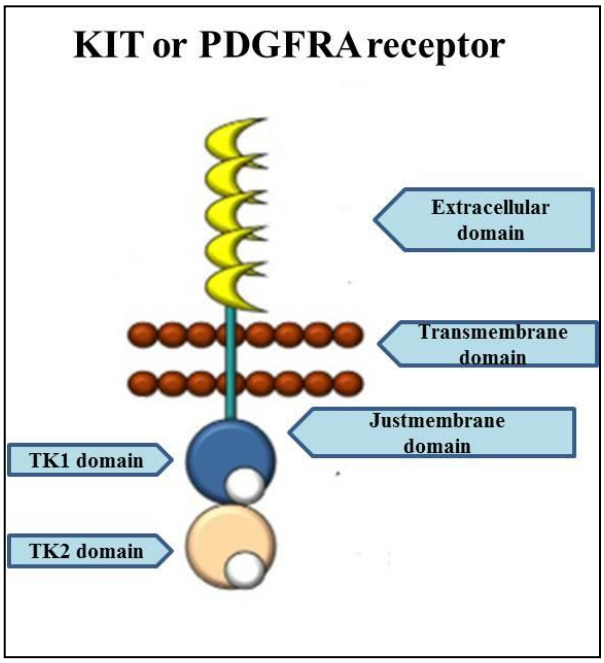

Figure 3. Structure of RTK

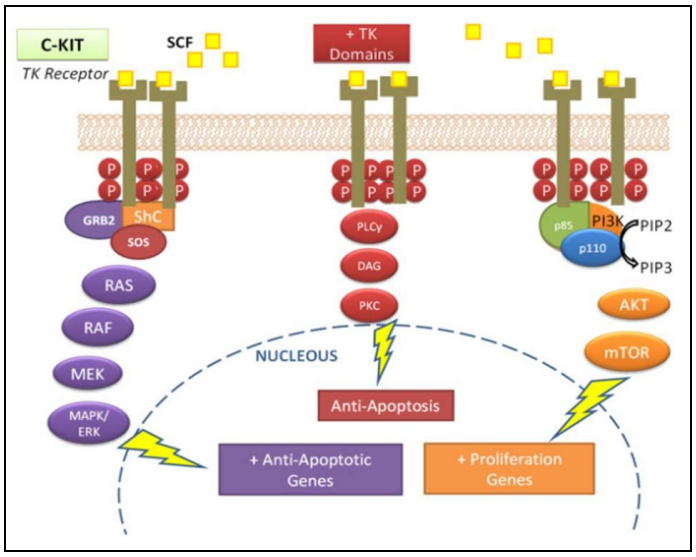

Figure 4. Main pathways activated by the tyrosine-kinase receptor - KIT and its effects on carcinogenesis [22]
Figure from De Melo et al, 2012

In KIT, different tyrosine residues including Tyr 568, Tyr 570, Tyr 703, Tyr 721, Tyr 730, Tyr 823, Tyr 900, and Tyr 936 may be phosphorylated. Phosphorylated tyrosines, and adjacent aminoacidic residues, form specific binding sites for downstream signaling molecules and promote activation of specific downstream signaling pathways (Figure 5) [23]. For example, it has been reported that Tyr 721 acts as the docking site for the activation of PI3 kinase and its downstream signaling pathway regulates cell survival and proliferation; Tyr 703 and Tyr 936 are docking sites for activation of Grb2 protein, which is involved in activation of RAS/RAF/MEK/ERK signaling cascade [23].

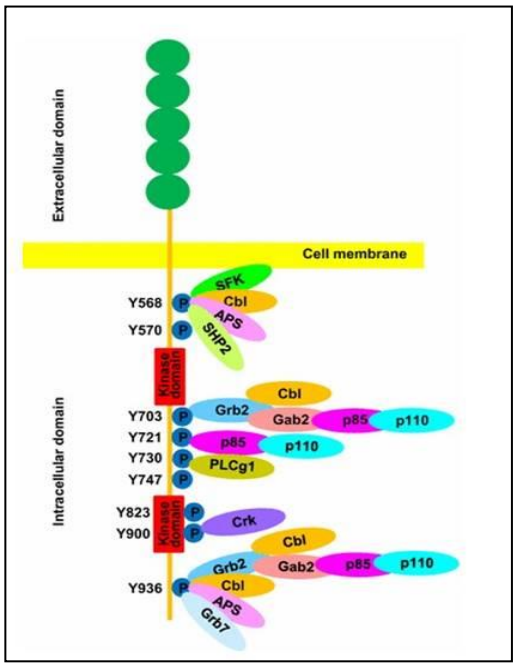

Figure 5. Schematic representation of the Tyr residues that may be phosphorylated and their interaction molecules

Genetic alterations in *KIT* or *PDGFRA* genes involve two main regions, the receptor regulatory domains (dimerization region in the EC and JM domains) and the enzymatic domains (TK1 and TK2).

The mutations characterizing GISTs are gain of function mutations and lead to a constitutive receptor activation, in a ligand-independent manner.

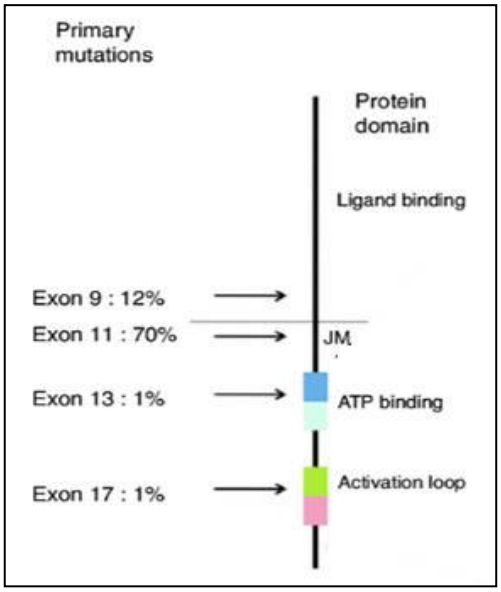

Figure 6. Schematic representation of *KIT* exons harboring primary mutations in GISTs

Approximately 80% of GISTs carry *KIT* pathogenic activating mutations, whereas 5% to 10% harbor activating mutations of the *PDGFRA* [24,25]. Regarding KIT receptor, in GISTs the majority of mutations (~65%) involve the JM domain (exon 11) followed by mutations involving the EC dimerization domain (exon 9), retrieved in about 10% of cases. Primary KIT mutations can also involve exon 13 (TK1) and exon 17 (TK2), but these mutations are quite rare (~2%) (Figure 6) [26].

With regard to *PDGFRA*, the most common *PDGFRA* mutation involves the exon 18 at codon 842 (~5%), and leads to a substitution of an aspartic acid (D) with a valine (V) (D842V) [27], while mutations on exon 12 and 14 are less frequent [27]. *KIT* and *PDGFRA* oncogenic alterations are mutually exclusive in GISTs and are driver events in GIST pathogenesis [28].

1.4.1. Mutations in *KIT* gene

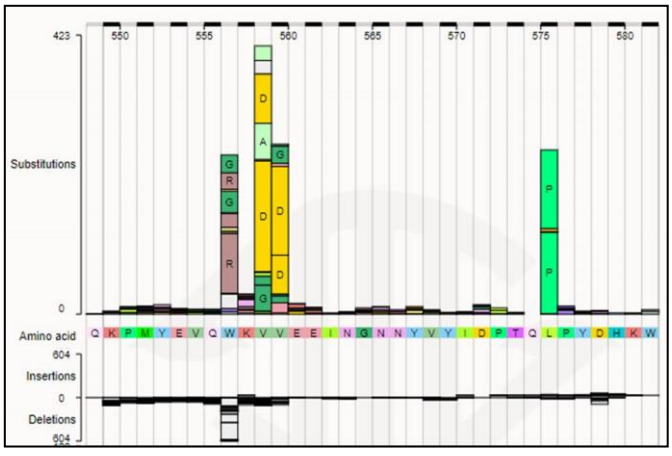

Figure 7. Schematic representation of main mutations in *KIT* exon 11

As mentioned before, the majority of mutations in *KIT* involve exon 11 and exon 9. Mutations can be aminoacid substitutions, *in-frame* deletions or insertions. With regard to exon 11, it has been observed that these kinds of alterations are associated with rupture of

secondary structure of JM domain**,** leading to dimerization and receptor autophosporylation with consequent activation. The kinds of mutations occurring in this hot-spot are heterogeneous, including *in-frame* deletions of variable sizes, point mutations, deletions preceded by substitutions or a combination of these. The most common site of *KIT* mutations is in the 5'end of exon 11. In general, exon 11 deletions are associated with a more aggressive behavior if compared with the single aminoacid substitution; in particular, deletions affecting codons WK557–558 indicate a poor prognosis. Another hot spot, but less frequent, is located at the 3' end of exon 11, that is characterized mostly by internal tandem duplication. GISTs with these type of mutations usually show a more indolent clinical evolution [29]**.** Figure 7 shows the major mutations harbored in *KIT* exon 11 (K549 to W581) reported in COSMIC. It is possible to observe the wide heterogeneity in genetic alterations' type. The main hot spots are aminoacids 557-558 and 559-560 [30,31]**.** With regard to exon 9, the most frequent mutation is represented by a duplication of six nucleotides (nts) encoding Ala-Tyr (at position 502–503) at the COOH terminus of the EC domain. Usually, GISTs harboring *KIT* exon 9 mutations have small bowel location and an aggressive clinical behavior [32]**.**

1.4.2. Mutations in *PDGFRA* gene

GISTs with *PDGFRA* mutations represent a small subset; it has been previously reported that tumors with these specific alteration arise primarily in the stomach, mesentery and omentum [33]. *PDGFRA* mutant GISTs have an epithelioid morphology, while spindle cells dominate the *KIT* mutant ones; in addition, up to 40% of these tumors are weak or negative for KIT expression in IHC. The mutational hot-spot in *PDGFRA* is codon 842 on exon 18, but other codons may be involved in aminoacid substitution or *in-frame* deletions and deletion/substitutions, as codon 845 to 848. *PDGFRA* exon 18 mutations are believed to aberrantly stabilize the kinase activation loop [34]. The principal difference with respect to *KIT* mutant GISTs is the location of primary mutations. Indeed, the majority of *KIT* mutations in GISTs arise in the JM domain (exon 11), but only ~10% of *PDGFRA* mutations are in this region (exon 12). On the contrary, mutations in the activation loop

of KIT (exon 17) are rare events (<1%), but they are predominant in *PDGFRA* mutant GISTs (exon 18) [33]. The tumor genotype and specific type of *KIT/PDGFRA* mutation are important for the clinical outcome to TKIs and they will be discussed in the following paragraphs.

1.5. *KIT/PDGFRA* wild-Type GISTs

1.5.1. SDH-*deficient* GISTs

About 10-15% of adult GISTs and 85% of the pediatrics do not present any alteration in *KIT* or *PDGFRA* genes and are referred to as *KIT/PDGFRA* wild-type (WT) GISTs. The major part of these are associated with hereditary syndromes, including neurofibromatosis type 1 (NF1), Carney triad (CT), Carney-Stratakis syndrome (CSS), and hereditary paraganglioma/pheocromocitoma (HPGL/PCC) syndrome. In the last years, substantial advances in knowledge of GISTs led to understand that *KIT/PDGFRA* WT GISTs are a heterogeneous group of different diseases [35]. Indeed, it is well known that between 20-40% of all *KIT/PDGFRA* WT GISTs are succinate dehydrogenase complex (*SDH)-deficient* GISTs. SDH is a mitochondrial enzyme composed of four subunits, each of which encoded by four different genes *SDHA*, *SDHB*, *SDHC*, and *SDHD* [6]. *KIT/PDGFRA* WT-(SDH*)-deficient* GISTs are recognized by IHC SDHB loss of expression, often due to germline and/or somatic loss of function mutations in any of the four SDH subunits. Frequently, SDH deficiency in tumor cells is due to a combination of a loss of function germline mutations in one of the *SDH* subunit genes and somatic loss of function mutations in the tumor cells, promoting inactivation of both alleles [36]. Recently, several papers have reported that SDH inactivation may involve also epigenetic mechanisms as methylation of *SDHC* promotor [37]. The

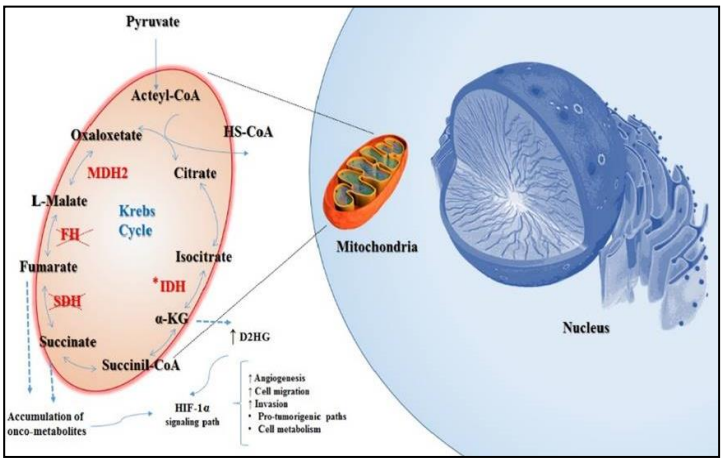

Figure 8. SDH deficiency promotes accumulation of oncometabolites, which leads to HIF1α-pathway activation

SDH-complex takes part in the Krebs cycle and is responsible for conversion of succinate to fumarate. Therefore, SDH-*deficient* cells accumulate succinate, which promotes HIF1α overexpression and HIF translocation into nucleus. Overexpressed HIF proteins leads to aberrant transcription factors and to expression of hypoxia-associated tumorigenic responses and angiogenesis (Figure 8) [36]. SDH-*deficient* GISTs are characterized by a peculiar gene expression signature that differs from the one observed in *KIT/PDGFRA* mutant GISTs; among the group of genes differentially expressed, one of the most important is the insulin-like growth factor 1 receptor (IGF1R), which is overexpressed in SDH-*deficient* GISTs but lost in *KIT/PDGFRA* mutant ones [38,39]. SDH-*deficient* GISTs show a number of clinically unique features such as young age, female gender predilection, gastric localization, mixed epithelioid and spindle cell morphology, diffuse KIT and DOG1 IHC positivity, frequent lymphnode metastatic involvement, and an indolent behavior [35,40].

1.5.2. *BRAF/RAS* mutant GISTs

Besides SDH-*deficient*, other subsets of *KIT/PDGFRA* WT GISTs have been characterized. Indeed, it has been reported that 5-13% of *KIT/PDGFRA* WT GISTs harbor a *BRAF* V600E mutation; BRAF is a pivotal intracellular protein kinase, involved in the RAS/RAF/MEK/ ERK signaling pathway. More than 90% of *BRAF* mutations occur in exon 15, resulting in the substitution of valine at codon 600 with a glutamic acid (V600E) [41]. The V600E mutation increases BRAF activity due to creation of a salt bridge with K507. This interaction V600E - K507 mimics the conformational changes that happen during dimerization, and for this reason, *BRAF* V600E does not depend on dimerization for increased kinase activity [42]. Usually, these *BRAF* mutant GISTs arise in the small intestine, in middle-aged females, and have a high mitotic rate and early metastasis [6,35,43].

KRAS mutations in GISTs have a low frequency, spanning from ~1% to 11% of *KIT/PDGFRA* WT GISTs [41]. These alterations may be present with *KIT* or *PDGFRA* mutations or as genetic event in *KIT*/*PDGFRA* WT GISTs [44,45]. In a recent study from Hechtman *et al*. in 267 GISTs, one single

KIT/PDGFRA WT GIST carried a *KRAS* mutation (p.G12V), which showed an aggressive behavior and resistance to multiple TKIs [46].

1.5.3. *NF1* mutant GISTs

A hereditary condition leading to an increased incidence of GIST is an autosomal-dominant inherited disease referred to as NF1. NF1 is characterized by specific nerve, dermal and ocular manifestations, including café-au-lait spots, dermal neurofibromas and ocular manifestations, Lisch nodules, and optic glioma.

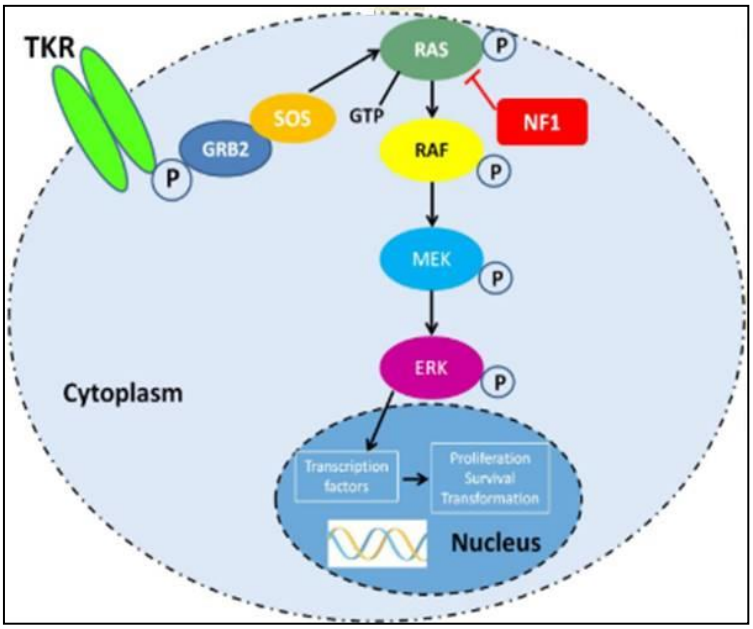

Figure 9. The signaling pathway displays the oncogenic Ras signaling pathway as well as tumor suppressor NF1**.**

NF1 gene has more than 60 exons and represent one of the largest human genes; it encodes neurofibromin, a tumor suppressor that downregulates the RAS/RAF/MEK/ERK via (Figure 9). ~7% of NF1 patients develop a GIST during their lifetime. GISTs arising in the setting of NF1 are SDHB positive and immunohistochemically positive for IGF1R expression [35,40]. The majority of NF1-associated GISTs arise in the small intestine, with infrequent gastric exceptions. Morphologically, NF1-associated GISTs present spindle cells, are correlated with Cajal cell hyperplasia and associated with GI motility disorders [6]. GISTs with mutations in *BRAF/RAS* or *NF1* might be referred to as RAS-pathway (RAS-P) mutant GIST.

1.5.4. Quadruple WT GISTs

Recently, Pantaleo and coworkers, through massively parallel sequencing and gene expression analyses, reported for the first time the existence of an additional subset of *KIT/PDGFRA* WT GISTs [47]. This subgroup has been named as *quadruple* WT *(*q-WT*)* because no genetic alterations

in *KIT/PDGFRA/SDH/RAS* have been found. Transcriptome profile of this small group is deeply different from other GISTs, and q-WT GISTs could represent another unique group within the family of GISTs [35,47]. To date, even if additional research groups have extensively worked on this new group of tumors, it has not been identified a common genetic driver event. On the contrary, a great molecular heterogeneity, with various and probably mutually exclusive mutational events, has been described [35]. Figure 10 summarizes the majority of mutations retrieved in q-WT GISTs.

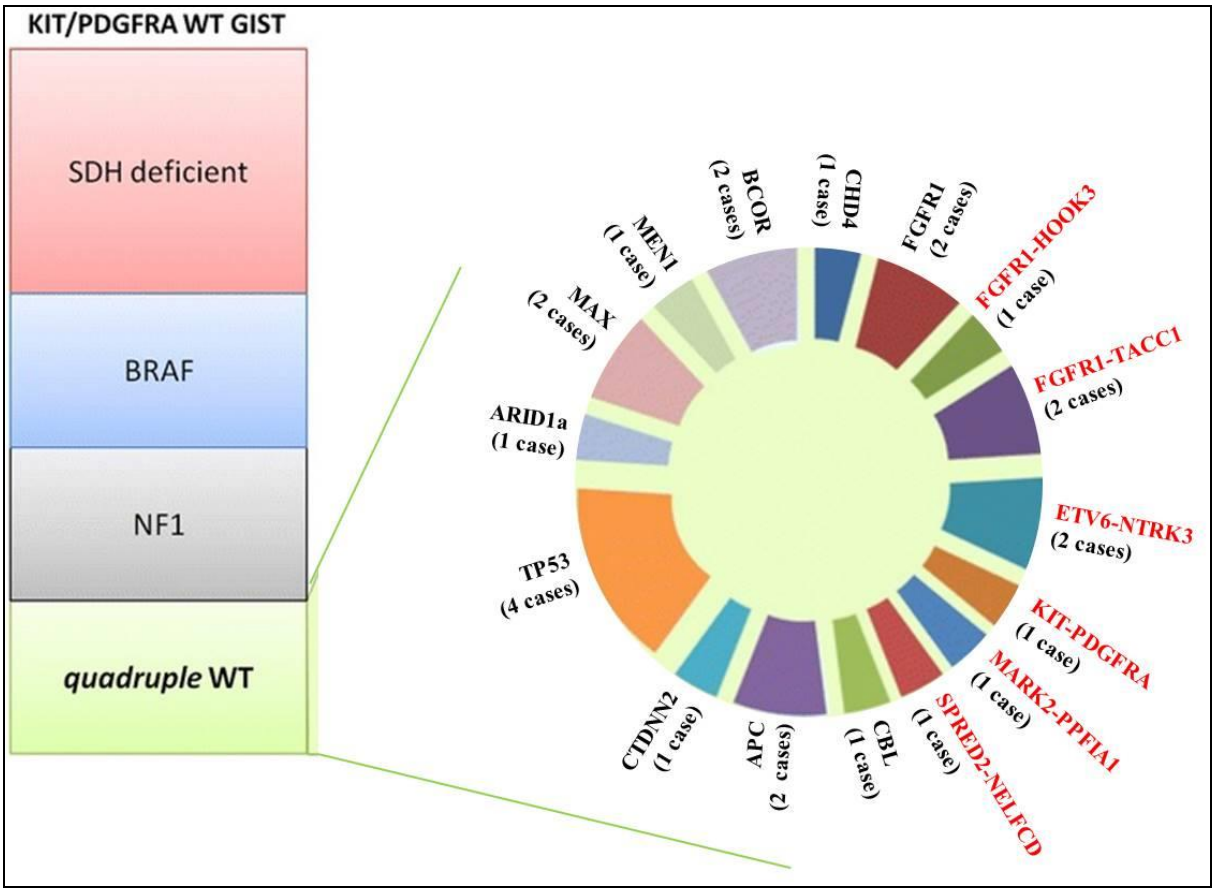

Figure 10. q-WT GISTs are a heterogeneous family of tumors with different genetic events.
Figure edited from Nannini et al, 2017

However, given this pronounced molecular heterogeneity and besides the unquestionable GIST morphology, q-WT GISTs could represent a different disease than GISTs, deriving from a distinct population of ICCs.

1.6. Treatment of GISTs

The standard chemotherapy is not effective in GISTs. However, until the introduction of TKIs at the beginning of 2000, doxorubicin and ifosfamide were used with low activity in GISTs compared to other soft tissue sarcomas, with a response rate < 5% [48]. The median survival was approximately 9 months [49]. Today, GIST management for immunohistologically confirmed GISTs plans: i) surgical resection for resectable GISTs without metastasis; ii) administration of TKIs such as imatinib for unresectable, metastatic, or recurrent GISTs [9,50,51]. The standard treatment for localized and resectable GISTs is the complete surgical resection of the lesion, with no tumor rupture. Indeed, tumor rupture is associated with a high risk of relapse and, for this reason, the laparascopic approach is discouraged for patients with large tumors. Ideally, the excision should have margins clear of tumor cells. GISTs sized up to 5 cm are managed through laparoscopic surgery which show terrific survival rates (92–96%) [1]. Larger GISTs need open surgery and broad resections. Total gastrectomy may be needed for very large or multiple and recurrent GISTs including SDH-*deficient* GISTs in young patients. After surgical resection, the risk of relapse may be considerable, as defined by available risk classifications [52]. 3 years of adjuvant treatment with imatinib (see below) is considered the standard approach for patients with a high risk of relapse. On the contrary, adjuvant therapy should not be considered when the risk is low, whereas decision-making should be discussed when the risk is intermediate [53].

1.6.1. Imatinib mesylate

In locally advanced inoperable and metastatic patients, imatinib is the standard treatment. Imatinib has been introduced in management of GIST at the beginning of 2000, led to a terrific improvement of prognosis of patients [5,54].

Imatinib mesylate (formerly STI571, Gleevec® (United States) or Glivec® (Europe), Novartis) represents one of the most successful example of target therapy. In the late ‘80s, scientists at Ciba

Geigy (now Novartis), started a project on the identification of compounds with inhibitory activity against protein kinases. The most promising molecule was STI571, which in vitro showed potent activity against all of the ABL tyrosine kinases, including ABL, viral ABL (v-ABL), and BCR-ABL. In contrast, STI571 was inactive against serine/threonine kinases, did not inhibit the epidermal growth factor (EGF) receptor intracellular domain, and showed weak or no inhibition of the activity of the receptors for vascular endothelial growth factor (VEGFR-1 and VEGFR-2), fibroblast growth factor receptor 1 (FGFR-1), c-MET, and nonreceptor tyrosine kinases of the SRC family (FGR, LYN, and LCK). In 1998, a phase 1 trial with imatinib started in patients with chronic myeloid leukemia (CML), revolutionizing the treatment of this kind of blood tumor [55]. Imatinib is a selective inhibitor, which binds competitively the ATP binding site of the target kinases including ABL, BCR-ABL, KIT, PDGFRA, PDGFRB, and receptor of macrophage-colony stimulating factor (CSF1R). This binding is due to the fact that imatinib mimics adenosine triphosphate (ATP) and can compete with ATP (Figure 11) [56].

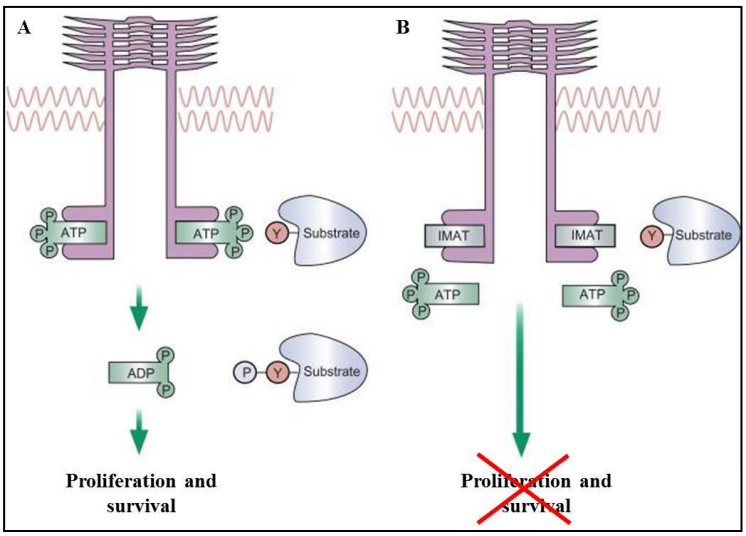

Figure 11. Mechanism of action of imatinib. A) Physiological conditions: ATP binds KIT or PDGFRA, promoting proliferation and survival. B) Imatinib binds the ATP structure and binds ATP binding pocket, preventing proliferation and survival. Figure edited by Rubin et al, 2007

In GIST cells, ATP binds to the active site of KIT or PDGFRA where it donates a phosphate to either KIT or PDGFRA, resulting in autoactivation, or to substrate molecules, resulting in activation of signal transduction. Imatinib, binding to the same site as ATP, prevents phosphorylation of downstream substrates and leads to inhibition of KIT or PDGFRA signaling [56].

The first patient treated with imatinib in 2000 had a rapidly progressive metastatic GIST that was resistant to chemotherapy; after 4 weeks of imatinib treatment, the patient had a complete metabolic response and many of the liver metastases became hypodense (Figure 12) [57]. The success in treating this patient quickly led to a multicenter trial which involved the Dana-Farber Cancer Institute, Fox-Chase Cancer Center, Oregon Health & Science University Cancer Institute, and the University of Helsinki [5]. In the trial, 147 adult patients, with a histologically confirmed, unresectable or metastatic GIST which expressed CD117, were enrolled. Patients were randomly treated either with 400 mg or 600 mg of imatinib; the tumor response was evaluated after one month, three months, and six months, and every six months. No patient had a complete response, but ~54% of the patients had a partial response; in addition, ~28% of patients had stable disease, and disease progression was noted in 14% of patients within three months after study entry. In general, imatinib was well tolerated, with adverse effects from mild to moderate and similar to those reported in patients with CML [5]. Similar results were observed in another phase I trial from the European Organization for Research and Treatment (EORTC). Based on the results from these two trials, imatinib was approved by the US Food and Drug Administration (FDA) for the treatment of unresectable and metastatic GIST on February 1st, 2002. Overall, imatinib achieved disease control in 70–85% of patients with KIT-

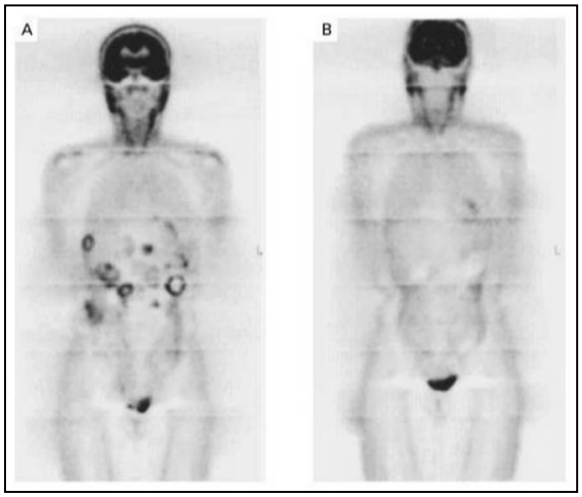

Figure 12. PET Studies with [18F]Fluorodeoxyglucose.
A) Before STI571 therapy there were multiple metastases in the liver and upper abdomen. **B)** After four weeks of treatment, there was no abnormal uptake of tracer in the liver or right kidney

positive GIST, with a median progression free survival (PFS) of 20–24 months, and an estimated overall survival (OS) over 36 months [49].

1.6.1.1 Correlation of kinase genotype and imatinib clinical outcome

The first study investigating the correlation between the tumor genotype and imatinib clinical response dates back to 2003 [58]. In particular, Heinrich *et al* analyzed the tumor genotype and the clinical outcome of 127 patients enrolled onto a phase II trial of imatinib for metastatic GISTs [5], but a larger study involving 428 GIST cases was conducted later, in 2008, by the same authors [59]. The results reported by the studies were concord, and showed that *KIT* exon 11 genotype had favorable impact on the imatinib response compared with GISTs with a *KIT* exon 9 mutation or WT genotypes. No significant difference in OS between patients whose tumors had a *KIT* exon 9 mutant or a WT genotype were observed [59]. In addition, it was reported that patients with *KIT* exon 9 mutant GISTs, who were treated with imatinib 800 mg, had a higher objective response rate compared with patients who were treated with imatinib 400 mg [59]. With regard to *PDGFRA* mutations, GISTs with *PDGFRA* point mutations D842V showed a primary resistance to imatinib therapy, consistent with *in vitro* data [58].

In general, according to the Clinical practice guidelines for GISTs released in 2018 by the European Society of Medical Oncology (ESMO), the standard dose of imatinib is 400 mg daily [9]. However, data have shown that patients with tumors harboring the *KIT* exon 9 mutation have significantly better PFS on an 800 mg daily dose, which is considered the standard treatment in this subgroup. In metastatic GISTs, treatment with imatinib should be continued indefinitely, considering that stopping treatment is generally followed by relatively rapid tumor progression.

1.6.1.2 Resistance to imatinib treatment

As described below, ~80% of GISTs patients get benefits from imatinib treatment, however, after a median time of 24 months, a remarkable number of them become resistant [60]. It has to be considered that KIT receptor may either be configured in an “open/on” conformation which allows ATP to bind or a “closed/off “ conformation which facilitates phosphorylation of substrates.

Imatinib can bind KIT receptor only when it is in the open conformation and maintains the receptor in this state. The majority of *KIT* and *PDGFRA* mutations lead to the open conformation, thereby reducing the efficacy of imatinib [60]. The term *primary resistance* is used to indicate patients showing progression within 3–6 months of initiating imatinib; approximately 15–20% of patients are primary resistant and most of the WT GISTs and *PDGFRA* D842V mutant patients display primary resistance [61]. On the contrary, progression after more than 6 months of clinical response is defined as secondary or acquired resistance. Secondary mutations have only been found in patients with primary *KIT* mutations and rarely in those with primary *PDGFRA* mutations. Resistant mutations are most often found in the ATP-binding pocket of the kinase domain (exons 13 and 14) or in the kinase activation loop (exons 17 and 18) [61]. Despite the acquisition of secondary mutations, mechanisms of delayed resistance may include: i) overexpression of KIT due to genomic amplification, (ii) loss of KIT expression with activation of an alternative tyrosine kinase, and (iii) ABC transporters overexpression, which may also represent a method for tumor cells to become resistant to TKIs.

Therapeutic options for GIST patients progressed on imatinib consider dose escalation from 400 to 800 mg /daily or switch to the second and third line TKIs.

1.6.2. Sunitinib malate

For those patients who progress under imatinib treatment or are intolerant to imatinib, sunitinib is the standard second line therapy, a second generation TKI [62].

Sunitinib malate (formerly SU11248, Sutent®, Pfizer) is an oral oxindole multitarget kinase inhibitor, that inhibits specific tyrosine kinases including VEGFRs (types 1 and 2), PDGFRs (PDGFRA and PDGFRB), KIT, FMS-like tyrosine kinase-3 (FLT3), glial cell line derived neurotrophic factor receptor (RET) and CSF1R [63] (Figure 13). Similar to imatinib, sunitinib interacts with the adenosine triphosphate (ATP) binding pocket of these kinases and acts as a competitive inhibitor of ATP.

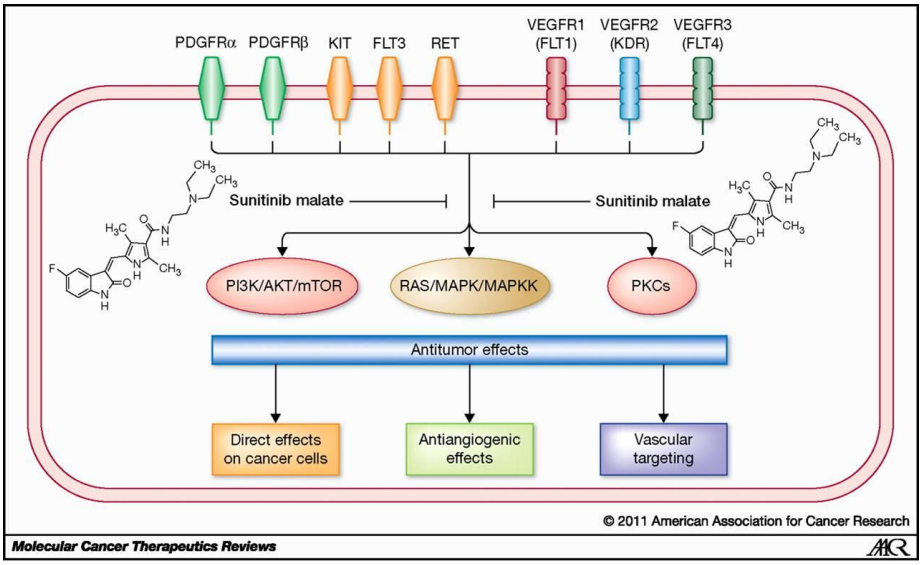

Figure 13. Specific RTKs are blocked by sunitinib; sunitinib inhibition of signaling pathways PI3K/AKT/mTOR, MAPK, and PKC triggers different antitumor effects [64]

The inhibition of these RTKs blocks signal transduction, thereby affecting various cellular processes, including tumor growth and progression, angiogenesis, and metastasis [64].

Besides the similarity with imatinib, sunitinib is effective in imatinib resistant GISTs, through unique binding characteristics and a broader spectrum of kinase inhibition. Primary and secondary mutations in the kinase powerfully influence sunitinib activity [65]. For example, it has been reported that sunitinib showed higher clinical benefits and the objective response rates in patients with primary *KIT* exon 9 mutations with respect to GISTs with exon 11 mutations (clinical benefit rates: 58% *vs* 34%; objective response rates: 37% *vs* 5%); moreover PFS and OS were significantly longer in *KIT* exon 9 mutant or *KIT/PDGFRA* WT patients compared to *KIT* exon 11 mutant ones [65]. With regard to *KIT* secondary mutations, *in vitro* and *in vivo* studies have shown that sunitinib is more effective against acquired mutations harbored in the ATP binding pocket, encoded by exon 13 and 14, than those in the activation loop *(KIT* exon 17 or 18) [65].

1.6.3. Regorafenib

After confirmed progression under sunitinib, a prospective placebo-controlled randomized trial showed that regorafenib can significantly prolong PFS. This treatment was approved as standard third line therapy for patients progressing on or failing to respond to imatinib and sunitinib, on February 25th, 2013 by FDA [66]. Regorafenib (formerly BAY73-4506, Stivarga®, BAYER) is an orally available multikinase inhibitor with activity against multiple targets, including KIT, PDGFR, VEGFR-1 -2 -3, TIE2, RET, FGFR-1, RAF, and p38 mitogen-activated protein kinase (MAPK) [66]. Many patients, after the development of resistance to imatinib and sunitinib, progress even under regorafenib. Currently, unfortunately there are no other therapeutic options and the rechallenge of imatinib or sunitinib may represent a reasonable option in advanced GIST patients after failure of previous treatments [67]. Figure 14 summarizes the management of advanced/metastatic GISTs, according the guideline by ESMO released in 2018.

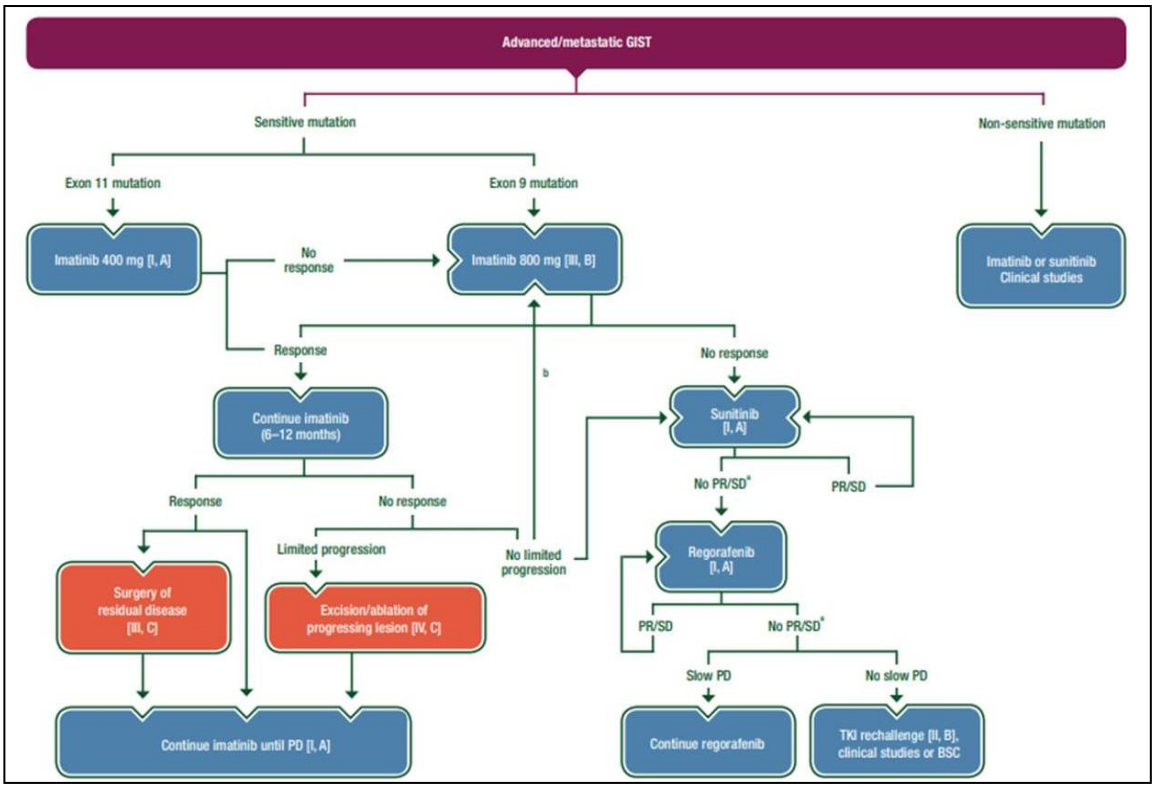

Figure 14. Management of advanced/metastatic GISTs. [a]Surgery of limited progression may be considered. [b]If previously treated with 400 mg imatinib. BSC: best supportive care; PD: progressive disease; PR: partial response; SD: stable disease

2. Pharmacogenetics and Epigenetics

According to ACCR Cancer Progress report 2017 [68], the number of global cancer-related deaths is arising, moving from 8.8 million in 2015 to 14.6 in 2035. This means that the impact of cancer will grow significantly in the next years if new and powerful tools for cancer prevention, detection and treatment will not be established or improved [68]. Therefore, a better knowledge of cancer landscape and the identification of novel potential biomarkers is urgently needed. The development of new techniques, as high-throughput screening, has led to a better characterization of many diseases, including cancer; on the other side, it is became clear that genetic code by itself is not the only player in disease development, as well as in clinical response. Indeed, DNA sequence and genetic factors alone cannot fully explain all the processes implicated in diseases initiation and development; on the contrary, it is now well understood that additional factors are involved in the resulting phenotype. Epigenetic modifications are heritable changes and key actors at the basis of physiological growth and differentiation. The term 'epigenetics' was introduced in 1941 by Conrad Waddington to define a '*branch of biology which studies the causal interactions between genes and their products, which bring the phenotype into being'.* Epigenetic mechanisms are divided in three main groups:

- DNA methylation,
- histone modifications
- non-coding RNAs (ncRNAs).

DNA methylation promotes gene silencing, compacting chromatin or through modification of histones; indeed the CH_3 group at CpG dinucleotides protrudes into the major groove of the double-stranded DNA, recruiting then proteins that favor those events.

Histones may be altered by different modifications, including methylation, acetylation, phosphorylation, ubiquitination. These types of changes affect 15–30 aminoacid N-terminal histone tails impacting chromatin condensation.

ncRNAs are also considerably involved in post-transcriptional modifications. ncRNAs can affect the expression of specific target genes and therefor may interfere with the biological processes in which those genes have a role. This “RNA interference” can be mediated by exogenous RNA molecules, known as small interfering RNAs (siRNAs) or by endogenous RNA-microRNAs (miRNAs).

3. microRNA

MicroRNAs (miRNAs) are a family of small non-coding RNAs (19–25 nucleotides -nts) that can regulate a plethora of biological processes via modulating expression of target genes at the post-transcriptional level [69].

The first miRNA discovered, Lin-4, dates back to 1993 [70]. Lin-4 is involved in development of *C. elegans*, through regulation of expression of the protein lin-14 [70]. Subsequently, many evidences reported existence of a huge number of miRNAs in both invertebrates and vertebrates, and some of them are highly conserved; this suggested that modulation of gene expression via miRNAs is a general and important regulatory mechanism [69]. Currently, according to Mirbase database, which is an archive of microRNA sequences and annotations, 48,885 mature miRNAs in 271 species are known, but, for most of them, function is unclear or unknown (updated to March 2018) [71]. Calin and colleagues published the first data, showing an involvement of miRNAs in cancer, in 2002. They observed a deletion in B-cell chronic lymphocytic leukemia cells, which contains two miRNA genes, miR-15a and miR-16-1, and reported that the majority of clinical chronic lymphocytic leukemia cases have low expression level or deletion [72]. miR-15a and miR-16-1 act as tumor suppressors and induce apoptosis through inhibiting Bcl-2, an anti-apoptotic protein overexpressed in malignant nondividing B-cells and in many solid malignancies [69]. In the last two decades, the research has focused on miRNAs, characterizing their function and mechanism of action to finely regulate expression of target genes. Today, it is well known that miRNAs play a pivotal role in many processes, such as cell growth development, cell cycle, apoptosis and many others. Compelling evidences have established that miRNA expression is dysregulated in human diseases including cancer; miRNAs deregulation may take place via different mechanisms such as deletion or amplification of miRNA genes, abnormal transcriptional control of miRNAs, epigenetic modifications in the miRNA biogenesis machinery (Figure 15) [73].

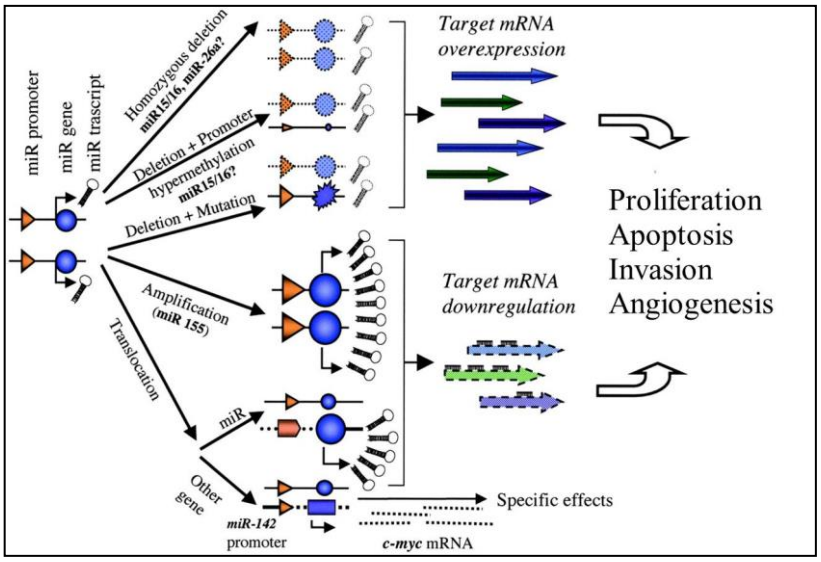

Figure 15. MiRNAs as cancer players: examples of mechanisms, which can lead to deregulation of miRNAs. Figure from Calin AD et al, PNAS 2004

MiRNAs may act as oncogenes or tumor suppressors and, depending on cellular context, a single miRNA may be both of them. Therefore, deregulation of miRNAs can affect the hallmarks of cancer, including sustaining proliferation, evading apoptosis and resisting cell death, promoting invasion and metastasis, and inducing angiogenesis.

3.1. **Biogenesis of miRNAs**

About 70% of miRNAs are located in introns and/or exons, and ~30% are located in intergenic regions [74]. The biogenesis of miRNAs begins with their transcription by RNA polymerase II, or by RNA polymerase III, resulting in a primary transcript, referred to as pri-miRNA, which contains a 33 bp hairpin stem, a terminal loop and a flanking single stranded sequence that can be 1-2 Kb in length [75,76]. Pri-miRNA is then cleaved by Drosha bound by its regulatory subunit DGCR8, to liberate a hairpin structured precursor, or pre-miRNA, of ~60–70 nts in the nucleus [77].

The pre-miRNA from nucleus is then exported to the cytoplasm by Exportin5 (Exp5) associated with its Ran cofactor coupled to GTP. Once in the cytoplasm, Exp5 releases its pre-miRNA cargo; subsequently, the pre-miRNA is cleaved by Dicer to produce a miRNA duplex intermediate of ~22-24 nts. Argonaute (Ago) binds the duplex and incorporates the mature miRNA (single-stranded)

into the Ago-RNA complex, whereas the second strand - the passenger strand or miRNA* - is discarded [78,79].

3.2. **Mechanism of action**

A single miRNA can modulate the expression of hundreds of mRNA targets and a miRNA target may be regulated by multiple miRNAs. A miRNA binds its target through 6-8 nts, which constitute the so-called *seed* sequence, and usually the 5′ region of miRNA contributes more to the specificity and activity in binding targets. miRNAs regulate the target expression by base pairing to sequence motifs in the 3'UTR of mRNAs with perfect or imperfect complementarity [80]. This imperfect base pairing makes miRNAs able to regulate the expression of multiple target genes, transcribed in the same cellular context as the miRNA. Besides this, it has been reported that miRNAs can bind even the 5'UTRs, but the evidence are less [81,82]. Considering the binding between miRNAs and 3'UTRs, miRNAs control their target expression acting through two mechanisms. If the miRNA-mRNA base-pairing is perfect, the mRNA can be endonucleolytically cleaved and degraded; if the miRNA-mRNA base-pairing is not perfect, there will be a block of translation. In both cases, the final result is a down-regulation of expression at the protein level [83].

3.3. **miRNAs and cancer**

The first indication that miRNAs are key player in human disease dates back to 2002, when Calin and colleagues showed that miR-15a/16-1 cluster is frequently deleted in chronic lymphocytic leukemia, implicating these miRNAs as tumor suppressors [72]. After that finding, a huge number of reports were published.

All the tumors analyzed have reported a specific miRNA signature, "*miRNome*", which is peculiar for tumor tissue and is often associated with clinico-pathological features of the tumors. In general, it has been observed that most miRNAs are down-regulated in cancers with respect to the normal

tissue counterparts, as indication of the general loss of differentiation of tumor cells. This is in agreement with studies *in vivo*, which showed that a global depletion of miRNAs by genetic deletion of the miRNA-processing machinery favorites cell transformation and tumorigenesis [84] [85]. This suggests that miRNAs deregulation is not a consequence of tumorigenesis but, rather, it has a causative role in cancer development. Beside a general down-regulation of miRNAs in cancers, diverse miRNAs are up-regulated, and have an oncogenic roles [86]. In general, as previous mentioned, a single miRNA, depending on the cellular context, may have a dual role and be a tumor suppressor or an onco-miR. For example, miR-221 and miR-222 are important in GIST because target the driver oncogene, *KIT*, and, as a consequence, they function as tumor suppressors [87]. However, in other solid tumors, including glioblastoma, prostate, and breast cancer, they also target important tumor suppressors - as PTEN, p27, p57 and TIMP3 - and function as oncogenic miRNAs by suppressing these tumor suppressors

4. Aim

GISTs are rare soft tissue sarcomas, which, however, represents the most common mesenchymal tumor of gastro intestinal tract. GISTs are considered a worldwide paradigm of molecular biology in solid tumors [89]. With the application of high throughput technologies into basic and translational research, molecular biology of GISTs has been progressively deepened and the GIST paradigm has been proven to be more complex than expected, due to an extensive molecular heterogeneity within all GIST tumors, and the identification of different subsets often characterized by peculiar genotype and phenotype [90]. Besides the importance of genomic alterations, epigenetics, including miRNA and methylation deregulation, could be a key player in driving tumorigenesis, as well as in clinical response and drug resistance. To date, it is well established that *KIT/PDGFRA* mutant and *KIT/PDGFRA* WT GIST patients are deeply different at both pathogenesis and molecular level. However, reports regarding miRNAs expression in GISTs are still a small number and often do not take into account tumor genotype and GIST molecular heterogeneity. For the above mentioned reasons, to identify novel potential biomarkers of GIST pathogenesis, I) the first aim of the PhD project was to investigate and characterize the differences in miRNAs expression levels, comparing *KIT/PDGFRA* mutant and *KIT/PDGFRA* WT GISTs.

II) Secondly, we aimed to characterize novel mechanisms of pharmacological resistance to a PI3KCA inhibitor in trial at Sant'Orsola Malpighi Hospital for GIST patients who previously failed imatinib and sunitinib. Indeed, all the treatment lines so far approved in GISTs are TKIs showing a similar mechanism of action, but the majority of patients experience disease progression. Therefore, it is extremely important to identify alternative therapeutic options with different mechanisms.

5. Fist aim: identification of potential novel biomarkers correlated with GIST pathogenesis

As already previously mentioned, little is known about differences in miRNA expression between *KIT/PDGFRA* mutant and *KIT/PDGFRA* WT GIST. In view of these considerations, we integrated multiple expression profiles of miRNA and mRNA to construct a miRNA-mRNA regulatory network in *KIT/PDGFRA* WT GIST patients. Subsequently we performed a series of functional *in vitro* studies to deepen the potential epigenetic network.

Part of the data reported below are reproduced from Epigenomics. 2016 Oct;8(10):1347-1366, with permission of Future Medicine Ltd.

5.1. Materials and Methods

Patients - To identify a miRNAs signature in GISTs, we profiled the expression of a cohort of GIST patients - discovery set - which included 9 *KIT/PDGFRA* mutant and 4 *KIT/PDGFRA* WT cases. A second cohort of patients, designed as validation set, was recruited to validate the capacity of specific miRNA to discriminate between *KIT/PDGFRA* mutants and *KIT/PDGFRA* WT disease. In the *KIT/PDGFRA* WT group, the SDH-*deficient* status was assessed by both IHC negativity for SDHB protein and genome sequencing of all four SDH subunits. The validation set consisted of 27 GISTs, of which 16 were not overlapping with the discovery cohort and included 7 *KIT/PDGFRA* WT and 20 *KIT/PDGFRA* mutant GIST cases (13 *KIT/PDGFRA* mutant and 3 *KIT/PDGFRA* WT cases not overlapping with the discovery set) (reproduced from Epigenomics, 2016 Oct;8(10):1347-1366). Subsequently, we were able to expand the validation set from 27 to 37 GIST cases (referred to as validation set II). The miRNAs, which maintained the statistical significance in the validation set, were finally tested in the validation set II.

RNA extraction - Total RNA (including miRNAs) was extracted from liquid nitrogen snap-frozen tumor samples using Qiagen miRNeasy Mini Kit (Qiagen, Hilden, Germany) according to manufacturer's instructions.

Genome-wide miRNA expression profiling - miRNAs expression was investigated using the Agilent Human miRNA microarray v.2 (#G4470B, Agilent Technologies, CA, USA). This microarray consists of 60-mer DNA probes synthesized in situ and contains 15,000 features, which represent 723 human miRNAs, sourced from the Sanger miRBase database (Release 10.1). Microarray results were analyzed by using the GeneSpring GX v.12 software (Agilent Technologies). Data transformation was applied to set all the negative raw values at 1.0, followed by a quantile normalization and a log2 transformation. Filters on gene expression were used to keep only the miRNAs expressed in at least one sample. Then, samples were grouped according to the presence or not *KIT/PDGFRA* mutations. Differentially expressed miRNAs were identified by a 2 fold-change filter followed by a moderated t-test, with $p<0.05$ by means of a moderated t-test with Benjamini-Hochberg correction. A principal component analysis (PCA) was applied to compress the multidimensional miRNAs expression data to three dimensions while maintaining the variance. The data have been submitted to Gene Expression Omnibus - GEO - (Entry series number: Submitted E-MTAB-4490) following the requirements of minimum information about a microarray experiment (MIAME).

Gene expression - Quality-controlled RNA was labeled according to Affimetrix expression technical manual before hybridization to HGU133 Plus 2.0 array following manufacturer's instruction. Gene expression data were quantified by the robust multi-array analysis (rma) algorithm. Unsupervised analyses were applied to a subset of genes whose standard deviation varied at least of 0.5. For hierarchical agglomerative clustering, Pearson's correlation coefficient and average linkage were respectively used as distance and linkage methods in DNA-Chip Analyzer (dChip) software. Differentially expressed genes were selected through supervised techniques using

SAM (Significance Analysis of Microarrays) package in R, with a two class unpaired (*KIT/PDGFRA* WT and mutated samples) T-statistic and permutated 1,000 times. Only genes with 0% q-value cut-off level were considered to be differentially expressed and selected for subsequent analysis. The data have been submitted to GEO (Entry series number: GSE20708), following the requirements of minimum information about a microarray experiment (MIAME).

Identification of validated mRNA/miRNA targets - The validated targets were obtained from the miRTarBase database (http://microrna.sanger.ac.uk/) that contains miRNA–target interactions (MTIs) with experimental support (2DGE, immunoprecipitation, Luciferase reporter assay, Mass spectrometry, Microarray, qRT-PCR, Western blot, Next Generation Sequencing (NGS), ELISA, IHC. Using these information, miRNA and mRNA arrays were analyzed to highlight pairs of mRNA/miRNA that were discordant (UP *vs* DOWN and viceversa). Potential miRNA-mRNA interactions and miRNA/mRNA expression profiles were used to construct functional interaction networks using Ingenuity Pathway Analysis (IPA, Ingenuity Systems, CA, USA).

Functional annotation, GO and pathway analysis - IPA was performed to identify the molecular pathways and functional groupings. Gene interaction networks, bio-functions and pathway analysis were generated using differentially expressed genes (DEGs) into known functions, pathways, and networks primarily based on human and rodent studies. The DEGs were organized in Gene Ontology Bio-Functions and Regulatory Effect Networks available from the Ingenuity database. The significance was set at a p-value of 0.05. IPA pathway explorer and miRNA/mRNA interactions were used to find a link between deregulated genes and deregulated miRNAs in array experiments.

Validation of miRNA array - miRNA array expression profiles of selected miRNAs were evaluated by TaqMan miRNAs assays (Applied Biosystems, CA, USA), and RNU48 and RNU44 were used as internal normalizer reference. The analysis was conducted according to standard TaqMan miRNAs assay protocol and run on a 7900 HT Fast Real-Time PCR System (Applied Biosystems).

Each sample was analysed in triplicate. Quantitative analysis was performed by the ΔΔCt method. The miRNAs chosen for validation included the top up- and down- regulated miRNA; furthermore, we selected miRNAs whose expression differed significantly and target genes known to be interesting for GISTs and novel genes for GISTs as well.

Western blotting - IGF1R, CD44 and CDK6 expressions were analyzed in 7 *KIT/PDGFRA* WT-SDH-*deficient* and 11 *KIT/PDGFRA* mutant cases. Frozen tumor samples were diced in ice-cold lysis buffer (1% NP40, 50 mM Tris-HCl, pH 8.0, 100 mM sodium fluoride, 30 mM sodium pyrophosphate, 2 mM sodium molybdate, 5 mM EDTA, 2 mM sodium orthovanadate) on dry ice and homogenized; the cell lysate was then rocked overnight at 4°C. Lysates were cleared by centrifugation at 14,000 rpm for 30 min at 4°C, and lysate protein concentrations were determined using a Bradford method (Bio-Rad, CA, USA). Lysates were separated by gel electrophoresis using NuPAGE® 4–12% Bis-Tris gels (Invitrogen–Thermo Fisher Scientific, MA, USA) and blotted to nitrocellulose membranes. The hybridization signals were detected by chemiluminescence (ECL, Invitrogen, Thermo Fisher Scientific) and captured using ChemiDOC (Bio-Rad). Primary antibodies were IGF1R (Cell Signaling Technology,Inc., MA, USA; #3027), CDK6 (clone 8H4, Sigma-Aldrich, MO, USA), CD44 (Sigma-Aldrich) and β-actin (clone AC15, Sigma-Aldrich).

Cell cultures - GIST48 and GIST882 cell lines were kindly provided by Dr Fletcher (Brigham and Women's Hospital, Harvard Medical School, Boston, MA, USA). GIST48 was established from a patient that had progressed - after an initial clinical response - during imatinib therapy; this cell line is characterized by a primary, homozygous *KIT* exon 11 mutation (p.V560D) and a secondary, heterozygous *KIT* exon 17 mutation (p.D820A). Cells were cultured in IMDM (Gibco, Thermo Fisher Scientific), supplemented with 15% fetal bovine serum (FBS) and 1 mM L-Glutamine (Invitrogen). GIST882 was established from an untreated, human primary tumor harboring a homozygous imatinib sensitive mutation in *KIT* exon 13 (p.K642E). Cells were maintained in RPMI-1640 (Gibco), supplemented with 15% FBS and 1 mM L-Glu (Invitrogen). All experiments

were performed in newly thawed cell lines. GIST lines were routinely monitored by Sanger sequencing to confirm their *KIT* mutational status and to exclude additional secondary mutations in *KIT*.

Luciferase assay - The pMirNanoGlo dual-Luciferase vector, containing both the Renilla luciferase gene and the Firefly luciferase gene, was purchased from Promega (Promega, Madison, WI, USA) (Figure 16). pMirNanoGlo, containing a 2,051 bp IGF1R 3'UTR region, was generated as follow. The IGF1R 3'UTR region, containing all the miR-139-5p (positions 2,486-2,493 and 3,742-3,748) and

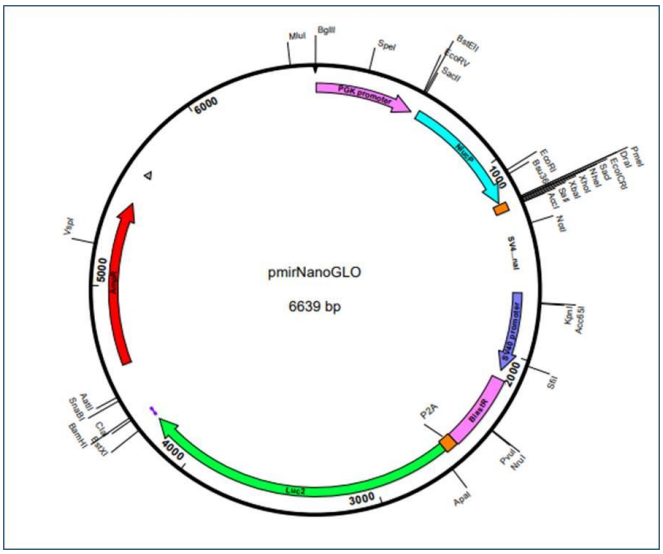

Figure 16. Circular plasmid map of pMirNanoGlo

miR-455-5p (position 3782-3788 and 4198-4204) binding sites, was amplified from human genomic DNA, introducing the NheI and XhoI restriction sites (Figure 17). First, this amplicon was cloned into a pGEM® vector using the pGEM-T Easy Vector Systems (Promega) according to the manufacturer's instructions. The amplified DNA fragments was then subcloned into the pMirNanoGlo vector, downstream of the Renilla luciferase stop coding region. All constructs were sequence-verified prior to be used. Primers are reported in table 1.

Table 1: List of primers

Primer	Sequence	Tmelting	Aim
IGF1R 2051 fwd	AGGCTAGCAGGAGTAAGAACAAAGCTGGGA	58°C	PCR
IGF1R 2051 rev	ATCTCGAGTGGGGTGGTCTGGGTCTT	58°C	PCR
IGF1R 2051 fwd	CGGCTTTTTTGCTGGTCA	43°C	Sanger
IGF1R 2051 rev	GCGTGGATGAGGTTACCAG	48°C	Sanger
IGF1R 2051 fwd	GGCAATTCCAGCCTAAGTGA	47°C	Sanger
IGF1R 2051 rev	CAGTACACACCAGCTCCTGCT	51°C	Sanger

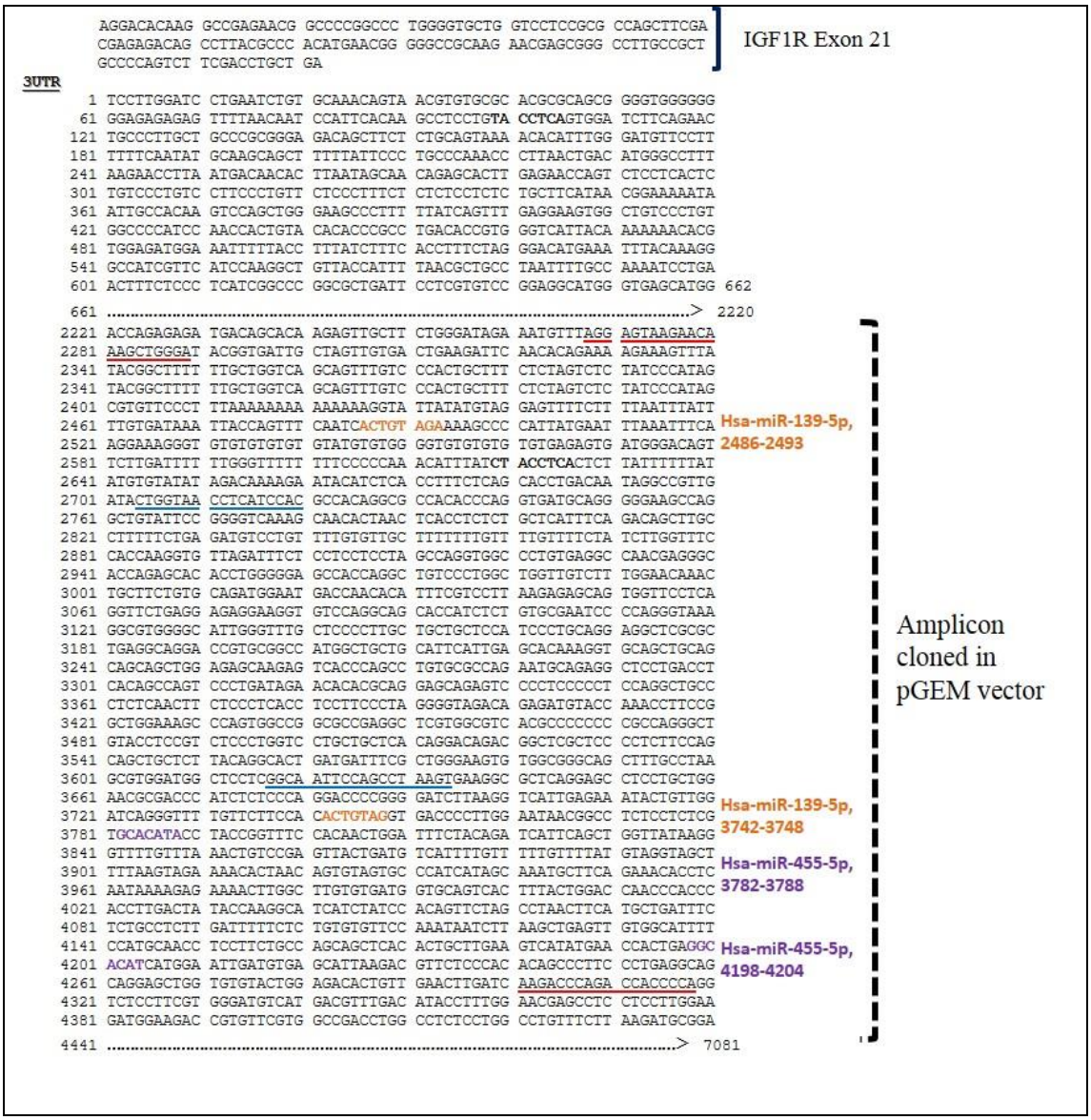

Figure 17. IGF1R 3'UTR cloned in pGEM and pMiRNanoGlo. In red are highlighted primers used to amplify, whereas in blue are highlighted primers used to sequence the amplicon

GIST882 and GIST48 cells were transfected using Amaxa Nucleofector II device (Lonza AG, Switzerland). In brief, 1×10^6 cells were resuspended in 100 µl Ingenio Electroporation solution (Mirus Bio, LLC; WI, USA) and mixed with 100 pmol of miRNA mimic (Mirvana miRNA mimic, Ambion, Thermo Fisher Scientific). Cells were then electroporated using the program T-20, and seeded in triplicate in a 96 wells plate. After 24h, Firefly and Renilla luciferase activities were quantified using the Dual luciferase system (Promega) through an EnSpire Multimode Plate Reader

(Perkin Elmer, Inc, MA USA). Renilla luciferase expression was normalized on the Firefly luciferase expression. Independent triplicate experiments were performed for each plasmid construct.

Site-Directed Mutagenesis - To evaluate the contribution of each of the two binding sites, we generated different constructs in which we individually deleted the seed sequences. To do that, we used the Phusion Site-Directed Mutagenesis Kit (Thermo Fisher Scientific); deletions were created by designing primers that border the deleted area on both sides (see figure 18 for a schematic presentation).

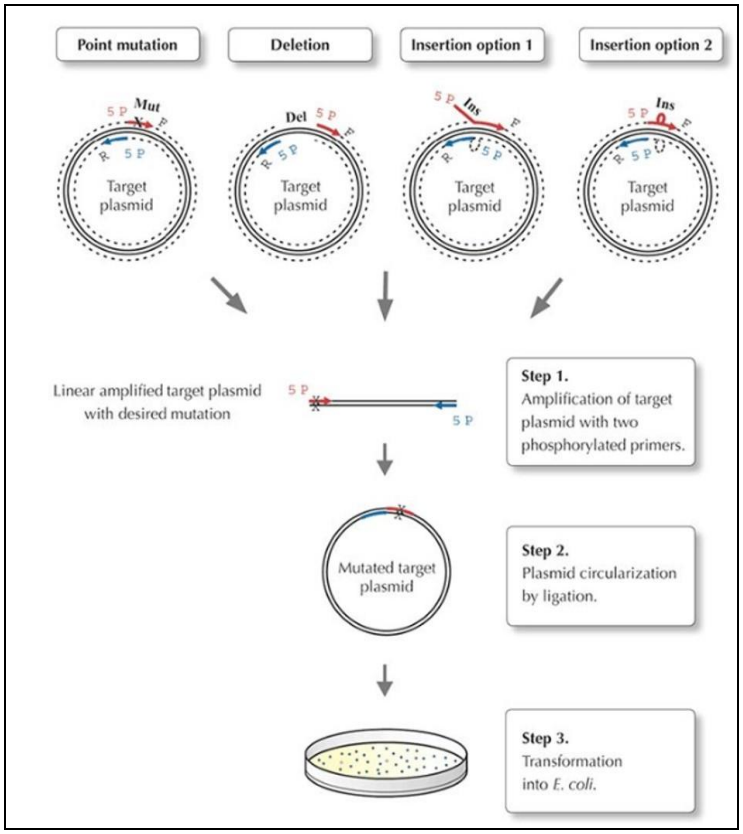

Figure 18. The Phusion Site-Directed Mutagenesis protocol

Transient transfection - Anti-miR-139-5p and anti-miR-455-5p were purchased from Ambion. Anti-miR-139-5p: UCUACAGUGCACGUGUCUCCAGU (#AM11749), anti-miR-455-5p: UAUGUGCCUUUGGACUACAUCG (#AM10529).

Anti-miR-139-5p and anti-miR-455-5p were transfected in GIST48 and GIST882 using RNAiMAX Lipofectamine (Invitrogen). A random miRNAs inhibitor pool was used as negative control. The

miRVANA microRNA inhibitors are single-stranded, chemically enhanced oligonucleotides designed to inhibit the endogenous miRNAs. Cells were transfected with 100 nM of the indicated oligonucleotide and we evaluated cell migration, apoptosis, cell cycle and proteins' expression.

Analysis of apoptosis - Apoptosis was assayed using the Guava Nexin kit (4500-0450, Merck Millipore, MA, USA) and the Guava PCA system (Guava Technologies, CA; USA). Cells were harvested 24 and 48 h after transfection treatment. Cells were then plated into a round bottom 96 well plate in triplicate, treated with 100 µl of Guava Nexin reagent according to the manufacturer's protocol, and incubated at room temperature for 20 min in dark. Samples were then analyzed using the Guava PCA system.

Cell migration assay - Migration of GIST cells treated with 100 nM miR inhibitor was investigated using Radius™ 24-Wells Cell Migration Assay (Cell Biolabs, CA, USA). In particular, $3x10^5$ cells were plated 24h before treatment. Then, cells were treated with 100 nM of anti-miR-139-5p/455-5p and were left to grow out until up to 96h and pictures were taken every 24 hours to monitor the cells migration.

Invasion assay - Invasion of GIST cells treated with miR inhibitor at 100 nM was investigated using CytoSelect™ 24-Wells Cell Migration and Invasion Assay (8 µm, Colorimetric Format) (Cell Biolabs). Cell suspensions containing $1x10^6$ cells/ml in serum free media were prepared (treated or not); 500 µL of media containing 10% FBS was added in the lower well of the migration plate. Then, 300 µL of the cell suspension solution was added to the inside of each insert and incubated 24 hours at 37°C. After that, the small chamber were collected and fixed by Cell Stain Solution. Each insert was then washed with 200 µL of Extraction Solution per well, then incubated 10 mins on an orbital shaker. Finally, 100 µL were transferred from each sample to a 96-wells plate and OD 560 nm measured.

5.2. **Results**

Differential miRNAs expression between KIT/PDGFRA mutant GISTs vs KIT/PDGFRA WT GISTs– miRNA profiling - The 3D PCA plot, distributing the samples into three dimensional space based on variance in miRNAs expression, clearly indicates that *KIT/PDGFRA* WT SDH-*deficient* GISTs (denoted thereafter as *KIT/PDGFRA* WT GISTs) clustered together in a distinctive pattern compared to mutant GISTs (Figure 19A). The array highlighted a total of 56 deregulated miRNAs out of the 723 analyzed (Figure 19B).

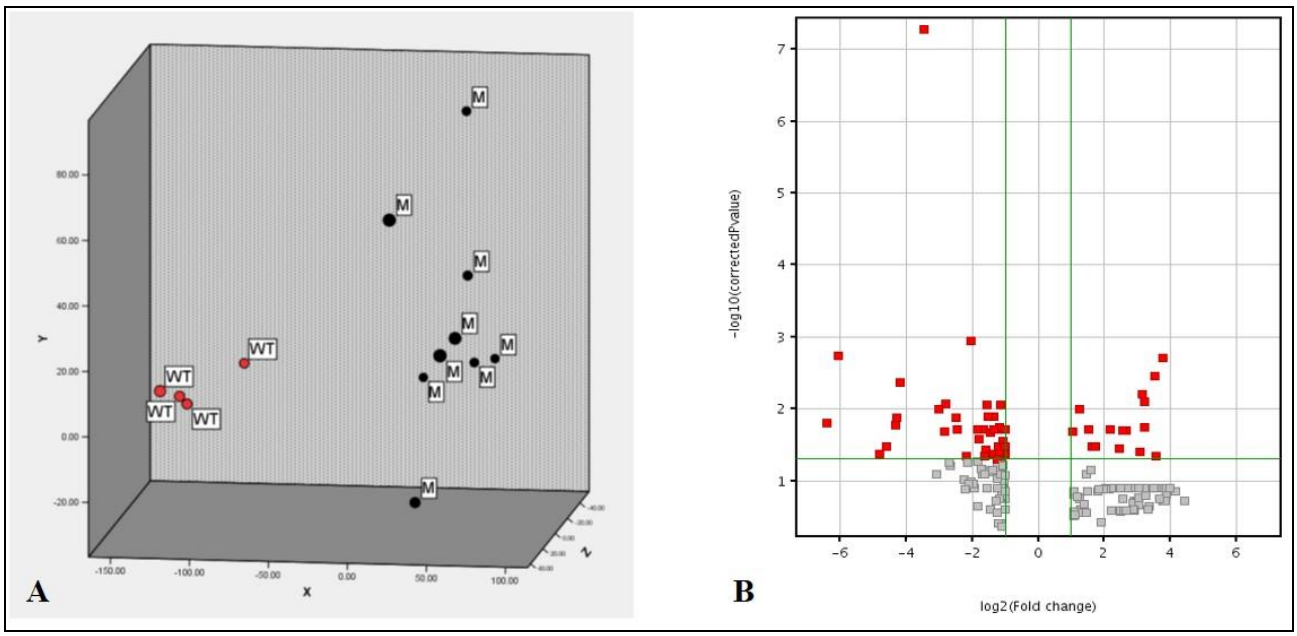

Figure 19. **A)** PCA of the miRNA profile in *KIT/PDGFRA* mutant GISTs (M) compared to *KIT/PDGFRA* WT GISTs (WT). Red dot represent WT GISTs, while black ones represent *KIT* mutant (small) and PDGFRA mutant GIST (big). **B)** miRNAs modulated in *KIT/PDGFRA* mutant GISTs compared to *KIT/PDGFRA* WT GISTs. Volcano plot depicting the 56 statistically significant (fold change ≥ 2 and a $P < 0.05$) deregulated miRNAs (red plot) in *KIT/PDGFRA* mutant GISTs compared to WT GISTs. The gray plot represent miRNAs with no significant expression changes

In particular, the expression of 16 miRNAs was up-regulated and 40 miRNAs were down-regulated in *KIT/PDGFRA* mutant GISTs compared to *KIT/PDGFRA* WT GISTs. All the differentially expressed miRNAs are reported in Table 2.

Table 2. miRNAs found to be significantly deregulated in *KIT/PDGFRA* mutant GISTs compared to *KIT/PDGFRA* WT GISTs.

miRNA name	**Regulation**	**Absolute Fold change**	**Corrected *P*-value**
hsa-miR-330-3p	Up-regulated	13,47	0,0019
hsa-miR-886-3p	Up-regulated	11,49	0,0034

hsa-miR-455-5p	Up-regulated	8,88	0,0061
hsa-miR-455-3p	Up-regulated	9,15	0,0077
has-let-7b	Up-regulated	2,37	0,0099
hsa-miR-335*	Up-regulated	9,26	0,018
hsa-miR-139-5p	Up-regulated	6,28	0,019
hsa-miR-148°	Up-regulated	5,80	0,019
hsa-miR-193b*	Up-regulated	4,54	0,019
hsa-miR-193b	Up-regulated	2,82	0,019
has-let-7c	Up-regulated	2,03	0,020
hsa-miR-497*	Up-regulated	3,29	0,033
hsa-miR-152	Up-regulated	3,02	0,033
hsa-miR-195*	Up-regulated	5,38	0,034
hsa-miR-199b-5p	Up-regulated	8,32	0,038
hsa-miR-487b	Up-regulated	11,76	0,045
hsa-miR-129-1-3p [#]	Down-regulated	11,13	$5{,}12 \times 10^{-8}$
has-miR-491-5p	Down-regulated	4,16	0,0011
has-miR-129-5p	Down-regulated	67,11	0,0018
has-miR-450a	Down-regulated	18,54	0,0041
hsa-miR-424	Down-regulated	7,16	0,0082
*hsa-miR-214**	Down-regulated	2,96	0,0086
hsa-miR-151-3p	Down-regulated	2,24	0,0086
has-miR-876-5p	Down-regulated	8,24	0,0099
hsa-miR-542-3p	Down-regulated	19,97	0,013
hsa-miR-584	Down-regulated	5,66	0,013
hsa-miR-328	Down-regulated	2,90	0,013
hsa-miR-769-5p	Down-regulated	2,57	0,013
hsa-miR-129-2-3p [§]	Down-regulated	87,08	0,015
hsa-miR-542-5p	Down-regulated	20,57	0,016
hsa-miR-590-5p	Down-regulated	2,27	0,017
hsa-miR-876-3p	Down-regulated	5,63	0,019
hsa-miR-34b*	Down-regulated	3,57	0,019
hsa-miR-326	Down-regulated	3,22	0,019
hsa-miR-1237	Down-regulated	2,57	0,019
hsa-miR-214	Down-regulated	2,55	0,019
hsa-miR-374b	Down-regulated	2,39	0,019
hsa-miR-30e*	Down-regulated	2,05	0,019
hsa-miR-199a-5p	Down-regulated	2,03	0,019
hsa-miR-338-3p	Down-regulated	7,18	0,020
hsa-miR-933	Down-regulated	2,81	0,021
hsa-miR-186	Down-regulated	3,53	0,026
hsa-miR-28-5p	Down-regulated	2,11	0,027
hsa-miR-873	Down-regulated	24,66	0,033
hsa-miR-361-3p	Down-regulated	2,36	0,033
hsa-miR-1225-3p	Down-regulated	2,05	0,033
hsa-miR-191*	Down-regulated	2,08	0,034
hsa-miR-34a	Down-regulated	2,37	0,036

hsa-miR-551b	Down-regulated	28,58	0,041
hsa-miR-490-5p	Down-regulated	2,56	0,041
hsa-miR-197	Down-regulated	2,27	0,041
hsa-miR-425*	Down-regulated	2,06	0,041
hsa-miR-101*	Down-regulated	3,11	0,044
hsa-miR-490-3p	Down-regulated	4,62	0,045
hsa-miR-30c-1*	Down-regulated	2,41	0,050
hsa-miR-15a	Down-regulated	2,18	0,050
Previously: # hsa-miR-129*; § has-miR-129-3p In Italic are highlighted miRNA selected for validation.			

Hierarchical clustering of all samples separated *KIT/PDGFRA* mutant GIST and *KIT/PDGFRA* WT GISTs into two distinct clusters (Figure 20), confirming the prior PCA results.

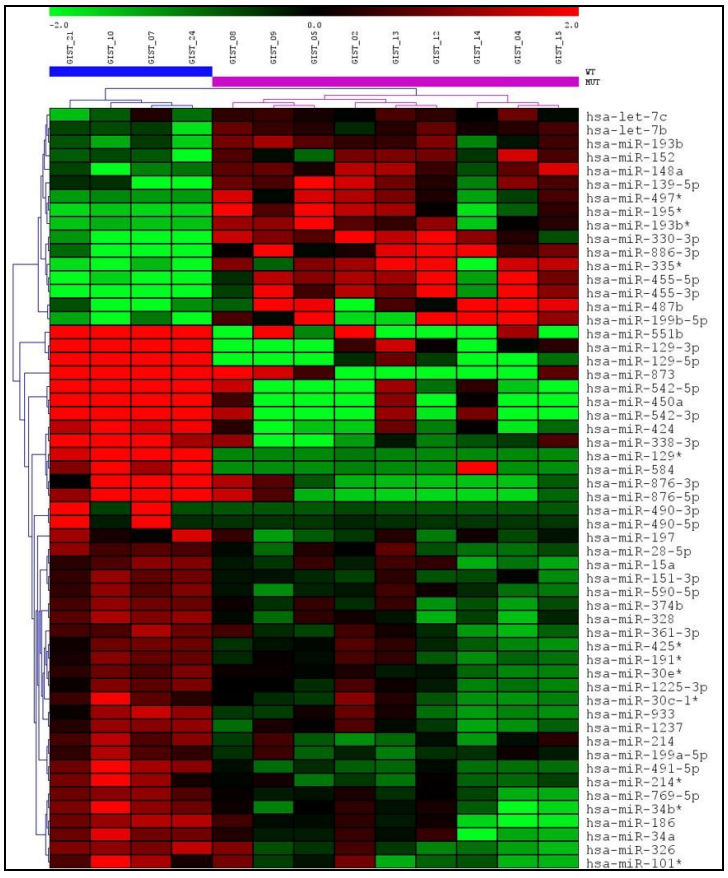

Figure 20. miRNA hierarchical clustering. The miRNAs identified as differentially expressed between *KIT/PDGFRA* mutant GISTs and *KIT/PDGFRA* WT GISTs were selected as markers for unsupervised hierarchical clustering.

Different mRNA expression between KIT/PDGFRA mutant GISTs vs KIT/PDGFRA WT GISTs – mRNA profiling - A comparative analysis between *KIT/PDGFRA* mutant GISTs *vs KIT/PDGFRA* WT GISTs revealed 235 differentially expressed genes with a false discovery rate of 0. In particular

123 genes were down-regulated (fold range: -0.7 to -5.5; Table 3) while 112 genes were up-regulated (fold range: 0.98 to 7.10; Table 3) (Figure 21A).

Table 3. The most deregulated mRNAs in *KIT/PDGFRA* mutant GISTs compared to WT GISTs.

Down-expression			**Over-expression**	
Gene	**fold change**		**Gene**	**fold change**
FBXL16	-5,058		SCG5	7,163
IGF1R	-4,934		LY6H	5,969
42074	-4,864		PRTFDC1	5,320
CRLF1	-4,418		TNFRSF19	5,043
LHX2	-4,099		FAM19A1	4,996
ASRGL1	-4,00		KCNT2	4,722
DNER	-3,936		IGDCC4	4,675
KIRREL3	-3,927		CFH	4,389
FGF4	-3,829		NIPAL2	4,300
GRIA1	-3,700		TSPYL5	4,285
CBLN2	-3,641		PIK3CG	4,213
FAM84B	-3,565		SPATA18	4,125
PPP2R2B	-3,485		PLBD1	4,050
CYP3A7	-3,462		RBP1	4,010
CDH2	-3,399		TMEM150C	3,944
CXADR	-3,376		DNAJC15	3,898
DPYSL4	-3,335		ME1	3,886
ISM1	-3,277		PDZD2	3,872
GLRB	-3,252		RHOBTB3	3,730
ELAVL3	-3,081		BASP1	3,707
PHLDA2	-3,041		CEP41	3,691
FOXO6	-3,035		SLC2A10	3,637
ADAMTS19	-2,952		ACKR3	3,628
ZNF804A	-2,926		KCNE4	3,498
MBNL1-AS1	-2,838		PTPLAD2	3,458
SV2C	-2,812		SERPINB9	3,423
BMP8B	-2,809		PLA2G16	3,415
ADARB1	-2,750		SERP2	3,413
COLGALT2	-2,699		LOC728613	3,400
C1orf145	-2,684		SOCS2	3,400
KCND3	-2,611		IQCA1	3,387
EFNA2	-2,589		CPQ	3,353
ERBB3	-2,588		PTER	3,292
NPNT	-2,535		SQRDL	3,253
PRDM16	-2,533		C16orf89	3,251

DAPK1	-2,435		IL1R1	3,240
EVA1A	-2,433		CLIC2	3,211
TBX21	-2,429		EPHX2	3,152
CD44	-2,401		CAPS2	3,105
NRCAM	-2,390		ALDH7A1	3,048
PDE4DIP	-2,383		FBXO4	3,046
P4HA3	-2,382		MINA	3,045
ARSB	-2,343		C9orf64	3,042
GPD2	-2,309		SERPINB1	3,023
SLC1A1	-2,276		TMEM173	3,020
FAM46C	-2,249		CPNE8	3,006
TAPBPL	-2,236		CYSLTR1	3,004
TMEFF1	-2,227		ZNF423	2,977
FAM43A	-2,226		RANGRF	2,932
KIF21B	-2,224		COX7A1	2,926
DAAM1	-2,217		GPX7	2,895
EFR3B	-2,213		C8orf88	2,861
USP53	-2,206		PARVA	2,854
TMEM59L	-2,179		WWTR1	2,846
ARX	-2,111		CREB3L1	2,773
MAGI2-AS3	-2,103		PLIN2	2,715
SLC4A7	-2,081		MCTP2	2,714
TARBP1	-2,070		SLC9A9	2,683
RIMBP2	-2,050		PDLIM4	2,681
TESK2	-2,012		S100A13	2,665
PHKA1	-2,009		CHCHD10	2,661
LSR	-2,005		TP73-AS1	2,622
FGFBP3	-1,994		PHLDA1	2,568
LRCH2	-1,869		HTATIP2	2,544
42066	-1,866		ZNF22	2,509
NRG3	-1,843		FMOD	2,484
42068	-1,841		FAM213A	2,464
FAM3C	-1,788		SELENBP1	2,417
CDH23	-1,787		LOC728819	2,416
TMEM30A	-1,783		CDIP1	2,365
PPM1B	-1,762		FAM50B	2,357
ARHGAP5	-1,740		MXRA7	2,333
DNAH12	-1,720		RNF135	2,332
DDAH1	-1,711		IMPACT	2,269
ENAM	-1,640		GYPC	2,199
DNAJB4	-1,627		CD40	2,106
TTLL7	-1,614		PBX3	2,067
EGFL7	-1,606		GLRX	2,066

NPC2	-1,597		DENND1B	2,020
MPP5	-1,580		CYB561	2,005
USP33	-1,530		NPEPL1	2,002
HEXA	-1,520		SETD9	2,000
SPPL2A	-1,506		TMEM220	1,997
ARRB1	-1,478		ZNF239	1,984
GPR63	-1,448		MAPK10	1,983
TMEM74B	-1,414		OCIAD2	1,975
SLC25A48	-1,411		PHF19	1,970
GALT	-1,405		GSE1	1,968
C1orf21	-1,384		ZNF621	1,964
ST7	-1,339		N6AMT2	1,963
EPN2	-1,338		CYP27A1	1,894
TMEM14C	-1,323		RHOD	1,889
PATZ1	-1,267		TTC12	1,888
GRN	-1,250		ACAA2	1,881
NDUFAF4	-1,241		LOC730102	1,855
NT5E	-1,236		C8orf48	1,854
NENF	-1,221		CLMP	1,786
SPEF2	-1,210		LOC100049716	1,757
ERP29	-1,206		EPHX1	1,750
DENND2C	-1,188		RFESD	1,710
CPEB3	-1,179		MYD88	1,707
ATP6V1D	-1,162		LOC101927027	1,691
RECK	-1,160		ENKD1	1,677
SIRT2	-1,159		DDB2	1,665
MBNL1	-1,126		MAP1LC3A	1,611
AKT3	-1,095		CTSF	1,5717
EFNA3	-1,075		HAUS7	1,530
ECI2	-1,060		PRR5	1,424
TMEM14B	-1,060		PPM1M	1,370
PTP4A1	-1,033		VILL	1,316
NCSTN	-1,025		TPST1	1,094
HAGHL	-1,023		ATG12	0,981
SIPA1L1	-1,004			
LUZP1	-0,999			
ABL2	-0,991			
ZFYVE1	-0,991			
KIAA1522	-0,950			
SMARCD3	-0,846			
ELFN1	-0,824			
CPNE9	-0,760			
APC2	-0,758			

RIMBP3	-0,735			
SDCBP2-AS1	-0,734			
False discovery rate=0				

In the figure 21B the most deregulated genes are summarized. Several markers were validated by qRT-PCR and previously reported [91]. The validated genes, which included IGF1R, LHX2, and KIRREL3, confirmed a good correlation with the differential expression observed in the array.

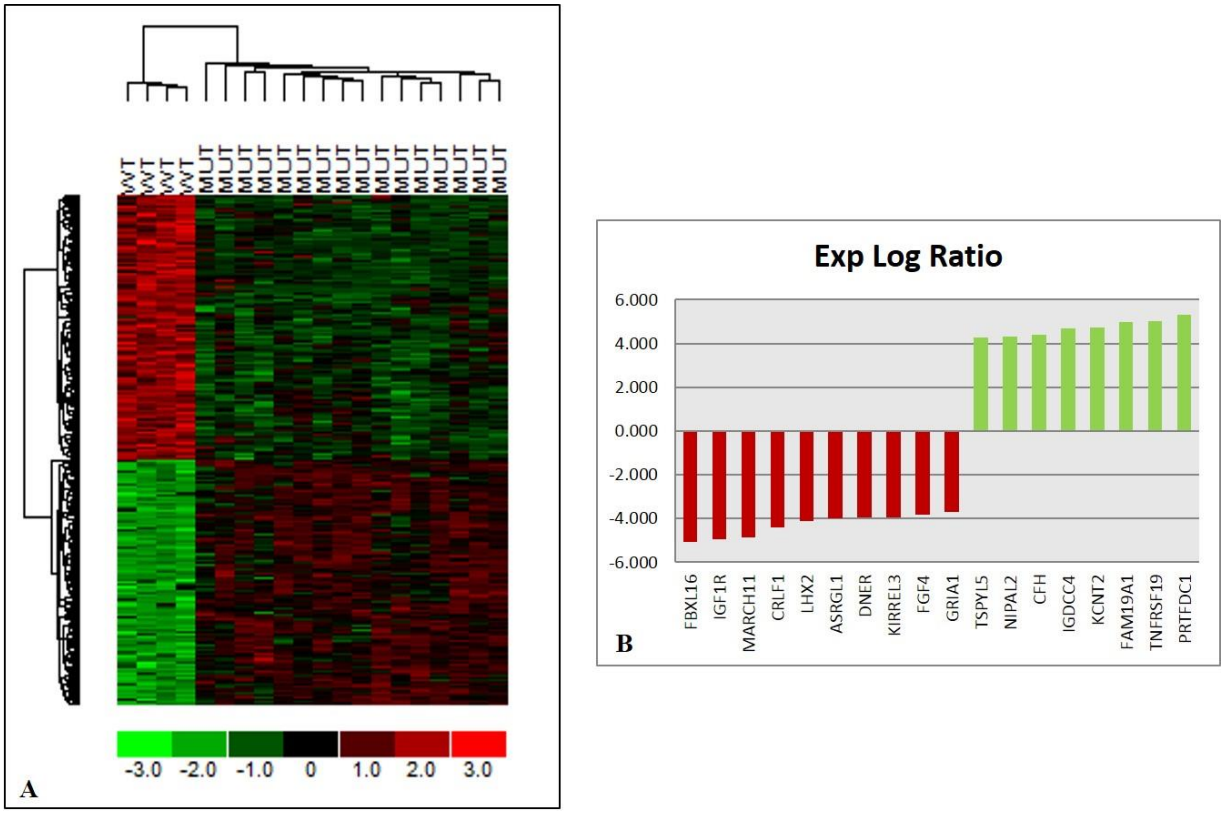

Figure 21. A) mRNA hierarchical clustering. The mRNA identified as differentially expressed between KIT/PDGFRA mutant GISTs and KIT/PDGFRA WT GISTs were selected as markers for unsupervised hierarchical clustering. **B)** The top scored deregulated genes.

Differentially expressed genes between KIT/PDGFRA mutant GISTs vs KIT/PDGFRA WT GISTs - bioinformatics analysis - All genes transcripts underwent GO term classification, which included Biological Process, Cellular Component and Molecular Function, and gene term enrichment analysis. Results showed a significant clustering of these differentially expressed genes. Genes were mainly involved in developmental processes and, to a less extent, in metabolic and cellular processes (Figure 22).

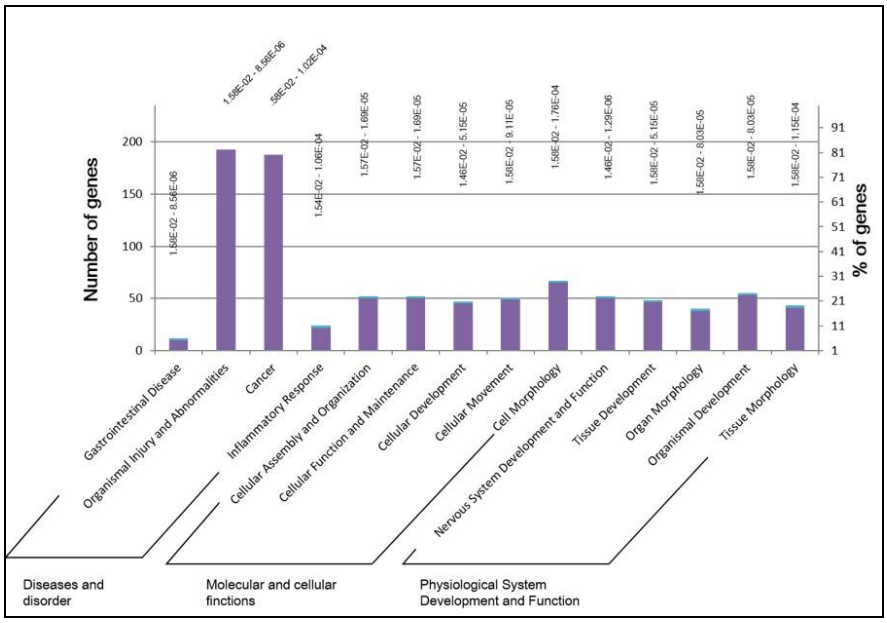

Figure 22. GO functional enrichment analysis of up- and down-regulated genes.

miRNA and mRNA arrays correlation - To construct miRNA-DEGs networks, we downloaded the experimentally verified associations between human miRNAs and their targets from miRTarBase, which has accumulated more than 400,000 miRNA-target interactions, collected by manually surveying pertinent literature after systematic data mining of the text. This dataset contained miRNA-target interactions consisting of 963 miRNAs and 12,518 mRNAs. The results are reported in table 4. Among 56 deregulated miRNAs retrieved by our data, 44 had verified associations with their targets. Among the targets with an inverse expression compared to the miRNA expression, we were able to identify 17 mRNA-miRNA networks (Table 4). *miRNA validation* - Among the 44 miRNAs, 29 were validated in the validation set. In addition, to avoid missing significant results, we predict the miRNA targets using different in silico software, including miRTarBase, DianaLab, MiRDB, microRNA.org, PicTAR, PITA, MiRanda, and a target had to be predicted by at least 5 software to be considered as true. In particular, we chose 9 up-regulated and 21 down-regulated miRNAs (Table 2, reported in italic). Among the up-regulated set of data, 5 miRNAs (139-5p P=0.0109; 148a P=0.0040; 193-3p P=0.0013; 330-3p P=0.0003; 455-5p P=0.0109) maintained statistical significance, whereas let-7b reached borderline significance (P=0.054). Among the down-regulated, 3 miRNAs were confirmed as significantly deregulated (miR-129-1-3p, P=0.03; miR-

129-2-3p, P=0.03; miR-876-5p, P=0.0176). Taking into account the significantly altered miRNAs, miRNA-mRNA interaction network analysis through IPA returned three direct interactions: IGF1R → miR-139-5p/miR-455-5p/let-7b, CDK6 → miR-139-5p, CDK6 → let-7b and CD44 → miR-330 (Figure 23).

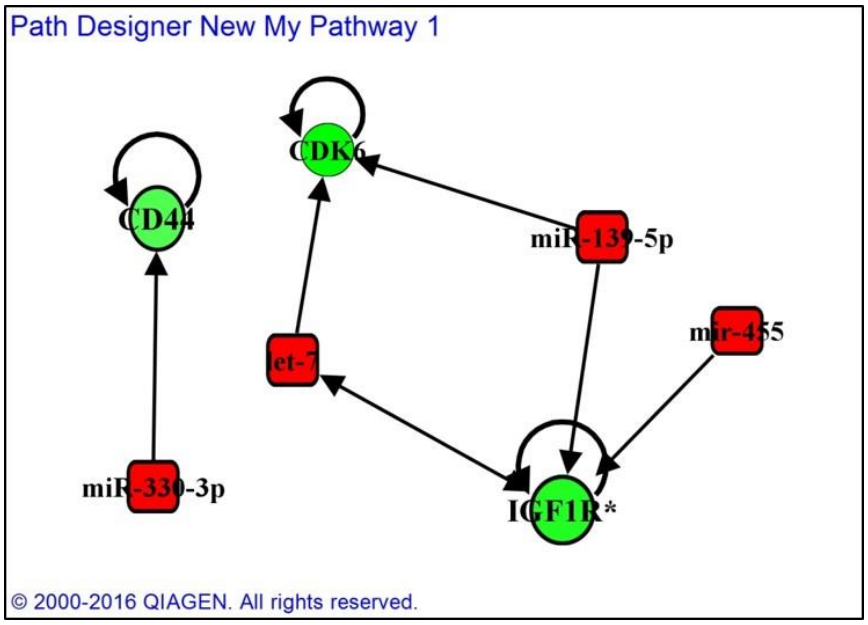

Figure 23. Integrated miRNA-mRNA regulatory networks by IPA. The red rectangle represents miRNA, while the green circle indicated target genes. Arrows denote direct interactions between a miRNA and its target

Analysis of the putative binding sequences at 3'UTR target genes - Taking into account that miRNAs bind the mRNA at their 3'UTR, we further analyzed the putative target sequence at the 3'UTRs of IGF1R, CDK6 and CD44 genes, through TargetScan in silico program (http://www.targetscan.org).

Table 4. Summary of mRNA-miRNA regulatory networks retrieved by IPA software.

	↑ miRNA (KIT/PDGFRA mutant vs WT GISTs)														
	let-7b	let-7c	**miR-139-5p**	**miR-148a-3p**	miR-152-3p	**miR-193b-3p**	miR-195-5p	miR-199b-5p	**miR-330-3p**	miR-335-5p	miR-455-3p	**miR-455-5p**	miR-487b-3p	miR-497-5p	miR-886-3p
↓ mRNA	**CDK6**	IGF1R	**IGF1R**	-	IGF1R	-	CDK6	-	**CD44**	IGF1R	-	NCSTN	-	IGF1R	-
	IGF1R		**CDK6**				TAB3			EPN2		**IGF1R**			
	CPEB3														
	↓ miRNA (KIT-PDGFRA mutant vs WT GISTs)														
	miR-1225-3p	**miR-1237**	**miR-129-1-3p**	**miR-129-2-3p**	**miR-15a-5p**	**miR-186-5p**	**miR-191-5p**	**miR-197-3p**	**miR-199a-5p**	**miR-214-3p**	**miR-28-5p**	**miR-30c-1***	**miR-30e-5p**	**miR-326**	**miR-328-3p**
↑ mRNA	-	-	-	-	-	-	-	-	-	LZTS1	-	-	-	-	-
	miR-338-3p	miR-34a	miR-34b-5p	miR-424-5p	miR-425-5p	miR-450a	miR-490-3p	miR-490-5p	miR-491-5p	miR-542-3p	miR-542-5p	miR-590-5p	miR-769-5p	miR-876-3p	**miR-876-5p**
↑ mRNA	-	-	-	-	-	-	-	-	MMP2	-	-	-	-	-	-

In bold are highlighted miRNAs confirmed in the validation step; miRNA let 7b had a borderline significance ($P = 0.054$).
-: no correspondence between the significant mRNA and verified miRNA targets.

As shown in figure 24A, with regard to IGF1R 3'UTR, we identified two potential binding sites for miR-139-5p at position 2486-2493 and 3742-3748, two for miR-455-5p at position 3777-3783 and 4193-4199, and three for let-7b at position 99-105, 2619-2626, 6661-6667. With regard to the CDK6 3'UTR, we observed four potential binding sites for miR-139-5p at positions 7989-7995, 3550-3556, 6966-6972 and 10177-10183 (Figure 24B). On the contrary, we found no potential direct binding sites for CD44/miR-330-3p and CDK6/let-7b at their 3'UTR regions.

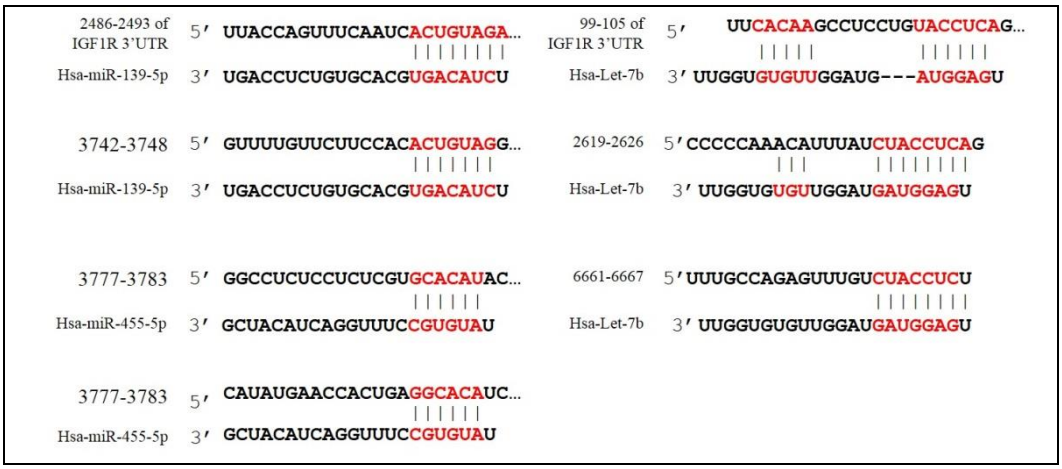

Figure 24. A) IGF1R - miRNA binding sites on its 3'UTR. Computational analysis of the IGF1R 3'UTR showed that miR-139-5p, 455-5p and let-7b have potential binding sites. Predicted binding sequences of miR-139-5p, 455-5p and let-7b to IGF1R are in red.

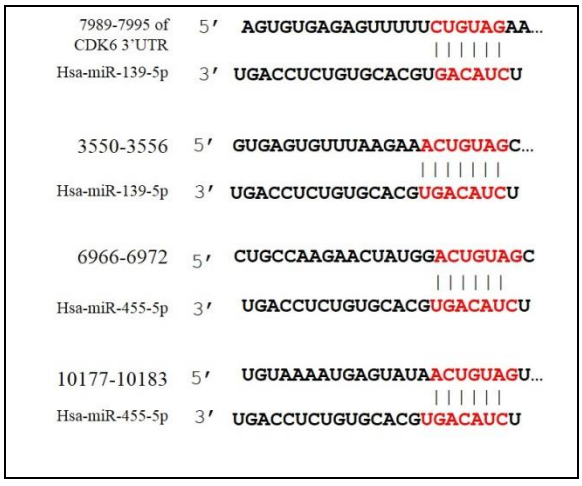

Figure 24. B) CDK6 - miRNA binding sites on its 3'UTR. Computational analysis of the CDK6 3'UTR showed that miR-139-5p had four potential binding sites. Predicted binding sequences are in red.

Western blotting analysis - In order to confirm miRNA–mRNA network at the protein level, a western blotting analysis was performed. Analysis confirmed IGF1R was strongly expressed in all *KIT/PDGFRA* WT-SDH *deficient* GIST, while no expression was detected in *KIT/PDGFRA* mutant

cases (Figure 25). With regard to CD44 and CDK6, no change in expression was observed (data not shown).

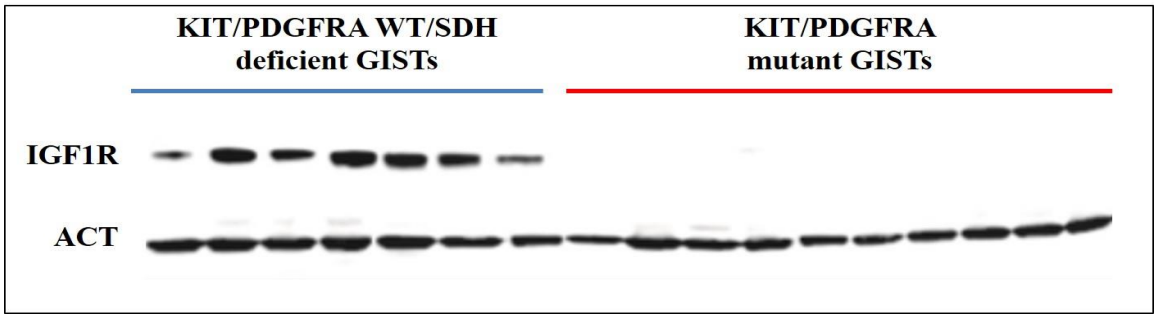

Figure 25. Western blotting confirmed a difference in IGF1R expression. Actin was used as internal control

Expression levels of miR-139-5p/miR-455-5p/let-7b - After having confirmed the IGF1R differential expression at the protein level in the two subsets of GISTs, we focused our attention on its epigenetic network by miR-139-5p, miR-455-5p and let-7b.

We added 9 new GIST cases to the validation cohort (for a total of 37 GISTs, of which 27 were *KIT/PDGFRA* mutant and 10 were *KIT/PDGFRA* WT) and checked the expression level of the 3 miRNAs. Moreover, we evaluated miR-139-5p, miR-455-5p and let-7b expression in two GIST cell lines. As highlighted in figure 26, miR-139-5p and miR-455-5p maintained the statistical significance, even after Bonferroni correction; let-7b did not maintain a significant difference after Bonferroni correction.

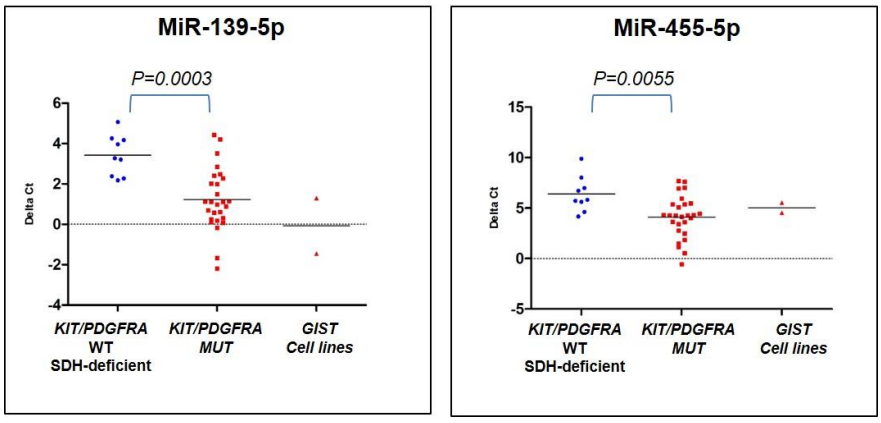

Figure 26. miR-139-5p and miR-455-5p expression levels were analysed in an extended cohort of 36 GIST patients, of which 27 were KIT/PDGFRA mutant and 9 were KIT/PDGFRA WT /SDH deficient. Moreover, we evaluated the same miRNAs in two GIST cell lines.

For this reason, our attention was then focused only on miR-139-5p and miR-455-5p and proceeded with a luciferase assay to verify interaction between the two miRNAs and IGF1R 3'UTR.

Luciferase assay – as shown in figure 27, we observed a reduction of luciferase activity in both GIST48 and GIST882 cell lines transfected with pMiRNanoGlo and miRNA mimics with respect to cells transfected with the plasmid alone.

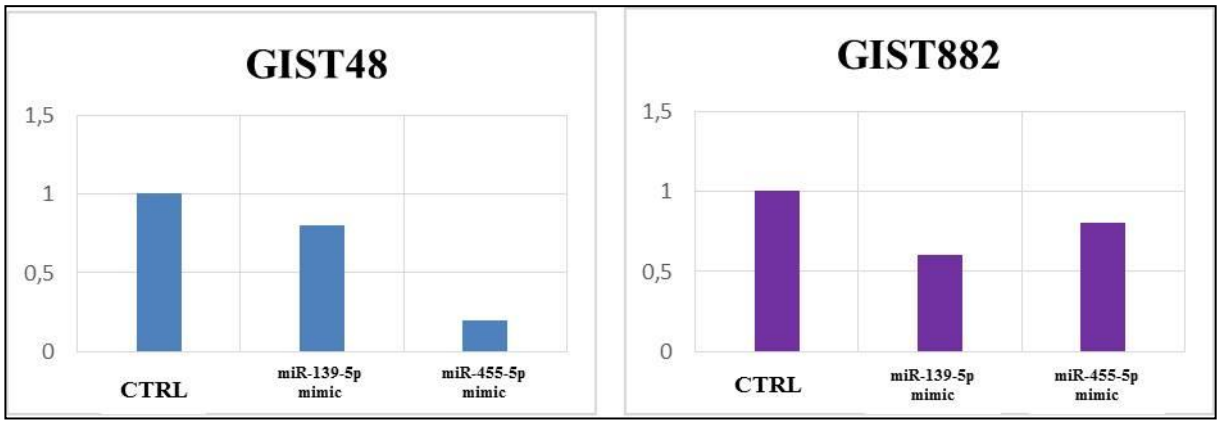

Figure 27. Luciferase assay results in GIST48 and GIST882. Control was set as 1.

Site-Directed Mutagenesis - All constructs were sequenced to confirm the deletion; an example is showed in figure 28.

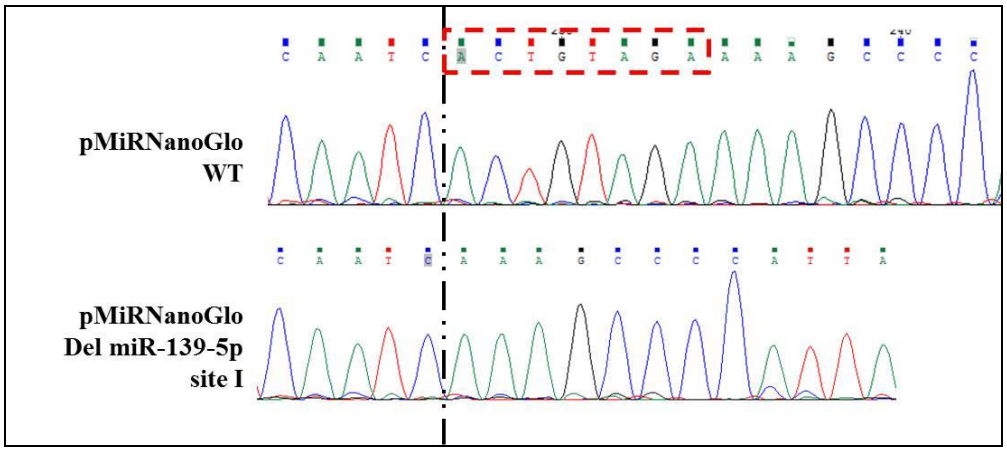

Figure 28. Sanger sequencing was used to confirm presence of miRNA binding site deletion

As showed in figure 29, luciferase assay was used to figure out which one between the two binding sites is important for miR-139-5p activity. The data highlighted that miR-139-5p regulates IGF1R via mainly binding the site in position 2486-2493.

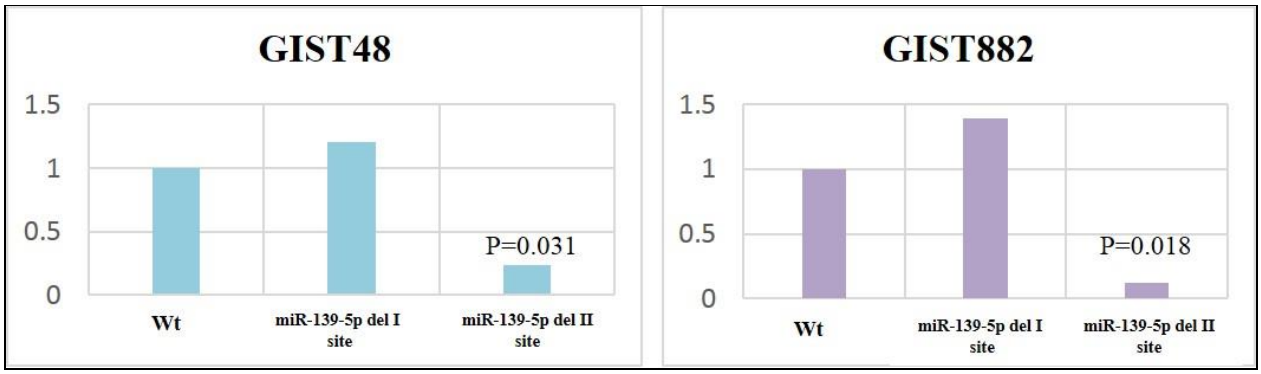

Figure 29. Luciferase assay with the 3 constructs (with WT miR-139-5p binding sites, with deletion of the first binding site and with deletion of the second one) in presence of miR-139-5p mimic

Indeed, deletion of second site (3742-3748), making available only the first one, led to an 80-90% reduction of luciferase activity in both the cell lines, compared with cells transfected with a Wt construct. This suggests that the first site is the one important in mediating IGF1R modulation.

On the contrary, deletion of any of the two miR-455-5p binding sites promoted higher luciferase activity in both the cell lines, compared to cells transfected with a WT construct (figure 30); increase in luminescence is index of a reduction of miRNA binding and activity and vice versa.

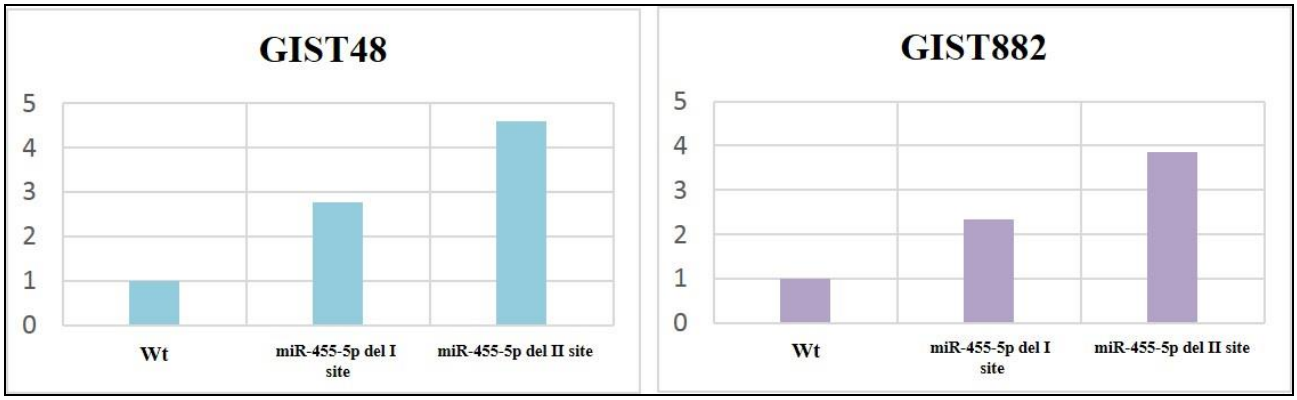

Figure 30. Luciferase assay with the 3 constructs (with WT miR-455-5p binding sites, with deletion of the first binding site and with deletion of the second one) in presence of miR-455-5p mimic. Values of luminescence were reported on Y axis; control was set as 1.

Analysis of apoptosis - Figure 31 summarized the results for analysis of apoptotic rate.

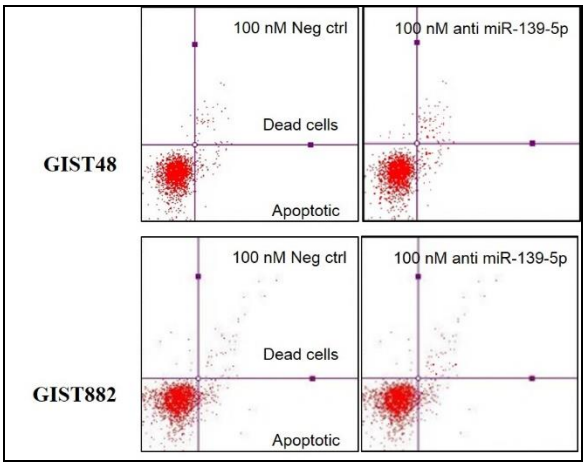

Figure 31. Results of analysis of apoptotic rate in cells transfected with negative control and cells transfected with 100nM of anti-miR-139-5p

We did not observed any difference in cells transfected with anti-miR-139-5p or with anti-miR-455-5p, compared to the ones transfected with negative control. This suggested that miR-139-5p and miR-455-5p do not play a role in apoptosis.

Cell migration assay - We observed that inhibition of miR-139-5p promoted a higher migration rate with respect to no transfected cells and transfected with negative control (in figure 32, only negative control is showed as control). This is more evident in GIST48 line. We did not highlight difference between cells transfected with anti-miR-455-5p and negative control.

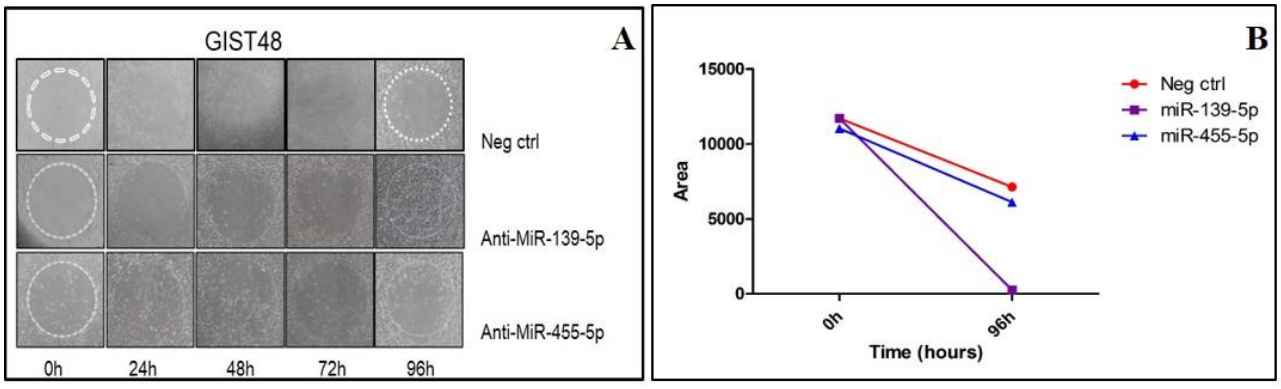

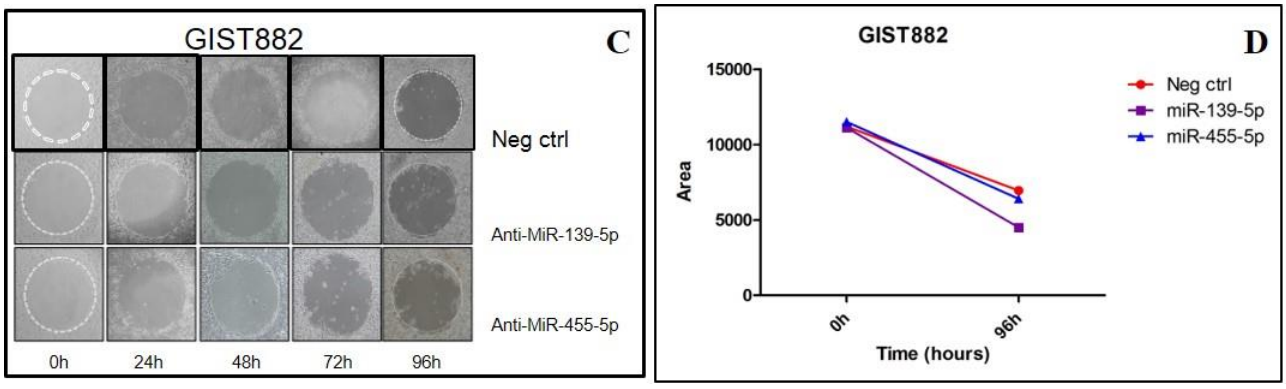

Figure 32. Migration assay was applied to detect the invasive capacities of GIST48 **(A)** and GIST882 **(C)** cells treated or not. **B)** and **D)**. Recover areas were calculated using Image J software

Invasion assay. We measured the value of OD 570nm; for each cell line, OD value was set as one. Invasion assay was applied to assess the invasion capacities of the cells treated or not with anti-miR-139-5p and anti-miR-455-5p. After transfection, the cell migration ability was increased in the cells treated with anti-miR-139-5p (figure 33)

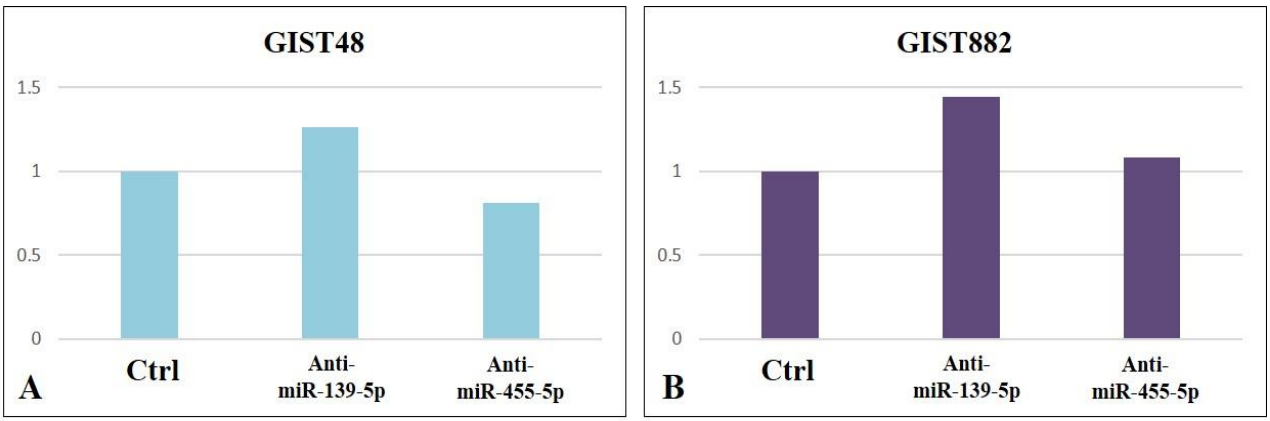

Figure 33. Invasion assay was applied to detect the invasive capacities of GIST48 (A) and GIST882 (B) cells treated or not

Western blotting - We evaluated IGF1R expression 48 hours after transfection with anti-miR-139-5p and anti-miR-455-5p. As showed in figure 34, we observed that IGF1R was expressed in the cells transfected with anti-miR-139-5p but not with anti-miR-455-5p. Moreover, we evaluated IGF1R activation, but no phosphorylation was detected.

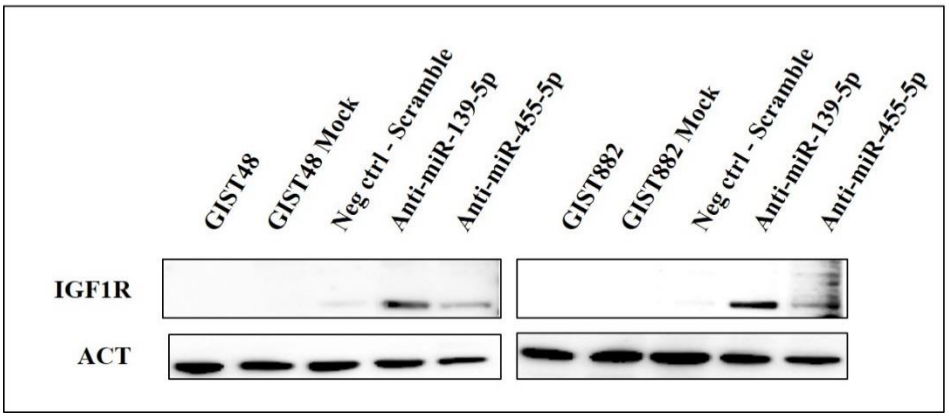

Figure 34. Expression of IGF1R at the protein level, evaluated through western blotting.

5.3. **Discussion**

A growing body of literature has shown the importance of miRNAs in a variety of biological processes, as well as in cancer development and progression [92]. A small number of studies have been published focusing on the significance of miRNAs in GIST development, classification, diagnosis and prognosis [for a review see ref. [93]]. In this context, even more scarce is the knowledge about the differences in miRNA expression between *KIT/PDGFRA* mutant and *KIT/PDGFRA* WT GIST. Basing on these forewords, we integrated multiple expression profiles of miRNA and mRNA to construct an original miRNA-mRNA regulatory network. We analyzed gene expression and miRNA arrays data comparing *KIT/PDGFRA* mutant *vs KIT/PDGFRA* WT GISTs. Taking into account that usually mRNA and miRNA expression has an inversion expression (i.e. ↓mRNA is associated with ↑miRNA and viceversa), we highlighted the existence of 3 potential regulatory networks, IGF1R → miR-139-5p/miR-455-5p/let-7b, CDK6 → miR-139-5p/let-7b, CD44 → miR-330-3p. Specifically, we identified 7 miRNAs (let-7b, let-7c, miR-139-5p, miR-152-3p, miR-335-5p, miR-455-5p, and miR-497-5p) that could affect the IGF1R expression.

In the second step, we performed miRNAs validation in an enlarged cohort of 37 GIST cases. This led us to confirm the significant deregulation of miR-139-5p and miR-455-5p, while, let-7b did not maintain the statistical significance. For this reason, we focused only on the first two miRNAs and proceeded with functional *in vitro* studies. To this purpose, we used two GIST cell models, GIST48 and GIST882; the two cell lines are both *KIT* mutant and may not represent the best model. However, unfortunately, GIST cell lines are not commercially available, all the established lines harbour *KIT* mutations and there are not *KIT/PDGFRA* WT models.

First, through a luciferase assay we confirmed that both miR-139-5p and miR-455-5p may bind IGF1R 3'UTR and regulate its expression. This data suggest that IGF1R could be epigenetically modulated by miR-139-5p and miR-455-5p, which are up-regulated in *KIT/PDGFRA* mutant GISTs

and could therefore inhibit IGF1R via binding its 3'UTR. Subsequently, we analyzed the binding sites to understand which one is involved in this regulation. With regard to miR-139-5p, the results revealed that position 2486-2493 is the key seed sequence, whereas site on position 3742-3748 could represent an ancillary site not involved in IGF1R regulation. On the contrary, we did not find any difference in miR-455-5p binding sites (positions 3782-3788 and 4198-4204); indeed deletion of any of the two sites promotes higher luciferase activity compared to the control, which is index of diminished miR-455-5p/3'UTR binding. This led us to speculate that both the sites are equally important for miR-455-5p activity.

Finally, we performed a series of functional experiments to clarify the role of miR-139-5p and 455-5p. With regard to IGF1R, we observed that inhibition of miR-139-5p, but not miR-455-5p, restored its expression in both GIST48 and GIST882 lines. In addition, miR-139-5p seems to play a role in invasion and migration. Indeed, its inhibition increased cell migration and invasion capability in both cell lines.

In summary, we showed that miR-139-5p is down-regulated in *KIT/PDGFRA* WT GISTs and IGF1R is among the most up-upregulated genes in this subset of patients. In previous studies, IGF1R has been identifies as a target to suppress tumor cell proliferation, migration and invasion in gliomas, HeLa cells, non-small cell lung cancer, amongst others [94,95,96]. MiR-139-5p has been widely reported in literature as tumor suppressor [97,98,99]; our results are in agreement with these data and could represent a novel biomarker in *KIT/PDGFRA* WT GIST subset. This is the first report on the tumor suppressive function of this miRNA in GISTs; in addition, our results confirm the regulatory network miR-139-5p/IGF1R. To the best of our knowledge, this is the first time that epigenetic regulation is explained at the molecular level in GISTs. In particular our results suggested that miR-139-5p may represent a potential onco-miR marker in *KIT/PDGFRA* WT GISTs, characterized by IGF1R epigenetic-enhanced expression, driving the carcinogenesis and development of *KIT/PDGFRA* WT GIST. In this context, epigenetically IGF1R activation and over-expression would serve the same as the *KIT/PDGFRA* driver mutation. Therefore, this miRNA

signature has the potential to represent an important diagnostic tool and therapeutic target in *KIT/PDGFRA* WT GISTs, and in particular in the SDH-*deficient* subset. In conclusion, we are aware of the limitation of the present study, in particular the small sample size that could have mask the significant effect of some of the miRNA, and consequently leading to the non-identification of important miRNA-mRNA networks.

Obviously, further identification of additional aberrantly expressed miRNAs in a larger GIST population, and the elucidation of their functional roles will be helpful in understanding the pathogenesis of GIST disease, and has the potential to represent a rational therapeutic strategy for the treatment of *KIT/PDGFRA* WT-SDH-*deficient* GISTs.

6. Second aim: Characterization of novel mechanisms of pharmacological resistance to a PI3KCA inhibitor from an *omic* point of view

As widely previously described in the introduction, with the arrival of imatinib, GIST became the best example of target therapy in solid tumors [24,21,5]. The major part of patients with advanced GISTs under imatinib have persistent measurable disease and typically within 24-36 months eventually progress [100]. During these almost 20 years since imatinib approval, to face emergence of pharmacological resistance, a second and a third line – sunitinib and regorafenib, respectively, have been introduce in the GIST management. As imatinib, sunitinib and regorafenib are TKIs and act with the same mechanism of action. Compared with first-line imatinib, benefits produced by sunitinib and regorafenib are quite limited and the majority of patients often experience tumor progression; this depends on the emergence of multiple drug resistant KIT mutations within an individual tumor [62,101,102,103]. Besides TKIs, to date, there are no other therapeutic options and, for this reason, the identification of novel *druggable* targets and a better characterization of resistance process may represent a key starting point to fine tune a clinical approach different from TKIs. Recently, a phase 1b trial started to evaluate a novel PI3KCA inhibitor - BYL719 (Novartis) - in GIST patients who previously failed imatinib and sunitinib (NCT01735968). Indeed, one of the strategies to fight resistance in GISTs could be represented by inhibiting PI3K pathway, which is downstream of KIT/PDGFRA. This pathway is deregulated in many human cancers, including GISTs [104,105,106,107,108]. Specifically, BYL719 is a selective inhibitor of the PI3K catalytic p110a subunit [109], and showed a significant antitumor effect in patient-derived xenograft models of GIST [110]. This led to a trial for GIST patients, who previously failed imatinib and sunitinib (NCT01735968), but it is still ongoing and there are no results yet. The interesting preclinical results prompted us to focus our attention on the cells' behavior treated with this new molecule, but

not from a canonical point of view. We generate two *in vitro* models of acquired resistance and performed an *omics*-based analysis by integrating miRNA profiling, RNA-sequencing and methylation profiling in sensitive and resistant cells. The aim of this work was to comprehensively characterize genomic and transcriptomic changes, which take place during noticing of resistance and how cancer cells evolve from drug-sensitive from an *omic* point of view.

6.1. Materials and methods

Cell culture and treatment - Two human established imatinib resistant GIST cell lines, GIST48 and GIST48B, were used. Cell lines were kindly provided by Dr Fletcher (Department of Pathology, Brigham and Women's Hospital, Harvard Medical School, Boston, MA). GIST48 has a primary, homozygous KIT exon 11 missense mutation (V560D) and a heterozygous secondary KIT exon 17 mutation (D820A), activating kinase loop [111]. This cell line was established from a GIST that ceased to respond to imatinib, while GIST48B is a subline of GIST48, which expresses KIT transcript but not the protein, and preserves activating *KIT* mutation in all cells [112]. Cells were cultured in IMDM (Gibco) supplemented with 15% FBS (Gibco) and 1% penicillin (10,000 U/ml)/streptomycin (10 mg/ml) (Lonza) and maintained at 37°C in a humified atmosphere of 5% CO2. To generate BYL719 resistant sublines, GIST48 and GIST 48B were cultured with increasing concentrations of BYL719 (Selleckchem), starting with 0.05 µM and to 5 µM. Fresh drug was added every 3-4 days and resistant cells, able to grow in 5 µM BYL719, were established after about 50 weeks of culture with the drug. GIST48 and GIST48B resistant cells are referred to as GIST48-R and GIST48B-R. RNAs and DNAs were isolated at the time zero of each change of concentration. KIT-mutant cell lines were authenticated by KIT sequencing and KIT TKI sensitivity experiments. GIST cell lines were routinely tested for mycoplasma contamination and were found to be negative.

MTT assay and IC50- IC50 was evaluated with the MTT [3-(4,5-dimethyl-2-thiazolyl)-2,5-diphenyl-2H-tetrazolium bromide] assay as previously described [113]. Briefly, $1x10^4$ cells were

seeded in a 96 well plate, and the day after serially diluted BYL719 was added by medium replacement. After 48h, the cells were washed with HBSS and then incubated with MTT (5 mg/mL) in HBSS for 2 h. After removal of MTT and further washing, the formazan crystals were dissolved with isopropanol. The amount of formazan was measured (570 nm) with a spectrophotometer (TECAN®, Spectra model Classic, Salizburg, Austria).

DNA isolation - Genomic DNA was extracted from each cell lines using QIAamp DNA Mini Kit (QIAGEN), according to the manufacturer's recommendations

KIT and PI3KCA DNA analysis - Mutational analyses of KIT (exons 9, 11 13, 14, 17 and 18) and PI3KCA (exons 9 and 20) were performed on genomic DNA from GIST48, GIST48B, GIST48-R and GIST48B-R. Briefly, each exon was amplified with PCR amplification using specific primer pairs. Then, PCR products were purified and sequenced on both strands using the Big Dye Terminator v1.1 Cycle Sequencing kit (Applied Biosystems). Sanger sequencing was performed on ABI 310 Genetic Analyzer (Applied Biosystems).

RNA isolation - Total RNA was isolated from parental (GIST48 and GIST48B) and BYL719 resistant (GIST48-R and GIST48B-R) cultured cells using RNeasy® mini Kit (QIAGEN) following manufacturer's instructions.

ABC transporter genes expression levels - Total RNA was retro-transcribed to cDNA using High Capacity RNA-to-cDNA kit. The cDNA was then loaded in TaqMan® Human ABC Transporter Arrays, which allow quantitative gene expression analysis of human ABC transporter genes important in drug discovery. The array contains 64 gene expression assays (50 targets and 14 controls) arrayed in triplicate in 384 wells. Arrays were normalized using GAPDH and 18S as endogenous controls, and the data were analyzed using the $2^{-\Delta\Delta Ct}$ method. Genes with Ct>35 were considered as not expressed and excluded from further analysis

RNA sequencing- Whole-transcriptome RNA libraries were prepared in accordance with Illumina's TruSeq RNA Sample Prep v2 protocol (Illumina, San Diego, California). Poly(A)-RNA molecules from 500 ng of total RNA were purified using oligo-dT magnetic beads. Subsequently, mRNA was

fragmented and randomly primed for reverse transcription followed by second-strand synthesis to generate double-stranded cDNA fragments. These cDNA fragments went through a terminal-end repair process and ligation using paired-end sequencing adapters. The products were then amplified to enrich for fragments carrying adapters ligated on both ends and to add additional sequences complementary to the oligonucleotides on the flow cell, thus creating the final cDNA library. 12pM paired-end libraries were amplified and ligated to the flowcell by bridge PCR, and sequenced at 2x75bp read length for RNA, using Illumina Sequencing by synthesis (SBS) technology.

Bioinformatic analysis - After demultiplexing and FASTQ generation (using bcltofastq function developed by Illumina), the paired-end reads were trimmed using AdapterRemoval (https://github.com/MikkelSchubert/adapterremoval) with the aim of removing stretches of low quality bases (<Q10) and Truseq/Nextera rapid capture adapters present in the sequences. Sequences coming from RNA-seq were mapped with TopHat/BowTie pipeline and PCR or optical duplicates were removed with the function *rmdup* of Samtools.

SNV calling - Variant calling was performed with SAMtools and SNVMix2, thus identifying all the point mutations and INDELs. Variants included in dbSNP and 1000 Genomes, ExAc and EVS with frequency > 1% were excluded. All variants from the matched normal-tumor pairs that were unique in the tumor sample were called as somatic.

Gene expression analysis - In order to compare the gene expression profile between sensitive and BYL-719 resistant GIST cell lines, RNA seq data were analyzed After the alignment procedure, the BAM file obtained was manipulated with SAMtools in order to remove the optical/PCR duplicate, and to sort and index it. The function HTSeq-count (Python package HTSeq) was adopted to count the number of reads mapped (cpm) on known genes, included in the Ensembl release 72 annotation features (http://www.ensembl.org).

miRNA expression evaluation - 300 ng of total RNA were reverse transcribed using TaqMan® MicroRNA reverse transcription kit (ThermoFisher Scientific) using Megaplex RT primers Human Pool A and Pool B. cDNAs were load on TaqMan Arrays Human MicroRNA A and B Cards

(ThermoFisher Scientific) and run on 7900HT Real-Time PCR system, in accordance with the manufacturer's procedure. The miRNA data were analyzed with SDS Relative Quantification Software version 2.4. (Applied Biosystems) and miRNAs with Ct>35 were considered as not expressed and excluded from further analysis; miRNA expression levels were normalized using U6 and RNU48 as endogenous controls. Normalization was carried out by subtracting the mean Ct from individual Ct values. R-Bioconductor package Limma was adopted to evaluate the differential expression profile between the parental and BYL719 resistant GIST cell lines

Global methylation profile-. 600 ng of genomic DNA per sample were bisulfite-converted using EZ DNA methylation Kits (Zymo research), and DNA methylation was measured using the Illumina Infinium HD Methylation Assay with Infinium MethylationEPIC BeadChips according to Illumina's protocol. Raw data (idat files) were processed in R Bioconductor (minfi27). Quality of each sample was analyzed and probe signal was removed when the detection p-value was above 0.05, or >1% of the dataset contained no data, or if probes contained single nucleotide polymorphisms. None of the samples included in the study was flagged as outliers [114]. Statistical analyses were carried out using GenomeStudio, normalizing idats with the controls provided by Illumina; the methylation score of each CpG is represented as a β-value and differences between βvalues of treated and untreated cells represent alteration in methylation level. The CpGs selected were those absolute methylation differential value of >0.2 or <-0.2 [115,114]. To identify CpGs on promoter regions, we considered as UCSC refgene group only TSS200 or TSS1500.

Identification of validated miRNA targets - Targets of significant miRNAs were identified through specific *in silico* tools which allow predicting the most probable targets. Six programs were used (TargetScan, mirbase, MIRanda, mirtarget2, PicTAR, and miRTarBase), and the targets were considered reliable if at least 4 out of 6 were in agreement.

miRNA and mRNA correlation - Using these information, miRNA and mRNA arrays were analysed to highlight pairs of mRNA/miRNA that were discordant (UP *vs* DOWN and vice versa). Potential

miRNA-mRNA interactions and miRNA/mRNA expression profiles were used to construct functional interaction networks.

Methylation profile and gene expression correlation - To integrate methylation profile and gene expression profile (GEP), we considered only CpGs on promoter regions which shown an absolute methylation differential value of >0.2 or <-0.2 in parental lines *versus* BYL719 resistant ones; promoter regions were defined as the upstream 1500 bp and downstream 200 bp from the transcription start site (TSS) of each gene. For each differentially methylated gene, we checked the expression level deriving from RNA sequencing

6.2. **Results**

KIT and PI3KCA analysis - We did not detect additional mutations in BYL719 resistant cell lines in *KIT* gene. With regard to PI3KCA, we specifically analysed exon 9 and exon 20 - both codifying for the catalytic p110a subunit - given that these exons are mutational hotspots in a wide portion of human cancers [116 117]. All the samples were WT.

ABC transporter genes - Given the well-recognized role of ABC transporter genes in mediating drug resistance, we firstly analyzed a custom panel of 50 genes in sensitive and resistant cell lines. However, we could not observed any significantly deregulated gene after treatment with BYL719.

RNA-seq: Gene expression - For this reason, we decided to carry on a comparative analysis between GIST48 and GIST48B *vs* GIST48-R and GIST48B-R. The comparative analysis showed 95 differentially expressed genes with a false discovery rate =0 and p-value ≤0.001 (Table 5)

Table 5. List of genes differentially expressed in parental and resistant cell lines

Up-regulated genes in BYL719 resistant cell lines				Down-regulated genes in BYL719 resistant cell lines			
Gene_name	**logFC**	**Pvalue**	**FDR**	**Gene_name**	**logFC**	**Pvalue**	**FDR**
H19	2.23	8.61E-12	1.08E-07	C16orf89	-2.21	0.000000	0.000001
RAB3IP	3.23	1.19E-09	3.93E-06	MXRA5	-1.90	0.000000	0.000004
ANXA3	1.81	8.24E-08	0.000148	BRINP1	-3.82	0.000000	0.000121
LXN	2.57	2.9E-07	0.000304	CUX2	-2.27	0.000000	0.000215
CHAC1	2.41	1,00E-06	0.000841	SLC4A7	-1.57	0.000000	0.000215

TNFSF10	3.12	1.53E-06	0.001043	PCSK6	-1.78	0.000000	0.000215
CLMN	2.40	1.8E-06	0.001078	SGK1	-2.46	0.000001	0.000535
ACSM3	2.26	5.71E-06	0.002987	GPC2	-1.79	0.000001	0.001010
PDE5A	1.52	9.67E-06	0.004328	FN1	-1.54	0.000003	0.001451
DSG2	2.60	1.39E-05	0.005618	RHBDF1	-1.43	0.000007	0.003245
ASNS	1.30	1.58E-05	0.00619	SAMD11	-1.38	0.000008	0.003622
PSAT1	1.48	1.96E-05	0.007033	VCAM1	-1.67	0.000017	0.006486
SNX10	2.00	2.51E-05	0.008495	ID3	-1.69	0.000019	0.006898
LMO4	1.29	2.64E-05	0.008495	SMAD9	-1.28	0.000029	0.008963
SEMA3C	2.39	3,00E-05	0.009034	SLC14A1	-3.15	0.000030	0.009034
GLRB	2.02	3.22E-05	0.009306	TSHZ2	-2.18	0.000033	0.009306
ADD2	1.62	4.99E-05	0.012541	MME	-1.47	0.000035	0.009897
EGR1	2.46	7.05E-05	0.017026	RP11-54O7.1	-2.01	0.000041	0.010885
MAL2	2.82	7.84E-05	0.017893	PHF2P2	-1.39	0.000042	0.011066
PRIMA1	2.06	8.88E-05	0.018896	TYRO3	-1.42	0.000097	0.019908
TBC1D2B	1.47	9.25E-05	0.019348	NUAK1	-1.45	0.000105	0.020765
GAB2	2.19	0.000108	0.020816	PHLDB2	-1.64	0.000106	0.020765
PROCR	1.89	0.000129	0.023094	DACT3	-1.43	0.000104	0.020765
ICA1	2.05	0.000132	0.023302	GTF2IP3	-2.01	0.000109	0.020816
PRKCQ-AS1	1.56	0.000142	0.024358	ID2	-1.25	0.000117	0.021688
DOCK9	1.77	0.000171	0.0276	EFNB2	-1.59	0.000137	0.023811
LAMP3	1.22	0.000232	0.035097	IQGAP2	-1.14	0.000144	0.024358
TRIB1	1.25	0.000232	0.035097	RBM18	-1.17	0.000170	0.027600
TBC1D8B	1.62	0.000266	0.038374	SOSTDC1	-1.84	0.000189	0.030100
SFRP1	1.10	0.000358	0.048283	F2R	-1.48	0.000225	0.034926
TNFAIP8	1.29	0.000407	0.052689	ADGRD1	-1.54	0.000262	0.038374
SAMD12	2.06	0.000424	0.053714	GAREM	-1.46	0.000297	0.042399
JUNB	1.43	0.000444	0.055782	SOX4	-1.23	0.000306	0.043207
DAAM2	1.21	0.000483	0.05878	SMAD6	-1.21	0.000350	0.047754
IGSF3	1.13	0.000487	0.05878	SH3BP5-AS1	-1.66	0.000347	0.047754
LGI2	1.90	0.000521	0.061597	PREX2	-1.06	0.000369	0.049242
CALB2	1.72	0.000525	0.061597	BCRP3	-1.76	0.000420	0.053714
PDE3B	1.39	0.000552	0.063588	COL16A1	-1.15	0.000449	0.055782
GPC3	1.71	0.000574	0.064953	PDLIM3	-1.45	0.000463	0.056947
TNFRSF19	2.17	0.000571	0.064953	ADAMTS2	-1.65	0.000512	0.061195
FOXP2	1.57	0.00061	0.06843	WTIP	-1.16	0.000531	0.061674
BST2	1.18	0.000619	0.068795	MYO1B	-1.27	0.000626	0.068960
HUNK	1.30	0.000647	0.070631	SORBS1	-1.55	0.000703	0.075396
FAM19A4	1.76	0.000709	0.075396	PPARGC1B	-1.01	0.000794	0.081682
ARRB1	1.27	0.000737	0.07712	ATOH8	-2.31	0.000808	0.082507
CCDC181	1.55	0.000893	0.088251	ZDHHC11	-1.33	0.000832	0.084194
GLTSCR2	0.98	0.001004	0.098527	CTGF	-1.16	0.000869	0.087235

FOS	2.77	0.001014	0.098663	

In particular, 48 genes were up-regulated, while 47 genes were down-regulated. The significant DEGs are reported in table 5. GO functional enrichment analysis of up-regulated and down-regulated genes are showed in figure 35A. The top deregulated genes are shown in figure 35B.

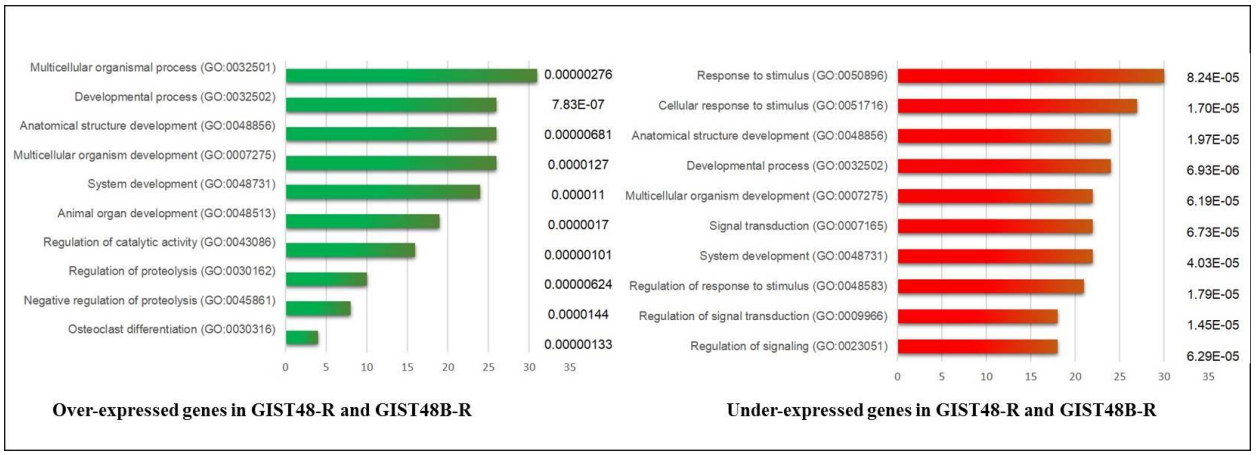

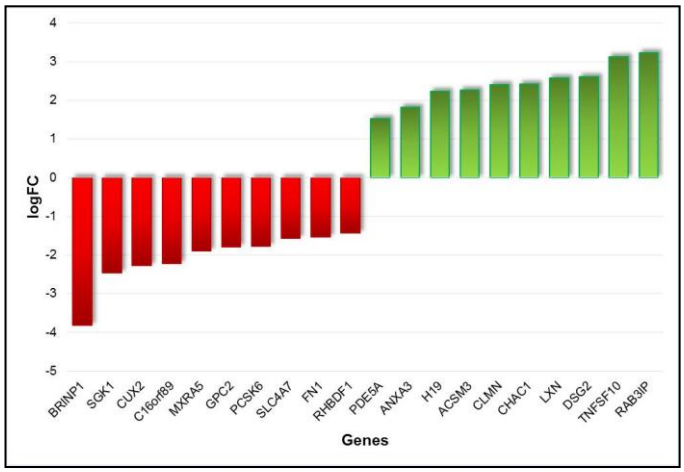

Figure 35. A) GO functional enrichment analysis of up-regulated and down-regulated genes**. B)** The top deregulated genes

SNV calling - Compared to the parental cell lines, we were able to identified 4 and 7 novel mutations respectively in GIST48-R and GIST48B-R (Table 6); the genes with novel mutations were not reported in literature as involved in PI3KCA downstream via. No one among those was in common between the two models. Therefore, we concluded that resistance to BYL719 was not linked to acquired mutations, as frequently happens in GISTs under TKIs.

Table 6. Novel acquired mutations in BYL719 resistant cells					
GIST48 vs GIST48-R			**GIST48B vs GIST48B-R**		
Gene	**Exon**	**AA change**	**Gene**	**Exon**	**AA change**
KIFC2	exon17	p.R732C	*FRY*	exon5	p.D168Y
RIF1	exon19	p.V666A	*PDGFB*	exon3	p.R51H
DPF1	exon9	p.C313G	*SYT14*	exon6	p.V359A
RPGR	exon6	p.Q171R	*EEF2KMT*	exon2	p.H52Q
			RARS2	exon1	p.C11X
			DCHS1	exon2	p.R168C

miRNA expression - The array highlighted a total of 44 deregulated miRNAs out of the 754 analyzed with a p-value <0.05, However, after correction, only 13 miRNAs maintained the statistical significance. In particular, the expression of 2 miRNAs was strongly up-regulated (has-miR-190b and has-miR-299-5p), and 11 miRNAs were down-regulated in resistant GIST cell lines compared to parental ones. All the differentially expressed miRNAs are reported in table 7.

Table 7. The most significant deregulated miRNAs		
miRNA	**Pvalue**	**Adjusted Pval**
hsa-miR-1243	2.94E-06	0.002232799
hsa-miR-520c-3p	1.27E-05	0.003316809
hsa-miR-190b	1.31E-05	0.003316809
hsa-miR-1289	2.72E-05	0.005164803
hsa-miR-1247-5p	0.000118	0.016017348
hsa-miR-22-3p	0.000126	0.016017348
hsa-miR-1267	0.000188	0.020418143
hsa-miR-299-5p	0.000237	0.022470219
hsa-miR-125b-5p	0.000294	0.024789505
hsa-miR-656-3p	0.000447	0.033993852
hsa-miR-331-5p	0.000591	0.040837133
hsa-miR-149-3p	0.000868	0.054998185
hsa-miR-30d-5p	0.001126	0.065812471

Hierarchical clustering of all samples separated sensitive and resistant GIST cell lines into two distinct clusters (Figure 36A).

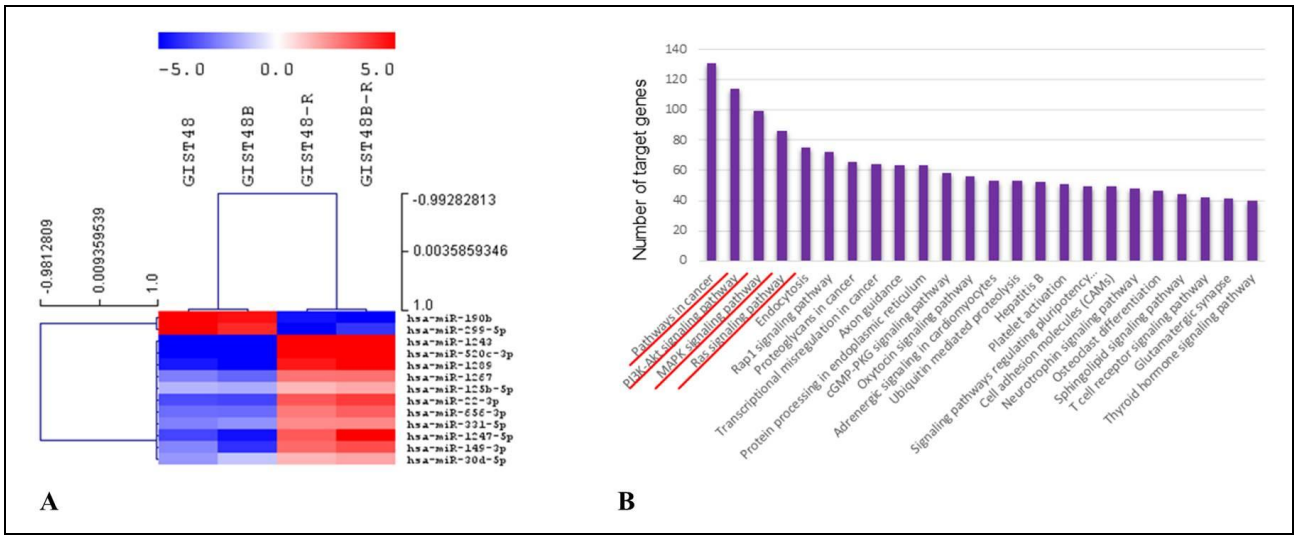

Figure 36. A) Hierarchical clustering analysis of miRNA expression**. B)** miRNA regulatory roles and identification of controlled pathways through miRPath 3.0

Through miRPath 3.0 we assessed miRNAs regulatory roles and identified their pathways [118]. Interestingly, among the pathways potentially modulated by those deregulated miRNAs (summarized in figure 36B), the most significant and with the greatest number of target genes, are PI3K/AKT- MAPK and Ras cascades, which are involved in BYL719 mechanism of action.

Global methylation profile- We performed a genome-wide DNA methylation profiling in both parental and resistant GIST48 and GIST48B cell lines to determine whether acquired resistance involves modifications in DNA methylation. We identified 3305 CpGs differentially methylated pre and post treatment (Δβ value <-0.2 or >0.2). Figure 37 shows the unsupervised hierarchical cluster analysis of the demethylated genes; the analysis divided the sample set into two main clusters: sensitive and resistant cell lines (Figure 37).

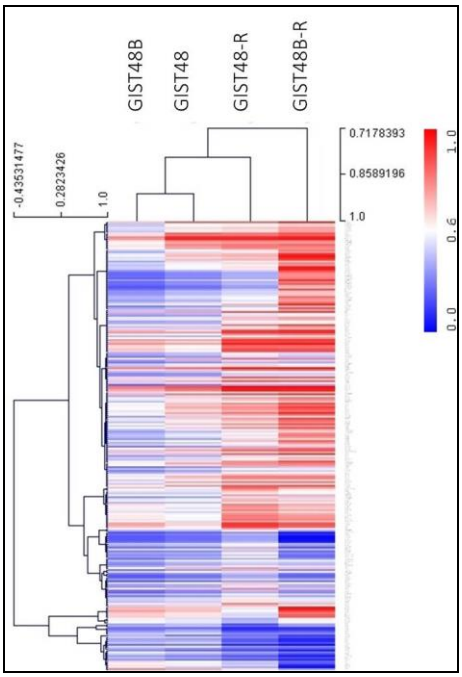

Figure 37. The heatmap shows the DNA methylation profiles of parental and resistant cell lines (Δβ value <-0.2 or >0.2).

Interestingly, as shown in figure 38A, B and C, the resistant cells showed significantly more promoter hypermethylation of the CpG islands than their parental counterparts.

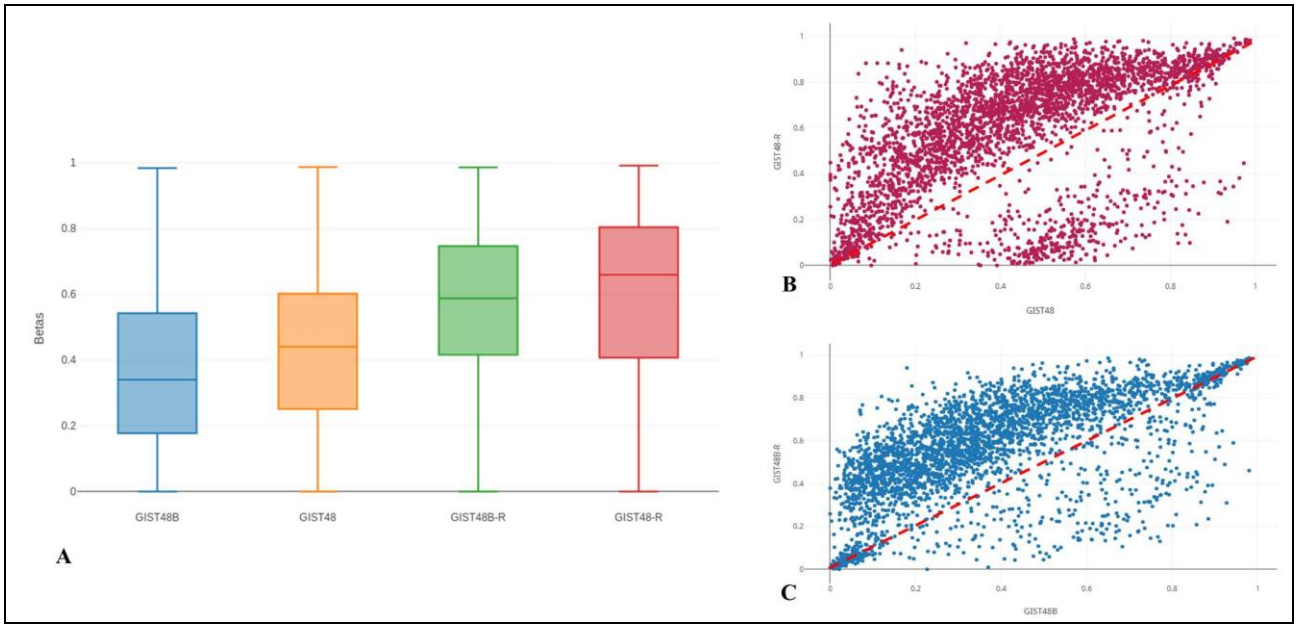

Figure 38. A) Box-plots show the β values of the CpGs at the promoters (only CpG islands); a general hypermethylation is more common in the resistant cell lines. B, C) Scatter plots of genome-wide DNA methylation levels (β). To highlight the general hypermethylation, in the two figures are reported the CpG islands with Δβ value <-0.2 or >0.2.

Among the 3305 CpGs, 2817 were hypermethylated, whereas 488 were hypomethylated. Among the hypermethylated CpGs, 547 were in promoter regions of 379 genes. With regard to the hypomethylated sites, 102 were in promoter regions of 70 genes.

miRNAs and mRNAs arrays correlation - To construct miRNAs-DEGs networks, we downloaded the experimentally verified associations between human miRNAs and their targets from miRTarBase, which encloses more than 400000 miRNAs-target interactions collected by manually surveying pertinent literature after systematic data mining of the text. This dataset contains miRNAs-target interactions consisting of 4076 miRNAs and 23054 mRNAs [119]. The results are reported in figure 39.

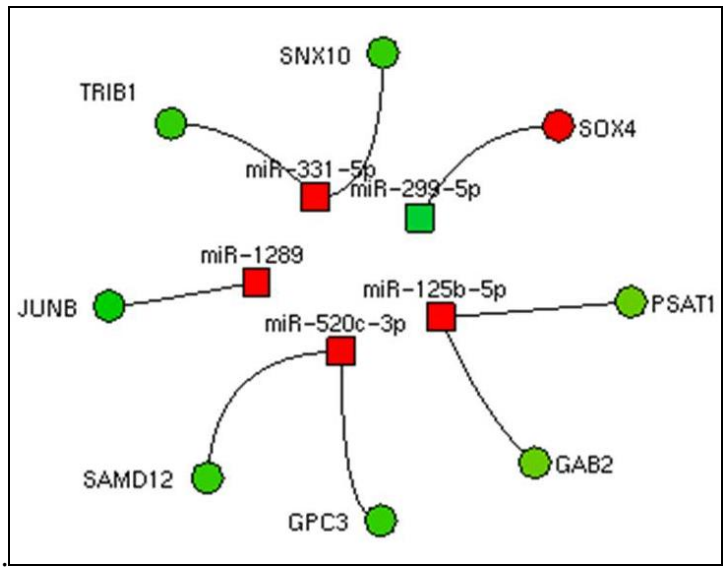

Figure 39. miRNAs-DEGs networks

Among the 13 deregulated miRNAs retrieved by our data, 7 (miR-331-5p, miR-125b-5p, miR-520c-3p, miR-1289, miR-299-5p, miR-30d-5p, miR-149-3p) had verified associations with their targets. However, taking into account of the typical inverse relationship between miRNAs and targets' expression, we were able to identify 8 mRNA-miRNA networks (Figure 39).

Methylation and mRNAs arrays correlation - We then integrated global methylation profile with DEGs. Some genes showed an association between changes in promoter hypermethylation and changes in gene expression. Among the genes with the strongest gene promoter hypermethylation

and concomitant increase in gene expression were: Calmin (CLMN), which encodes a member of the hedgehog-interacting protein family; Myelin and Lymphocyte protein (MAL), which encodes the T-lymphocyte maturation-associated protein and functions in T-cell differentiation. On the contrary, promoter hypermethylation and concomitant Teashirt zinc finger homeobox 2 (TSHZ2) down-regulation was observed, whereas, PSAT1, Phosphoserine aminotransferase 1, showed strong promoter hypomethylation associated with increased gene expression after treatment.

Integration of miRNAs, methylation profiles and gene expression - Finally, we integrated all the data deriving from GEP, miRNAs and methylation profiles. As mentioned before, regarding to gene expression modulation by miRNAs, we considered the canonical inverse correlation. We found a gene - PSAT1- up-regulated in resistant cell lines, which showed promoter hypomethylation and was potentially modulated by miR-125b-5p (Figure 40) (These results are from Ravegnini *et al*, 2019, Submitted).

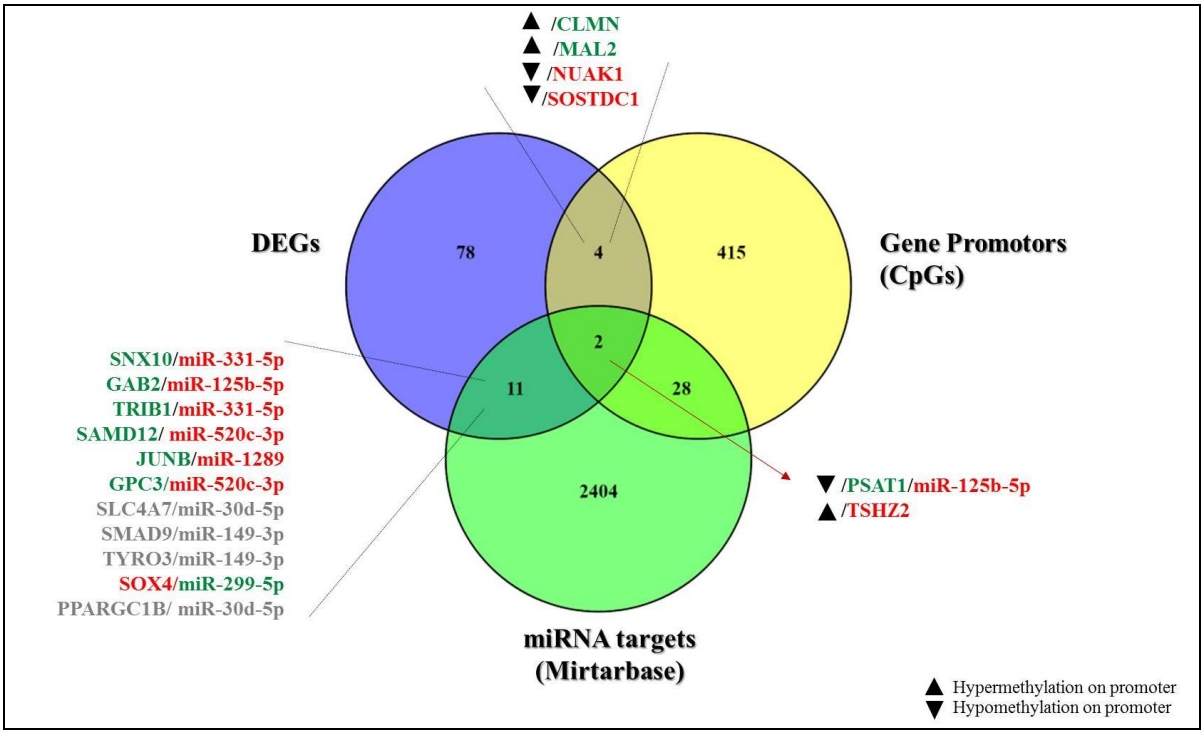

Figure 40. Integration of GEP, miRNAs and methylation profiles. In grey are shown genes and miRNAs with the same trend of expression, which were excluded. Red and green indicate respectively a down-regulation and an up-regulation

.

6.3. **Discussion**

GISTs represent a worldwide paradigm of target therapy. The introduction of imatinib in clinic has deeply revolutionized the GIST management, leading them from incurable disease to be a sort of chronic disease. Imatinib showed terrific improvement in prognosis, however, as often happens with TKIs, after a certain period, the majority of patients develop acquired mutations and progress. To contain the tumor progression, in these last 20 years, a second - sunitinib - and a third – regorafenib – line therapy have been introduced; unfortunately, all these treatments act with the same mechanism of action and the most of patients progress even under the third line. To date, unfortunately, there are no therapeutic options for whom have failed imatinib, sunitinib and regorafenib; for these reasons, it is pivotal and mandatory to individuate novel molecules and strategies to overcome the inevitable upcoming resistance. Recently, a new trial started for GIST patients who previously failed treatment with imatinib and sunitinib (NCT01735968). The trial is still ongoing but there are no published results. However, the preclinical results have shown promising results [110]. Our aim was to comprehensively characterize genomic and transcriptomic changes taking place during noticing of resistance, and understand how cancer cells evolve from being drug-sensitive to drug resistant, from an *omic* point of view. We generate two *in vitro* GIST models of acquired resistance to BYL719 and performed an *omics*-based analysis by integrating miRNAs profiling, RNA-seq and methylation profiling in sensitive and resistant cells.

The first difference that we observed compared with the standard TKIs treatment was the lack of novel mutations in BYL719 resistant cells. This is a quite novel mechanism in GISTs, in which drug resistance is usually largely due to accumulation of additional kinase domain mutations [110]. Then, we took into account that among the known mechanisms of drug resistance, the overexpression of genes involved in drug efflux or transport is among the most common [120,121,122]. For this reason, we analyzed a precast panel of 50 well-characterized ABC transporters genes.

However, we could not observe any significant difference in resistant cell lines compared to the parental ones. The next step was then a deep characterization of these novel models of acquired resistance. Through RNA-seq, we could evaluate the appearance of additional point mutations or INDELs. Although novel alterations were found in resistant lines, however no mutations were shared by both models or harbored on hot-spot genes (including *PI3KCA*, *KIT*, or downstream effectors). This prompted us to assume that BYL719 resistance could be mediated by epigenetic mechanisms. In literature is widely reported that epigenetic modifications may represent alternative mechanisms to evade the pharmacological response [123,124,125]. Different trials evaluating epigenetic therapies in solid tumors as drug resistance modulators are ongoing [123]; in GISTs, many research efforts have been made to offer therapeutic options to bypass TKIs resistance. In recent years, epigenetic treatments raised among the future perspective [126,127], however, results are still at an early stage and further investigations are pivotal in this novel field in GISTs.

Here, through an *omic* approach, we characterized a peculiar resistance mechanism involving epigenetic alterations. Integrating miRNAs and methylation profiles with gene expression deregulation, we identified overexpression of PSAT1 as potentially modulated by its promotor hypomethylation and by downregulation of miR-125b-5p. Interaction between miRNAs, methylation and gene expression have been previously described in cancer [128], but not in GISTs.

Over-expression of PSAT1, which encodes for phosphoserine aminotransferase 1, has been reported as involved in resistance in different tumors, including colorectal and pancreatic cancer, melanoma, and non-small cell lung cancer [129,130]. PSAT1 belongs to serine biosynthesis pathway, which is a key actor in nucleotide and amino acid metabolism and specifically, the folate cycle contributes to nucleotide metabolism. The folate cycle provides nucleotide pool replenishment during cell proliferation, and DNA damage induces the production of nucleotides [130]. Moreover, serine synthesis enzyme levels have been shown to increase under conditions of DNA damage and genomic instability [130,131]. In addition, recently, Labuschagne *et al* reported that serine, but not glycine, supports one-carbon metabolism and proliferation of cancer cells [132]. GIST48-R and

GIST48B-R were characterized by up-regulation of PSAT1 and this could represent an advantage for resistant cells, which have to find novel *ploys* to live. Here, we showed that PSAT1 over-expression is modulated by both methylation and miRNAs. It is plausible that these epigenetic mechanisms may act concurrently or in a mutual manner, with the final goal to increase PSAT1 level. Among the genes with a differential methylation level, we found TSHZ2, which showed a down-regulation in resistant cells. TSHZ2, a zinc-finger homeobox nuclear protein, is supposed to be a tumor suppressor and is down-regulated in breast cancer [133]. Interestingly, Yamamoto *et al*, investigated the methylation level of TSHZ2 promoter, but they were not able to observe difference with respect to normal tissue, leaving a question of how TSHZ2 is down-regulated. On the contrary, we identified an epigenetic contribution for TSHZ2 regulation. We speculated that TSHZ2 might bind transcriptional regulators that control the expression of crucial genes in tumorigenesis and resistance acquisition. With regard to miRNAs deregulation, we identified 13 miRNAs significantly altered in resistant cells. Through miRPath 3.0 we assessed miRNA regulatory roles and identified the pathways. Interestingly, among the pathways potentially modulated by those deregulated miRNAs, the most significant and with the greatest number of target genes, were PI3K/AKT-MAPK and RAS cascades, which are involved in BYL719 mechanism of action. Integrating miRNA array and GEP, 5 miRNAs targeted 8 genes (TRIB1, GAB2, SNX10, SAMD12, JUNB, GPC3, SOX4). Among those genes, some have been reported involved in PI3K/AKT signaling pathway. TRIB1 is a downstream effector of PI3K [134]. GAB2, Grb2-associated binder 2, belong to a family of scaffolding or docking adaptor proteins; GAB2 cooperates with PI3K/AKT pathway in promoting malignant behavior in cells [135,136].

In conclusion, we identified a peculiar and novel mechanism of resistance in GISTs. Unfortunately, at the moment, we do not have patients in treatment with BYL719 to verify this preclinical data. However, these results suggest the existence of alternative pathways of resistance in GISTs and they should be take into account as alternative adaptive mechanism

7. Conclusion

In the last two decades, the research has progressively focused its attention on epigenetics. It is now clear that both genetic and epigenetic alterations are involved and contribute to cancer pathogenesis, development, progression, as well as treatment outcome. The knowledge in epigenome is continuously growing and we are gradually figuring out its importance in regulating gene expression and biological processes. However, to date, clinical translation has been very scarce, therefore there is an urgent need to translate the findings.

GISTs are rare sarcoma tumors, which represent the most common mesenchymal tumor of the GI tract, with an incidence of ~1-1.5 new cases/100000 per year.

In 2018, during the ESMO Sarcoma and GIST Symposium, epigenetics has been included among the new avenues in soft tissue sarcomas and GISTs [137]. In GISTs, excluding methylation, which has been studied more extensively than the other two epigenetic mechanisms (miRNAs and histones modifications), the advances have been quite scarce.

The research of my PhD project aimed to deeper feature the knowledge on epigenetics in GIST. Specifically, during my PhD program, the research had two aims; I) the first aim was to investigate and characterize the differences in miRNAs expression levels, comparing *KIT/PDGFRA* mutant and *KIT/PDGFRA* WT GISTs. II) Secondly, we aimed to elucidate mechanisms of pharmacological resistance to a PI3KCA inhibitor – BYL719 – in trial at Sant'Orsola Malpighi Hospital for GIST patients who previously failed imatinib and sunitinib – the first and the second lines approved for GIST. Indeed, all the treatment lines so far approved in GISTs are TKIs, showing a similar mechanism of action.

With regard to the first goal, we identified, for the first time in GIST, an epigenetic mechanism involved in regulating the IGF1R expression. In particular, in agreement with the literature, our data revealed that miR-139-5p has a role of tumor suppressor and its inhibition promoted cell migration and invasion.

With regard to the second aim, through an *omic* approach in *in vitro* models, we characterized a mechanism of resistance involving epigenetic alterations. Specifically, after having confirmed the absence of resistance mutations, we integrated miRNAs and methylation profiles with gene expression deregulation. This led us to speculate that BYL719 resistance could be mediated by alternative mechanisms, which, similarly to mutations, confer advantages to the cells.

Herein we showed that epigenetics in GIST could be more important than it has been thought so far. In particular, we showed that epigenetic mechanisms are involved in the pathogenesis, as well as in resistance. This highlights the importance to better understand the biology underlying this tumor. In addition, considering the emergence of new epigenetic therapies in solid tumors as drug resistance modulators, this could represent a chance too important to miss.

.

8. References

1. Miettinen, M. & Lasota, J. Gastrointestinal stromal tumors. *Gastroenterol. Clin. North Am.* **42,** 39Miettinen, M., Lasota, J. (2013). Gastrointest (2013).
2. Golden T, S. A. Smooth muscle tumors of the gastrointestinal tract and retroperitoneal tissues. *Surg Gynecol Obs.* **73,** 784–810 (1941).
3. Mazur, M. T. & Clark, H. B. Gastric stromal tumors. Reappraisal of histogenesis. *Am. J. Surg. Pathol.* **7,** 507–19 (1983).
4. Hirota, S. *et al.* Gain-of-function mutations of c-kit in human gastrointestinal stromal tumors. *Science* **279,** 577–80 (1998).
5. Demetri, G. D. *et al.* Efficacy and safety of imatinib mesylate in advanced gastrointestinal stromal tumors. *N. Engl. J. Med.* **347,** 472–80 (2002).
6. Mei, L. *et al.* Gastrointestinal Stromal Tumors: The GIST of Precision Medicine. *Trends in Cancer* **4,** 74–91 (2018).
7. Søreide, K. *et al.* Global epidemiology of gastrointestinal stromal tumours (GIST): A systematic review of population-based cohort studies. *Cancer Epidemiol.* **40,** 39–46 (2016).
8. Gatta, G. *et al.* Rare cancers are not so rare: The rare cancer burden in Europe. *Eur. J. Cancer* **47,** 2493–2511 (2011).
9. Casali, P. G. *et al.* Gastrointestinal stromal tumours: ESMO-EURACAN Clinical Practice Guidelines for diagnosis, treatment and follow-up. *Ann. Oncol. Off. J. Eur. Soc. Med. Oncol.* (2018). doi:10.1093/annonc/mdy095
10. Liegl-Atzwanger, B., Fletcher, J. A. & Fletcher, C. D. M. Gastrointestinal stromal tumors. *Virchows Arch.* **456,** 111–27 (2010).
11. Fletcher, C. D. M. *et al.* Diagnosis of gastrointestinal stromal tumors: A consensus approach. *Hum. Pathol.* **33,** 459–65 (2002).
12. DeMatteo, R. P. *et al.* Two hundred gastrointestinal stromal tumors: recurrence patterns and

prognostic factors for survival. *Ann. Surg.* **231,** 51–8 (2000).

13. Miettinen, M., Virolainen, M. & Maarit-Sarlomo-Rikala. Gastrointestinal stromal tumors--value of CD34 antigen in their identification and separation from true leiomyomas and schwannomas. *Am. J. Surg. Pathol.* **19,** 207–16 (1995).
14. Corless, C. L. & Heinrich, M. C. Molecular Pathobiology of Gastrointestinal Stromal Sarcomas. *Annu. Rev. Pathol. Mech. Dis.* **3,** 557–586 (2008).
15. Cancer.net. cancer.net/cancer-types/gastrointestinal-stromal-tumor-gist/risk-factors. Available at: https://www.cancer.net/cancer-types/gastrointestinal-stromal-tumor-gist/risk-factors.
16. Joensuu, H. Gastrointestinal stromal tumor (GIST). *Ann. Oncol. Off. J. Eur. Soc. Med. Oncol.* **17 Suppl 10,** x280-6 (2006).
17. Huizinga, J. D., Zarate, N. & Farrugia, G. Physiology, injury, and recovery of interstitial cells of Cajal: basic and clinical science. *Gastroenterology* **137,** 1548–56 (2009).
18. Laurini, J. A. & Carter, J. E. Gastrointestinal stromal tumors: a review of the literature. *Arch. Pathol. Lab. Med.* **134,** 134–41 (2010).
19. Hubbard, S. R. Juxtamembrane autoinhibition in receptor tyrosine kinases. *Nat. Rev. Mol. Cell Biol.* **5,** 464–71 (2004).
20. Pawson, T. Regulation and targets of receptor tyrosine kinases. *Eur. J. Cancer* **38 Suppl 5,** S3-10 (2002).
21. Angelini, S., Ravegnini, G., Fletcher, J. A., Maffei, F. & Hrelia, P. Clinical relevance of pharmacogenetics in gastrointestinal stromal tumor treatment in the era of personalized therapy. *Pharmacogenomics* **14,** (2013).
22. de Melo Maia, B. *et al.* Prognostic significance of c-KIT in vulvar cancer: bringing this molecular marker from bench to bedside. *J. Transl. Med.* **10,** 150 (2012).
23. Ke, H., Kazi, J. U., Zhao, H. & Sun, J. Germline mutations of KIT in gastrointestinal stromal tumor (GIST) and mastocytosis. *Cell Biosci.* **6,** 55 (2016).

24. Corless, C. L., Barnett, C. M. & Heinrich, M. C. Gastrointestinal stromal tumours: origin and molecular oncology. *Nat. Rev. Cancer* **11,** 865–78 (2011).

25. Indio, V. *et al.* Integrated Molecular Characterization of Gastrointestinal Stromal Tumors (GIST) Harboring the Rare D842V Mutation in PDGFRA Gene. *Int. J. Mol. Sci.* **19,** 732 (2018).

26. Heinrich, M. C. *et al.* Sorafenib Inhibits Many Kinase Mutations Associated with Drug-Resistant Gastrointestinal Stromal Tumors. *Mol. Cancer Ther.* **11,** 1770–1780 (2012).

27. Hirota, S. *et al.* Gain-of-function mutations of platelet-derived growth factor receptor alpha gene in gastrointestinal stromal tumors. *Gastroenterology* **125,** 660–7 (2003).

28. Lasota, J. & Miettinen, M. KIT and PDGFRA mutations in gastrointestinal stromal tumors (GISTs). *Semin. Diagn. Pathol.* **23,** 91–102 (2006).

29. Antonescu, C. in *Current topics in microbiology and immunology* **355,** 41–57 (2011).

30. COSMIC v85, released 08-M.-18. Cosmic. Catalogue Of Somatic Mutations In Cancer. Available at: https://cancer.sanger.ac.uk/cosmic.

31. Forbes, S. A. *et al.* COSMIC: exploring the world's knowledge of somatic mutations in human cancer. *Nucleic Acids Res.* **43,** D805-11 (2015).

32. Antonescu, C. R. *et al.* Association of KIT exon 9 mutations with nongastric primary site and aggressive behavior: KIT mutation analysis and clinical correlates of 120 gastrointestinal stromal tumors. *Clin. Cancer Res.* **9,** 3329–37 (2003).

33. Heinrich, M. C. *et al.* PDGFRA activating mutations in gastrointestinal stromal tumors. *Science* **299,** 708–10 (2003).

34. Dibb, N. J., Dilworth, S. M. & Mol, C. D. Switching on kinases: oncogenic activation of BRAF and the PDGFR family. *Nat. Rev. Cancer* **4,** 718–27 (2004).

35. Nannini, M., Urbini, M., Astolfi, A., Biasco, G. & Pantaleo, M. A. The progressive fragmentation of the KIT/PDGFRA wild-type (WT) gastrointestinal stromal tumors (GIST). *J. Transl. Med.* **15,** 113 (2017).

36. Miettinen, M. & Lasota, J. Succinate dehydrogenase deficient gastrointestinal stromal tumors (GISTs) - a review. *Int. J. Biochem. Cell Biol.* **53,** 514–9 (2014).

37. Urbini, M. *et al.* SDHC methylation in gastrointestinal stromal tumors (GIST): A case report. *BMC Med. Genet.* **16,** (2015).

38. Pantaleo, M. A. *et al.* Insulin-like growth factor 1 receptor expression in wild-type GISTs: a potential novel therapeutic target. *Int. J. cancer* **125,** 2991–4 (2009).

39. Janeway, K. A. *et al.* Strong expression of IGF1R in pediatric gastrointestinal stromal tumors without IGF1R genomic amplification. *Int. J. cancer* **127,** 2718–22 (2010).

40. Pantaleo, M. A. *et al.* Analysis of all subunits, SDHA, SDHB, SDHC, SDHD, of the succinate dehydrogenase complex in KIT/PDGFRA wild-type GIST. *Eur. J. Hum. Genet.* **22,** 32–9 (2014).

41. Huss, S. *et al.* Classification of KIT/PDGFRA wild-type gastrointestinal stromal tumors: implications for therapy. *Expert Rev. Anticancer Ther.* **15,** 623–8 (2015).

42. Dankner, M., Rose, A. A. N., Rajkumar, S., Siegel, P. M. & Watson, I. R. Classifying BRAF alterations in cancer: new rational therapeutic strategies for actionable mutations. *Oncogene* **37,** 3183–3199 (2018).

43. Agaimy, A. *et al.* V600E BRAF mutations are alternative early molecular events in a subset of KIT/PDGFRA wild-type gastrointestinal stromal tumours. *J. Clin. Pathol.* **62,** 613–6 (2009).

44. Ricci, R., Dei Tos, A. P. & Rindi, G. On the prevalence of KRAS mutations in GISTs. *Virchows Arch.* **463,** 847–847 (2013).

45. Miranda, C. *et al.* KRAS and BRAF mutations predict primary resistance to imatinib in gastrointestinal stromal tumors. *Clin. Cancer Res.* **18,** 1769–76 (2012).

46. Hechtman, J. F. *et al.* Novel oncogene and tumor suppressor mutations in KIT and PDGFRA wild type gastrointestinal stromal tumors revealed by next generation sequencing. *Genes. Chromosomes Cancer* **54,** 177–84 (2015).

47. Nannini, M. *et al.* Integrated genomic study of quadruple-WT GIST (KIT/PDGFRA/SDH/RAS pathway wild-type GIST). *BMC Cancer* **14,** 685 (2014).

48. Din, O. S. & Woll, P. J. Treatment of gastrointestinal stromal tumor: focus on imatinib mesylate. *Ther. Clin. Risk Manag.* **4,** 149–62 (2008).

49. Balachandran, V. P. & Dematteo, R. P. Targeted therapy for cancer: the gastrointestinal stromal tumor model. *Surg. Oncol. Clin. N. Am.* **22,** 805–21 (2013).

50. Akahoshi, K., Oya, M., Koga, T. & Shiratsuchi, Y. Current clinical management of gastrointestinal stromal tumor. *World J. Gastroenterol.* **24,** 2806–2817 (2018).

51. ESMO/European Sarcoma Network Working Group. Gastrointestinal stromal tumours: ESMO Clinical Practice Guidelines for diagnosis, treatment and follow-up. *Ann. Oncol.* **25,** iii21-iii26 (2014).

52. Joensuu, H. *et al.* Risk of recurrence of gastrointestinal stromal tumour after surgery: an analysis of pooled population-based cohorts. *Lancet Oncol.* **13,** 265–274 (2012).

53. Gronchi, A. *et al.* Adjuvant treatment of GIST with imatinib: solid ground or still quicksand? A comment on behalf of the EORTC Soft Tissue and Bone Sarcoma Group, the Italian Sarcoma Group, the NCRI Sarcoma Clinical Studies Group (UK), the Japanese Study Group on GIST, the French Sarcoma Group and the Spanish Sarcoma Group (GEIS). *Eur. J. Cancer* **45,** 1103–6 (2009).

54. Dematteo, R. P., Heinrich, M. C., El-Rifai, W. M. & Demetri, G. Clinical management of gastrointestinal stromal tumors: before and after STI-571. *Hum. Pathol.* **33,** 466–77 (2002).

55. Deininger, M., Buchdunger, E. & Druker, B. J. Review in translational hematology The development of imatinib as a therapeutic agent for chronic myeloid leukemia. (2005). doi:10.1182/blood-2004-08

56. Rubin, B. P., Heinrich, M. C. & Corless, C. L. Gastrointestinal stromal tumour. *Lancet (London, England)* **369,** 1731–41 (2007).

57. Joensuu, H. *et al.* Effect of the tyrosine kinase inhibitor STI571 in a patient with a metastatic

gastrointestinal stromal tumor. *N. Engl. J. Med.* **344,** 1052–6 (2001).

58. Heinrich, M. C. *et al.* Kinase Mutations and Imatinib Response in Patients With Metastatic Gastrointestinal Stromal Tumor. *J. Clin. Oncol.* **21,** 4342–4349 (2003).

59. Heinrich MC1, Owzar K, Corless CL, Hollis D, Borden EC, Fletcher CD, Ryan CW, von Mehren M, Blanke CD, Rankin C, Benjamin RS, Bramwell VH, Demetri GD, Bertagnolli MM, F. J. Correlation of kinase genotype and clinical outcome in the North American Intergroup Phase III Trial of imatinib mesylate for treatment of advanced gastrointestinal stromal tumor: CALGB 150105 Study by Cancer and Leukemia Group B and Southwest Oncology Gr. *J. Clin. Oncol.* **26,** 5360–5367 (2008).

60. Ksienski, D. Imatinib mesylate: past successes and future challenges in the treatment of gastrointestinal stromal tumors. *Clin. Med. Insights. Oncol.* **5,** 365–79 (2011).

61. Gounder, M. M. & Maki, R. G. Molecular basis for primary and secondary tyrosine kinase inhibitor resistance in gastrointestinal stromal tumor. *Cancer Chemother. Pharmacol.* **67,** 25–43 (2011).

62. Demetri, G. D. *et al.* Efficacy and safety of sunitinib in patients with advanced gastrointestinal stromal tumour after failure of imatinib: a randomised controlled trial. *Lancet (London, England)* **368,** 1329–38 (2006).

63. Papaetis, G. S. & Syrigos, K. N. Sunitinib. *BioDrugs* **23,** 377–389 (2009).

64. Aparicio-Gallego, G. *et al.* New insights into molecular mechanisms of sunitinib-associated side effects. *Mol. Cancer Ther.* **10,** 2215–23 (2011).

65. Heinrich, M. C. *et al.* Primary and secondary kinase genotypes correlate with the biological and clinical activity of sunitinib in imatinib-resistant gastrointestinal stromal tumor. *J. Clin. Oncol.* **26,** 5352–9 (2008).

66. George, S. *et al.* Efficacy and safety of regorafenib in patients with metastatic and/or unresectable GI stromal tumor after failure of imatinib and sunitinib: A multicenter phase II trial. *J. Clin. Oncol.* **30,** 2401–2407 (2012).

67. Bruno Vincenzi, Margherita Nannini, Giovanni Grignani, Elena Fumagalli, Silvia Gasperoni, Lorenzo D'Ambrosio, Giuseppe Badalamenti, Angelo Paolo Dei Tos, Lorena Incorvaia, Paolo G Casali, Daniele Santini, Giuseppe Tonini, Giovanna Catania, Mariella Spalat, M. A. P. Rechallenge in advanced GIST progressing to imatinib, sunitinib and regorafenib: An Italian survey. *J. Clin. Oncol.* **15,** 11038 (2017).

68. Tessmer, M. S. & Flaherty, K. T. *AACR Cancer Progress Report 2017:* Harnessing Research Discoveries to Save Lives. *Clin. Cancer Res.* **23,** 5325–5325 (2017).

69. Peng, Y. & Croce, C. M. The role of MicroRNAs in human cancer. *Signal Transduct. Target. Ther.* **1,** 15004 (2016).

70. Lee, R. C., Feinbaum, R. L. & Ambros, V. The C. elegans heterochronic gene lin-4 encodes small RNAs with antisense complementarity to lin-14. *Cell* **75,** 843–54 (1993).

71. miRBase Sequence Database -- Release 22. miRBASE. Available at: http://www.mirbase.org/.

72. Calin, G. A. *et al.* Frequent deletions and down-regulation of micro- RNA genes miR15 and miR16 at 13q14 in chronic lymphocytic leukemia. *Proc. Natl. Acad. Sci. U. S. A.* **99,** 15524–9 (2002).

73. Calin, G. A. *et al.* Human microRNA genes are frequently located at fragile sites and genomic regions involved in cancers. *Proc. Natl. Acad. Sci.* **101,** 2999–3004 (2004).

74. Sevignani, C., Calin, G. A., Siracusa, L. D. & Croce, C. M. Mammalian microRNAs: a small world for fine-tuning gene expression. *Mamm. Genome* **17,** 189–202 (2006).

75. Ha, M. & Kim, V. N. Regulation of microRNA biogenesis. *Nat. Rev. Mol. Cell Biol.* **15,** 509–524 (2014).

76. Romero-Cordoba, S. L., Salido-Guadarrama, I., Rodriguez-Dorantes, M. & Hidalgo-Miranda, A. miRNA biogenesis: biological impact in the development of cancer. *Cancer Biol. Ther.* **15,** 1444–55 (2014).

77. Graves, L. E. *et al.* Proinvasive properties of ovarian cancer ascites-derived membrane

vesicles. *Cancer Res.* **64,** 7045–9 (2004).

78. Graves, P. & Zeng, Y. Biogenesis of Mammalian MicroRNAs: A Global View. *Genomics. Proteomics Bioinformatics* **10,** 239–245 (2012).

79. Di Leva, G., Garofalo, M. & Croce, C. M. MicroRNAs in Cancer. *Annu. Rev. Pathol. Mech. Dis.* **9,** 287–314 (2014).

80. Cai, Y., Yu, X., Hu, S. & Yu, J. A Brief Review on the Mechanisms of miRNA Regulation. *Genomics. Proteomics Bioinformatics* **7,** 147–154 (2009).

81. Zhou, H. & Rigoutsos, I. MiR-103a-3p targets the 5' UTR of GPRC5A in pancreatic cells. *RNA* **20,** 1431–9 (2014).

82. Lytle, J. R., Yario, T. A. & Steitz, J. A. Target mRNAs are repressed as efficiently by microRNA-binding sites in the 5' UTR as in the 3' UTR. *Proc. Natl. Acad. Sci. U. S. A.* **104,** 9667–72 (2007).

83. Pereira, D. M., Rodrigues, P. M., Borralho, P. M. & Rodrigues, C. M. P. Delivering the promise of miRNA cancer therapeutics. *Drug Discov. Today* **18,** 282–289 (2013).

84. Kumar, M. S. *et al.* Dicer1 functions as a haploinsufficient tumor suppressor. *Genes Dev.* **23,** 2700–2704 (2009).

85. Lambertz, I. *et al.* Monoallelic but not biallelic loss of Dicer1 promotes tumorigenesis in vivo. *Cell Death Differ.* **17,** 633–641 (2010).

86. Volinia, S. *et al.* A microRNA expression signature of human solid tumors defines cancer gene targets. *Proc. Natl. Acad. Sci.* **103,** 2257–2261 (2006).

87. Koelz. Down-regulation of miR-221 and miR-222 correlates with pronounced Kit expression in gastrointestinal stromal tumors. *Int. J. Oncol.* **38,** (2011).

88. Garofalo, M., Quintavalle, C., Romano, G., Croce, C. M. & Condorelli, G. miR221/222 in cancer: their role in tumor progression and response to therapy. *Curr. Mol. Med.* **12,** 27–33 (2012).

89. Ravegnini, G. *et al.* Personalized Medicine in Gastrointestinal Stromal Tumor (GIST):

Clinical Implications of the Somatic and Germline DNA Analysis. *Int. J. Mol. Sci.* **16,** 15592–608 (2015).

90. Ricci, R., Dei Tos, A. P. & Rindi, G. GISTogram: a graphic presentation of the growing GIST complexity. *Virchows Arch.* **463,** 481–7 (2013).

91. Nannini, M., Biasco, G., Astolfi, A., Urbini, M. & Pantaleo, M. A. Insulin-like Growth Factor (IGF) system and gastrointestinal stromal tumours (GIST): present and future. *Histol. Histopathol.* **29,** 167–75 (2014).

92. Garzon, R., Calin, G. A. & Croce, C. M. MicroRNAs in Cancer. *Annu. Rev. Med.* **60,** 167–79 (2009).

93. Nannini, M. *et al.* MiRNA profiling in gastrointestinal stromal tumors: Implication as diagnostic and prognostic markers. *Epigenomics* **7,** (2015).

94. Xu, W. *et al.* MicroRNA-139-5p inhibits cell proliferation and invasion by targeting insulin-like growth factor 1 receptor in human non-small cell lung cancer. *Int. J. Clin. Exp. Pathol.* **8,** 3864–70 (2015).

95. Jia, C. Y. *et al.* MiR-223 Suppresses Cell Proliferation by Targeting IGF-1R. *PLoS One* **6,** e27008 (2011).

96. Hu, W., Zhang, W., Li, F., Guo, F. & Chen, A. miR-139 is up-regulated in osteoarthritis and inhibits chondrocyte proliferation and migration possibly via suppressing EIF4G2 and IGF1R. *Biochem. Biophys. Res. Commun.* **474,** 296–302 (2016).

97. Dai, S., Wang, X., Li, X. & Cao, Y. MicroRNA-139-5p acts as a tumor suppressor by targeting ELTD1 and regulating cell cycle in glioblastoma multiforme. *Biochem. Biophys. Res. Commun.* **467,** 204–210 (2015).

98. Zhang, L. *et al.* microRNA-139-5p exerts tumor suppressor function by targeting NOTCH1 in colorectal cancer. *Mol. Cancer* **13,** 124 (2014).

99. Liu, R. *et al.* Tumor-Suppressive Function of miR-139-5p in Esophageal Squamous Cell Carcinoma. *PLoS One* **8,** e77068 (2013).

100. Serrano, C. & George, S. Recent advances in the treatment of gastrointestinal stromal tumors. *Ther. Adv. Med. Oncol.* **6,** 115–27 (2014).

101. Demetri, G. D. *et al.* Efficacy and safety of regorafenib for advanced gastrointestinal stromal tumours after failure of imatinib and sunitinib (GRID): an international, multicentre, randomised, placebo-controlled, phase 3 trial. *Lancet* **381,** 295–302 (2013).

102. Hemming, M. L., Heinrich, M. C., Bauer, S. & George, S. Translational Insights into Gastrointestinal Stromal Tumor and Current Clinical Advances. *Ann. Oncol. Off. J. Eur. Soc. Med. Oncol.* (2018). doi:10.1093/annonc/mdy309

103. Liegl, B. *et al.* Heterogeneity of kinase inhibitor resistance mechanisms in GIST. *J. Pathol.* **216,** 64–74 (2008).

104. Serrano, C. *et al.* KRAS and KIT Gatekeeper Mutations Confer Polyclonal Primary Imatinib Resistance in GI Stromal Tumors: Relevance of Concomitant Phosphatidylinositol 3-Kinase/AKT Dysregulation. *J. Clin. Oncol.* **33,** e93-6 (2015).

105. Bauer, S., Duensing, A., Demetri, G. D. & Fletcher, J. A. KIT oncogenic signaling mechanisms in imatinib-resistant gastrointestinal stromal tumor: PI3-kinase/AKT is a crucial survival pathway. *Oncogene* **26,** 7560–8 (2007).

106. Vivanco, I. & Sawyers, C. L. The phosphatidylinositol 3-Kinase AKT pathway in human cancer. *Nat. Rev. Cancer* **2,** 489–501 (2002).

107. Patel, S. Exploring Novel Therapeutic Targets in GIST: Focus on the PI3K/Akt/mTOR Pathway. *Curr. Oncol. Rep.* **15,** 386–395 (2013).

108. Ríos-Moreno, M. J. *et al.* Differential activation of MAPK and PI3K/AKT/mTOR pathways and IGF1R expression in gastrointestinal stromal tumors. *Anticancer Res.* **31,** 3019–25 (2011).

109. Fritsch, C. *et al.* Characterization of the novel and specific PI3Kα inhibitor NVP-BYL719 and development of the patient stratification strategy for clinical trials. *Mol. Cancer Ther.* **13,** 1117–29 (2014).

110. Van Looy, T. *et al.* Phosphoinositide 3-kinase inhibitors combined with imatinib in patient-derived xenograft models of gastrointestinal stromal tumors: rationale and efficacy. *Clin. Cancer Res.* **20,** 6071–82 (2014).

111. Bauer, S., Yu, L. K., Demetri, G. D. & Fletcher, J. A. Heat shock protein 90 inhibition in imatinib-resistant gastrointestinal stromal tumor. *Cancer Res.* **66,** 9153–61 (2006).

112. Mühlenberg, T. *et al.* Inhibitors of deacetylases suppress oncogenic KIT signaling, acetylate HSP90, and induce apoptosis in gastrointestinal stromal tumors. *Cancer Res.* **69,** 6941–50 (2009).

113. Ulukaya, E., Colakogullari, M. & Wood, E. J. Interference by anti-cancer chemotherapeutic agents in the MTT-tumor chemosensitivity assay. *Chemotherapy* **50,** 43–50 (2004).

114. Barault, L. *et al.* Discovery of methylated circulating DNA biomarkers for comprehensive non-invasive monitoring of treatment response in metastatic colorectal cancer. *Gut* gutjnl-2016-313372 (2017). doi:10.1136/gutjnl-2016-313372

115. Moran, S., Arribas, C. & Esteller, M. Validation of a DNA methylation microarray for 850,000 CpG sites of the human genome enriched in enhancer sequences. *Epigenomics* **8,** 389–99 (2016).

116. Lai, K., Killingsworth, M. C. & Lee, C. S. Gene of the month: *PIK3CA*. *J. Clin. Pathol.* **68,** 253–257 (2015).

117. Samuels, Y. *et al.* High Frequency of Mutations of the PIK3CA Gene in Human Cancers. *Science (80-.).* **304,** 554–554 (2004).

118. Vlachos, I. S. *et al.* DIANA-miRPath v3.0: deciphering microRNA function with experimental support. *Nucleic Acids Res.* **43,** W460-6 (2015).

119. Chou, C.-H. *et al.* miRTarBase update 2018: a resource for experimentally validated microRNA-target interactions. *Nucleic Acids Res.* **46,** D296–D302 (2018).

120. Beretta, G. L., Cassinelli, G., Pennati, M., Zuco, V. & Gatti, L. Overcoming ABC transporter-mediated multidrug resistance: The dual role of tyrosine kinase inhibitors as

multitargeting agents. *Eur. J. Med. Chem.* **142,** 271–289 (2017).

121. Choi, Y. H. & Yu, A.-M. ABC transporters in multidrug resistance and pharmacokinetics, and strategies for drug development. *Curr. Pharm. Des.* **20,** 793–807 (2014).

122. Klukovits, A. & Krajcsi, P. Mechanisms and therapeutic potential of inhibiting drug efflux transporters. *Expert Opin. Drug Metab. Toxicol.* **11,** 907–920 (2015).

123. Brown, R., Curry, E., Magnani, L., Wilhelm-Benartzi, C. S. & Borley, J. Poised epigenetic states and acquired drug resistance in cancer. *Nat. Rev. Cancer* **14,** 747–753 (2014).

124. Knoechel, B. *et al.* An epigenetic mechanism of resistance to targeted therapy in T cell acute lymphoblastic leukemia. *Nat. Genet.* **46,** 364–370 (2014).

125. Salgia, R. & Kulkarni, P. The Genetic/Non-genetic Duality of Drug 'Resistance' in Cancer. *Trends in Cancer* **4,** 110–118 (2018).

126. Nervi, C., De Marinis, E. & Codacci-Pisanelli, G. Epigenetic treatment of solid tumours: a review of clinical trials. *Clin. Epigenetics* **7,** 127 (2015).

127. Bauer, S. *et al.* Phase I study of panobinostat and imatinib in patients with treatment-refractory metastatic gastrointestinal stromal tumors. *Br. J. Cancer* **110,** 1155–62 (2014).

128. Shivakumar, M. *et al.* Identification of epigenetic interactions between miRNA and DNA methylation associated with gene expression as potential prognostic markers in bladder cancer. *BMC Med. Genomics* **10,** 30 (2017).

129. Vié, N. *et al.* Overexpression of phosphoserine aminotransferase PSAT1 stimulates cell growth and increases chemoresistance of colon cancer cells. *Mol. Cancer* **7,** 14 (2008).

130. Ross, K. C., Andrews, A. J., Marion, C. D., Yen, T. J. & Bhattacharjee, V. Identification of the Serine Biosynthesis Pathway as a Critical Component of BRAF Inhibitor Resistance of Melanoma, Pancreatic, and Non–Small Cell Lung Cancer Cells. *Mol. Cancer Ther.* **16,** 1596–1609 (2017).

131. Markkanen, E., Fischer, R., Ledentcova, M., Kessler, B. M. & Dianov, G. L. Cells deficient in base-excision repair reveal cancer hallmarks originating from adjustments to genetic

instability. *Nucleic Acids Res.* **43,** 3667–3679 (2015).

132. Labuschagne, C. F., van den Broek, N. J. F., Mackay, G. M., Vousden, K. H. & Maddocks, O. D. K. Serine, but Not Glycine, Supports One-Carbon Metabolism and Proliferation of Cancer Cells. *Cell Rep.* **7,** 1248–1258 (2014).

133. Yamamoto, M., Cid, E., Bru, S. & Yamamoto, F. Rare and Frequent Promoter Methylation, Respectively, of TSHZ2 and 3 Genes That Are Both Downregulated in Expression in Breast and Prostate Cancers. *PLoS One* **6,** e17149 (2011).

134. De Marco, C. *et al.* Specific gene expression signatures induced by the multiple oncogenic alterations that occur within the PTEN/PI3K/AKT pathway in lung cancer. *PLoS One* **12,** e0178865 (2017).

135. Wang, Y., Sheng, Q., Spillman, M. A., Behbakht, K. & Gu, H. Gab2 regulates the migratory behaviors and E-cadherin expression via activation of the PI3K pathway in ovarian cancer cells. *Oncogene* **31,** 2512–2520 (2012).

136. Wang, W. J. *et al.* Grb2-associated binder 2 silencing impairs growth and migration of H1975 cells via modulation of PI3K-Akt signaling. *Int. J. Clin. Exp. Pathol.* **8,** 10575–84 (2015).

137. Frezza, A. M. *et al.* 2018 ESMO Sarcoma and GIST Symposium: ‘take-home messages’ in soft tissue sarcoma. *ESMO open* **3,** e000390 (2018).